CHAPTER 1

Literature Review

1.1 Structural features of carbon nanotubes (CNTs)

Carbon is a fascinating element that is very abundant and is the basis of life. Carbon has two features which make it quite unique; a carbon atom can bond with another carbon atom by using a range orbitals (different hybridization of the C atom), and can also bond with many other elements. Crystalline carbon can be found in essentially two categories in nature, namely graphite and diamond. The two categories correspond to the different hybridizations that carbon atoms can assume. The four valence electrons in carbon, when shared equally, form a sp^3 hybridized bond, which is found in diamond. When only three electrons are shared covalently between neighbours in a plane and the fourth electron is allowed to be delocalized among all carbon atoms (sp^2 hybridized), the resulting material is graphite. Carbon nanotubes and fullerenes belong to the architecture of sp^2 bonded carbon materials. Although diamond and graphite are formed from pure carbon their physical and chemical properties are different. For example, graphite is a zero gap semiconductor and is opaque, while diamond is a high band gap semiconductor and is transparent.

Carbon filaments which are carbon products in a tubular form were first discovered when electron microscopes came into wide use in the 1950s [1]. In the early 90s, some filamentous carbon material was observed to have diameters in the nanometer range [2] and these materials have ever since been called carbon nanotubes (CNTs). CNTs are made of graphene sheets rolled up into a cylinder, with ends that can be closed or open to give a fullerene like structures (Figure 1.1a and 1.1b). In ideal nanotubes, a hexagonal network of carbon atoms are arranged to make a seamless hollow cylinder. CNTs can be categorised according to the number of walls found in the material e.g., single-walled carbon nanotubes (SWCNTs) and multi-walled carbon nanotubes (MWCNTs). Ideally SWCNTs are made of a perfect graphene sheet, i.e. a polyaromatic monoatomic layer

made of a hexagonal display of sp^2 hybridized carbon atoms (Figure 1.1a), rolled up into a cylinder and closed by two caps (semi-fullerenes). The internal diameter of these structures can vary between 0.4 and 2.5 nm and the length can range from a few microns to several millimetres. MWCNTs can be considered as concentric SWCNTs with increasing diameter and coaxially disposed each other. The number of walls (graphene sheets) can vary from two (double-walled CNTs) to several tens, such that the external diameter can reach up to 100 nm or more, while the interlayer spacing remains close to that of graphite (0.34 nm). The inner diameter of MWCNTs varies from one nanometer up to a few nanometers and their outer diameter ranges from 2 nm up to 100 nm depending on the number of graphene sheets in the structure.

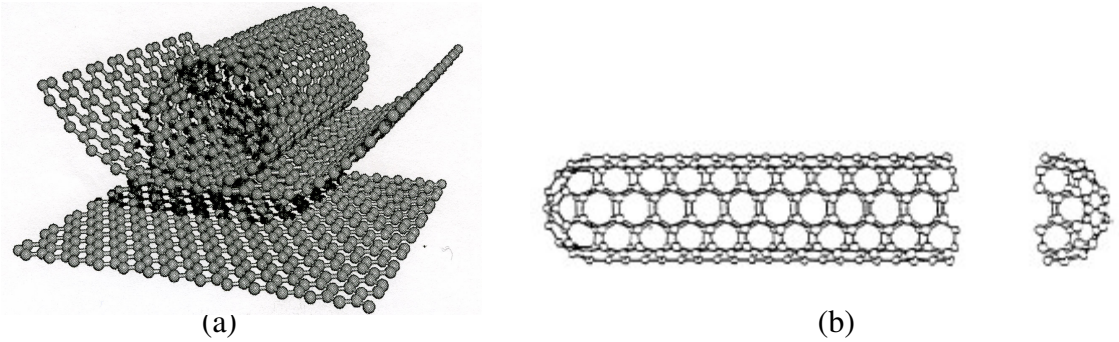

(a) (b)

Figure 1.1: (a) Schematic diagram of an open carbon nanotube [3], (b) a closed carbon nanotube [4].

1.2 Synthesis of carbon nanotubes

Since the studies of carbon tubes by Iijima [2], several techniques have been developed to produce CNTs. Such techniques include arc discharge, laser vaporization and a variety of chemical vapour deposition (CVD) methods. Two of the most promising methods for generating a good yield of CNTs are the "floating catalyst" CVD method or the injection CVD method, which are discussed in more detail later in this section. CVD methods can produce both MWCNTs and SWCNTs. Carbon nanotubes are found to grow under various conditions for example, CNTs are generally found to grow in the presence of supported metal catalysts while some CNTs can grow in the absence of a support,

suggesting different growth mechanisms. Although different techniques have been used to produce CNTs, evaluating the purity and quality of produced CNTs still remains a challenge to most researchers.

1.2.1 Arc-discharge technique

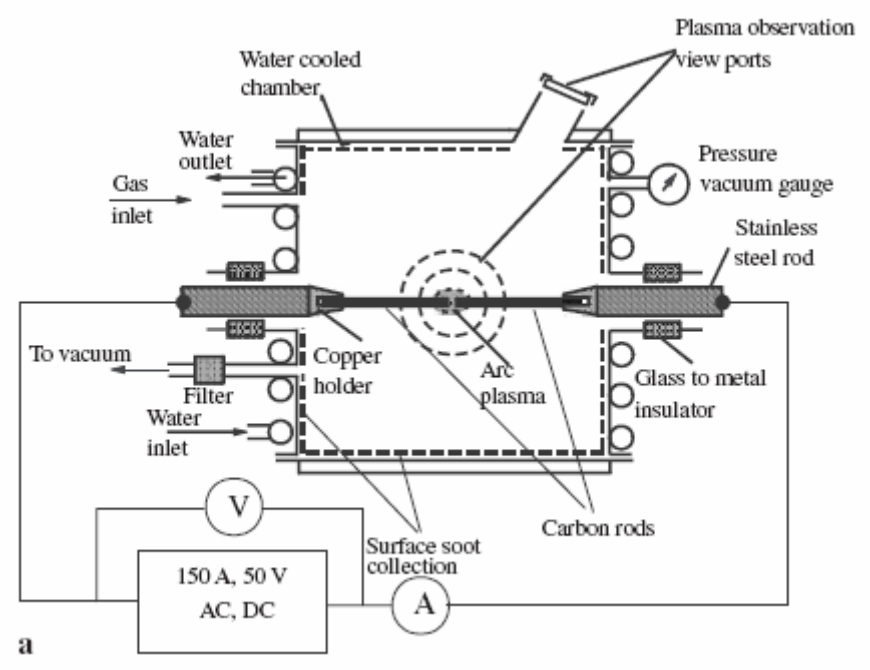

Figure 1.2: Arc discharge plasma experimental setup for production of CNTs [5]

The arc-discharge method for the preparation of carbon nanotubes is similar to that used for the synthesis of fullerenes (Figure 1.2). Iijima [2], Ebbesen and Ajayan [6] have used this process for the large-scale synthesis of nanotubes. An inert gas atmosphere (typically helium) is passed through a reaction vessel at a controlled pressure. Two graphite rods constitute the electrodes between which a potential difference is applied. As the rods are brought closer together, a discharge occurs resulting in the formation of a plasma. A deposit which may contain CNTs under certain conditions forms on a negative electrode (cathode) while a positive electrode (anode) is consumed. In the situation whereby a metal catalyst is used, a hole is drilled into the carbon anode and it is filled with the mixture of metal and graphite powder. When a metal catalyst is used most nanotubes are

found in the soot deposited on the arc-chamber wall [7]. Typically the outer diameter of the CNTs synthesised by the arc-discharge method range between 2 and 20 nm, while the inner diameters ranges between 1 and 3 nm [8]. The length of the nanotubes is micrometric. The obtained materials from the arc-discharge method consist of a mixture of nanotubes, nanofibers, nanoparticles and amorphous carbon.

In 1990, Krätschmer et al. [9] discovered CNTs as a by product in an arc-discharge method used in the synthesis of fullerenes. A medium pressure (500 Torr) helium-arc plasma was found to favour the efficient formation of MWCNTs. Arc co-evaporation of carbon and catalyst metal resulted in the formation of SWCNTs, usually found in the soot material. A higher density of SWCNTs was observed for binary catalysts than that with one metal alone [10]. Synthesis of SWCNTs by the hydrogen arc discharge method with a mixture of 2.6 % Ni, 0.7 % Fe, 0.7 % Co and 0.75 % FeS yielded more than 1.0 g of nanotubes per hour [11]. Sun et al. [12] used an anode filled with a mixture of Co metal powder and the inner black core of a cathode deposit to synthesise narrow MWCNTs with a diameter of the innermost nanotubes being ~ 0.5 nm.

Iijima and Ichihashi [13] have reported on the preparation of SWCNTs by co-vaporizing graphite and Fe in an Ar-CH_4 atmosphere. The CNTs produced had diameters in the 0.7-1.6 nm range and they often formed bundles. In this study, it was observed that no nanotubes were formed when the carbon arc reactor was operated in the absence of Ar, CH_4 and Fe components. Bethune et al. [14] have reported that co-vaporizing carbon and Co in an arc generator under a He atmosphere leads to the formation of SWCNTs of very small diameter (*ca* 1.2 nm). Zhou et al. [15] have also reported the observation of non-concentric carbon nanotube growth during the arc-discharge evaporation process when no catalyst was used.

1.2.2 Laser vaporization technique

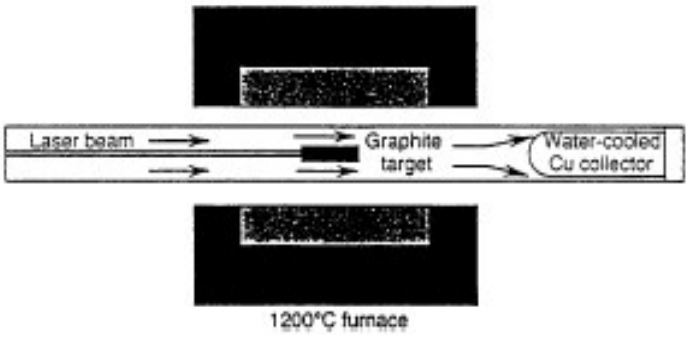

Figure 1.3: Schematic representation of the oven-laser vaporization apparatus [16]

In the laser vaporization method (Figure 1.3) CNTs are produced using a uniform laser vaporization of a graphite target. Historically, laser ablation was the first method to produce fullerene nanostructures in the gas phase [17]. In early experiments, only MWCNTs were produced from a pure graphite target [16, 18], but a high yield of CNTs was obtained at 1200 °C with graphite/bi-metal targets, such as Co/Ni [19] or Rh/Pd [20]. Zhang and Iijima [21] showed that a lower laser induced temperature (400 °C) could be used if purified C_{60} polycrystalline powder (pressed with Co/Ni powder as the catalyst) was used as the target material instead of graphite. In contrast to the arc discharge method, direct vaporization allows far greater control over their growth condition. It also allows continuous operation and produces nanotubes in higher yield (70-90%) as well as nanotubes of good quality. It was found that the SWCNTs synthesized by this method are arranged in bundles (called ropes), with similar spacing between the nanotubes [22]. Various mono- and bimetallic catalysts were also investigated as catalysts and it was found that Ni produced the highest CNT yield followed by Co. The bimetallic catalysts yielded SWCNTs with no formation of MWCNTs.

1.2.3 Catalysis methods

These methods involve the passage of a flow of gas containing a hydrocarbon (usually CH_4, C_2H_2, C_2H_4 and C_6H_6, usually as a mixture with H_2) or CO over small transition metal particles. Parameters such as temperature, time, gas composition, flow rate, catalyst nature and catalyst size affect the nature of the carbon species formed in the resulting material. These methods include the chemical vapour deposition method and the injection/floating catalyst method. Both methods are discussed in the sections below.

1.2.3.1 Catalytic chemical vapour deposition (CCVD) technique

The CCVD method is an efficient technique which can be used to scale up the production of CNTs and is the most widely used method for nanotube synthesis. The formation of carbon filaments and fibers from CCVD of carbon bearing reactants over different substrates has been known for a long time [23]. However CNTs {formed along with carbon nanofibers (CNFs)} were first synthesized by the catalytic decomposition of benzene vapours over iron catalyst at 1100 °C in 1988 by Endo [23d]. Since then hundreds of experiments have been performed to produce SWCNTs and MWCNTs over supported catalysts or with floating catalysts [5, 24]. The nanotube diameter can be controlled by varying the size of the active particles on the surface of the catalyst (usually the supported transition metals Fe, Co and Ni or their binary mixtures). The produced nanotubes can adopt different shapes and often have a carbon amorphous coating and catalyst particles embedded within their structure. The nanotubes grow from various catalyst impregnated substrates in the temperature range of 500-1200 °C. The resulting deposit may contain SWCNTs or MWCNTs with various diameter ranges and the nanotubes are usually arranged in bundles smaller than 100 nm in diameter that may be up to 100 μm long. Pan et al. [25] has reported on CCVD production of very long MWCNTs that reach about 2 mm in length, which is an order of magnitude longer than that described in most other reports.

The most popular CCVD method for the production of carbon nanofibers and nanotubes uses a horizontal furnace [23d, 26]. The horizontal furnace consists of a heated quartz tube in which the substrates/catalysts are placed (Figure 1.4).

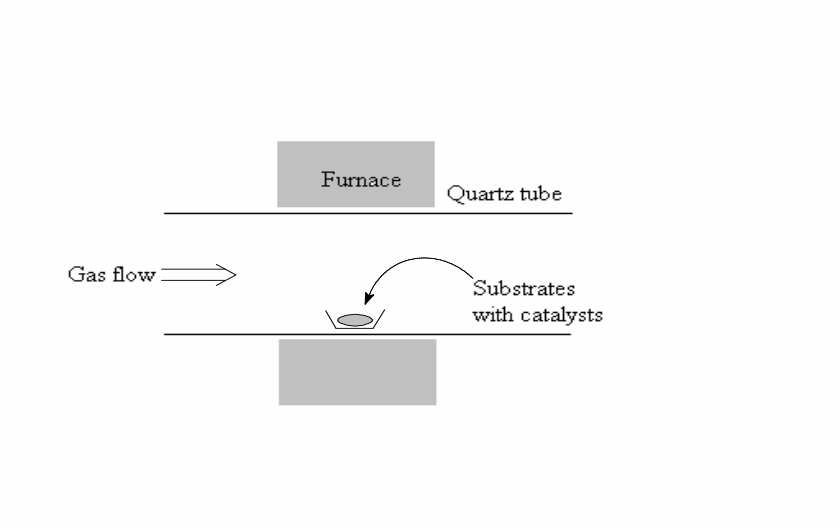

Figure 1.4: The horizontal furnace used for the catalytic CVD of nanofibers and nanotubes

The reactant gases flow over the substrates/catalysts which are placed in a removable ceramic boat/holder in the centre of the quartz tube. The horizontal furnace is advantageous because there is no temperature gradient within the heated zone. In most cases, the length of the CNTs/CNFs produced can simply be controlled by the length of the deposition time. The quartz tube reactor is first flushed with a carrier gas before the reaction starts. The most popular carrier gases are argon, hydrogen, and nitrogen [23d, 27]. The most commonly used carrier gas is argon since it can easily displace air and therefore forms an inert atmosphere in the chamber. The furnace is then heated up to the required growth temperature in the inert atmosphere. Hydrogen is often added to the gas flow to reduce the catalyst particles during heating and when the growth temperature is reached, the carbon feedstock is introduced. The reactions are usually conducted at a temperature below 1000 °C to minimize the formation of undesirable carbon deposits such as amorphous carbon [28] and graphite.

The amorphous carbon is formed by thermal decomposition (pyrolysis) of the carbon feedstock gas, whereas the CNTs/CNFs are produced from the catalytic decomposition of the carbon feedstock gas. The growth temperature affects the crystallinity of the structure produced, and a higher temperature leads to the formation of amorphous carbon. The formation of amorphous carbon can be reduced by decreasing contact time between the carbon feedstock and the substrates. This is achieved by using very high flow rates (in cases whereby only a carbon feedstock is used) or high dilution [29]. Normally there is an optimum ratio of carbon feedstock to carrier gas. For example, when using acetylene and nitrogen, the optimized combination was 9% by volume of the total gas flow [29a]. When the acetylene ratio was increased, amorphous carbon began to form due to the self-pyrolysis of the carbon feedstock and increased exposure of the sample to the carbon feedstock [29a]. A small amount of hydrogen in the gas flow is useful in keeping the catalyst particle active (reduced) and hydrogen also helps in reducing the formation of undesirable carbon deposits [30]. This is because hydrogen rehydrogenates the reactive carbon species in the gas phase.

Laser ablation and arc discharge methods do not permit easy control over the structure of SWCNTs during growth because of the high growth temperatures required when compared to the CVD method. In the CVD method, catalytic metal particles have a tendency to aggregate with each other at high temperature. Therefore, this results in a serious draw back in growing the SWCNTs with a uniformly distributed diameter.

In addition to the catalytic CVD method, various other CVD methods have been developed, including plasma enhanced CVD (PECVD), hot filament enhanced CVD (HFCVD) and hot wire chemical vapour deposition (HWCVD). The HFCVD method is a conventional method for depositing diamond films from a mixture of hydrocarbons and hydrogen [31]. In this technique, the filament which is typically placed near the substrate, acts as a thermal source for decomposing the gas, and often serves to heat the substrate as well. Compared to the common CVD method, the PECVD method is advantageous for the direct growth of CNTs films on the substrates at a low temperature due to the presence of a uniform plasma [32]. PECVD is the practical large area, low temperature, high throughput fabrication method for making thin film transistors in liquid crystal

displays. As a result, PECVD could be extensively used to fabricate the large area CNTs films that are suitable for field emission displays.

In the sub-sections below, the synthesis of various carbon nanostructures reported in the literature which are grown from various transition metal-supported catalysts in the presence of different carbon source is reviewed.

Synthesis of single-wall carbon nanotubes (SWCNTs) and double-wall carbon nanotubes (DWCNTs)

Many researchers have reported on the use of the horizontal CVD method to produce different carbonaceous materials using a variety of metals and supports. SWCNTs can be synthesized using metals supported on oxides such as SiO_2, Al_2O_3 , MgO [33] and La_2O_3 [34], where the metals adhere onto oxide surfaces, thus suppressing the aggregation of catalysts. Colomer et al. have reported that large scale synthesis of SWCNTs was achieved over Co, Ni, Fe and a binary mixture Co-Fe supported on MgO particles [33b]. They reported that 1g/day of SWCNTs was produced by this CVD method. The growth of SWCNTs with a narrow diameter distribution was produced over a Ni-MgO catalyst, when a mixture of acetylene and hydrogen gases were used [35]. Synthesis of SWCNTs has also been obtained when the catalysts; Fe, Ni and Co supported on spinel oxides using hydrogen and methane gas, were used [36].

SWCNTs with few defects, containing a very small amount of amorphous carbon coating, have been produced by the catalytic decomposition of C_2H_2 over a Fe-Mo bimetallic MgO supported catalyst [37]. Similarly, SWCNTs were also produced by the catalytic decomposition of ethylene over a Fe-Mo/MgO catalyst [38]. Kong et al. reported on the growth of SWCNTs by chemical vapour decomposition of methane over a supported transition metal oxide catalysts [39]. The catalyst support was found to play a crucial role in controlling formation of individual or bundled SWCNTs. Catalysts supported on crystalline alumina nanoparticles produced abundant individual small bundles and SWCNTs, while catalysts supported on amorphous silica particles produced only SWCNTs bundles. The decomposition of methane has been shown to be a crucial

step in the production of SWCNTs and DWCNTs over Fe, Co and Ni/MgO supported catalysts [40]. It was shown from the studies that the methane decomposition occurs on metal nanoparticles, and that the catalytic activity increased depending on the metal used in the order: Fe-Mo> Fe> Co> Ni. It was found that Mo increased the initial methane conversion and also prevented the rapid deactivation of the catalyst. The influence of the reaction atmosphere on the CVD growth of SWCNTs using Fe/MgO or Fe-Mo/MgO supported catalysts was investigated by comparing the different carbon deposits produced from methane decomposition in argon and nitrogen [41]. In an argon atmosphere, SWCNTs were synthesized on Fe/MgO and Fe-Mo/MgO catalysts, while in a nitrogen atmosphere the growth of the N-doped CNFs was obtained with a Fe/MgO catalyst. The growth of SWCNTs by decomposition of ethanol over Fe-Mo/Mgo supported catalyst using a fluidized bed has recently been reported [42]. Low temperature synthesis of high quality SWCNTs through microwave PECVD was demonstrated by the catalytic decomposition of methane over Fe-Mo bimetallic catalyst nanoparticles supported on porous MgO powders [43].

SWCNTs were grown by catalytic decomposition of both carbon monoxide and ethylene using Fe and Fe-Mo/Al_2O_3 supported catalysts [44]. The Fe and Mo catalysts were co-sputtered or sputtered separately onto an Al layer, which was pre-coated onto a SiO_2 substrate. It has been reported that highly graphitized SWCNTs could be synthesized by either co-sputtered or sputtered methods with the co-sputtering method producing highly graphitized CNTs [45]. SWCNTs and DWCNTs were simultaneously synthesized by catalytic decomposition of methane over a Fe-Mo/Al_2O_3 catalyst [46]. It was observed from HRTEM that the produced carbon materials consisted of about 70% SWCNTs and about 30% DWCNTs. A systematic investigation into the growth of SWCNTs on thin metallic films deposited on various substrates has been reported [47]. It was found from this study that aluminium-iron-molybdenum multi-layer thin films were deposited on the various substrates to determine which substrates promote the growth of SWCNTs over MWCNTs during the decomposition of methane gas. SWCNTs were synthesized by decomposition of methane over Fe_2O_3/Al_2O_3 and FeMo/Al_2O_3 supported catalysts using vertical CVD method [48]. Preparation of SWCNTs by a CVD method using a novel

aerogel supported Fe/Mo catalyst has also been reported by Su et al. [49]. A family of Co-Mo/SiO_2 supported catalysts has been found to be able to produce SWCNTs by catalytic decomposition of CO, with high selectivity depending on the Co:Mo ratio, the reaction temperature and the processing time [50]. The total weight of the nanotubes produced was found to be more than 200% the weight of the catalyst used. SWCNTs have been synthesized by CO disproportionation on Co:Mo/SiO_2 catalysts and high selectivity of SWCNTs was obtained when most of the Co in the sample was interacting with Mo, forming cobalt-molybdate surface layer [51]. Synthesis of SWCNTs on a Si substrate has been reported from an acetylene and hydrogen mixture by a HFCVD method using a carbon filament [52]. The catalyst used was silica supported Fe-Co, which was prepared by the sol gel method. A dendrimer-based Co_{32} nanocluster molecule was synthesized and then deposited on a SiO_2 support in an attempt to achieve diameter controlled growth of SWCNTs [53]. A synergistic effect between Co and Mo over a SiO_2 support using CO decomposition to produce CNTs has been studied by Alvarez et al. [54]. They observed exclusively SWCNT growth when both metals were used simultaneously but when used separately the metals were either inactive (Mo alone) or unselective (Co alone). A high purity and low temperature synthesis of SWCNTs from zeolite supported catalysts has been reported by Maruyama et al. [55]. They have reported the SWCNTs could be obtained by using alcohol as a carbon source and Fe/Co catalysts supported on a Y-type zeolite. Hiraoka et al. have reported the synthesis of double walled carbon nanotubes (DWCNTs) in high yield (80%) by the catalytic vapour deposition of acetylene over well dispersed metal particles (typically a Co/Fe binary system) embedded in a heat resistant zeolite (TS-1(Si/Ti = 50) at elevated temperatures [56]. The growth of SWCNTs over the natural minerals, magnesite and brucite, by pyrolysis of methane gas in the presence of Fe as a catalyst has been reported [57]. Okazaki et al. have prepared SWCNTs by HFCVD using alcohol vapour (ethanol, methanol, and 2-propanol) as a carbon source and Fe/Co Y-zeolite supported catalysts [58].

Synthesis of Multi-wall carbon nanotubes (MWCNTs)

Iron/molybdenum/magnesium mixed oxides prepared by the sol-gel method showed a high efficiency for the synthesis of MWCNTs from the catalytic decomposition of methane [59]. Ni-Y/Mo catalyst supported on MgO was found to be adequate for the mass production of MWCNTs by the CVD process [60]. Molybdenum acted as a promoter or activator while yttrium was inactive for the CVD production of CNTs but had a positive effect on the yield and morphology of the tubes when used in combination with nickel. MWCNTs formed in large amounts through low temperature decomposition of acetylene over Co/MgO catalyst have been studied [61]. It was observed that the yield of the nanotubes, the wall thickness and diameter of the tubes were influenced by the catalyst loading. Mauron et al. have reported CNT synthesis by a fluidized-bed CVD method using iso-pentane or acetylene as a carrier gas and $Fe(NO_3)_3.9H_2O/MgO$ as a catalyst [62]. MWCNTs and SWCNTs were observed with both iso-pentane and acetylene as carrier gases respectively at various temperatures.

The influence of several synthesis parameters on the growth of CNTs using the cobalt-catalyzed decomposition of ethanol on porous alumina substrates have been investigated by Zheng et al. [63]. CNTs produced by CCVD can be formed into loose agglomerates that can be fluidized during the growth process [64]. This method provides a way to synthesize high quality CNTs on a large scale at low cost in a nano-agglomerate fluidized-bed reactor using Fe/Al_2O_3 as a catalyst and high yields of 70-80% MWCNTs with a high production rate of 50 kg/day were obtained. Large amounts of amorphous CNTs fabricated by low temperature have been prepared with Ni/Al_2O_3 as catalyst in hydrogen gas atmosphere with methane as a carbon source [65]. Ordered, straight and hollow MWCNTs with high nanotexture were grown over an anodic titanium oxide template by the CVD method using acetylene as carbon source in the absence of a catalyst [66]. It was reported that the catalytic activity of Lewis acid sites inside the pores of titanium oxide is strong enough to catalyse the decomposition of acetylene, leading to the formation of CNTs. Growth of MWCNTs with junctions (Y, T, L) produced over Fe/Al substrate in an atmosphere of nitrogen using acetylene as a carbon source has been studied [67]. It was found that the formation of these junction CNTs was influenced by

temperature, excess carbon source and the Al substrate. Vertically aligned MWCNTs were grown by pyrolysing iron phthalocyanine (FePc), cobalt phthalocyanine (CoPc) and nickel phthalocyanine (NiPc) supported on silicon oxide substrates under Ar/H_2 atmosphere [68]. Aligned and curly MWCNTs have been synthesized from Fe/Al supported catalyst using mixtures of acetylene and ammonia under different reaction conditions [69]. Bamboo-shaped MWCNTs and herringbone nanofibers have been catalytically synthesized by decomposition of methane over Ni/Al catalysts under N_2 at low temperatures [70]. The CVD method was also used to grow well aligned MWCNTs on an anodic aluminium oxide template (AAO) with Co as catalyst and acetylene as carbon source [71]. Large scale aligned MWCNTs and MWCNTs bundles have been synthesized on smooth silica and rough polycrystalline ceramic substrates by pyrolysis of ferrocene/melamine mixtures under an argon atmosphere [72]. Aligned Fe-Co alloy-filled MWCNTs were synthesized on silica substrates by pyrolysis of a ferrocene/cobaltocene mixture under an Ar/H_2 atmosphere [73].

Catalytic CVD of hydrocarbons over metal supported zeolites is a widely used method for forming CNTs. It has been reported in the literature that a high yield synthesis of quasi aligned MWCNTs [74] can be obtained by pyrolysis of acetylene over well dispersed cobalt metal particles embedded in Y-type zeolites at low temperatures. MWCNTs have been formed at low temperature by a CVD method using Ni/Mo catalyst supported on Y-zeolite in the presence of acetylene [75]. Pyrolytic decomposition of acetylene on the surface of nickel, cobalt and iron containing ordered mesoporous MCM-41 silicas was investigated [76]. It was found that the iron and cobalt-based catalysts formed MWCNTs, while nickel-based catalyst formed carbon fibers. Mesoporous Co-MCM-41 molecular sieves with various Si/Co ratios were synthesized by direct incorporation of cobalt into the framework through hydrothermal method and then used as catalyst for the production of SWCNTs using acetylene as a carbon precursor [77]. Fe/SBA-15 mesoporous molecular sieves were prepared in acid solution from the sol-gel method and used to prepare MWCNTs by the decomposition of acetylene gas [78].

High purity MWCNTs were synthesized in the catalytic decomposition of acetylene over Fe, Co, or Fe-Co catalysts supported by $CaCO_3$ [79]. The preparation of MWCNTs by the CVD method using Co, Fe and Ni, as well as their bimetallic compounds supported on nanocrystalline $CaCO_3$ was investigated with acetylene as a carbon source [80]. It was found from the above study that nanocrystalline $CaCO_3$ is an improved support that can produce CNTs in high yield. MWCNTs were also synthesized in a catalytic reaction over an iron catalyst using $CaCO_3$ as a support and these nanotubes were used as supports for the Fischer –Tropsch reaction [81].

A simple spray coating method has been reported to be an efficient method for depositing a cobalt catalyst over quartz substrates that can be utilized in the production of CNTs by thermal CVD [82] using mixtures of ammonia and acetylene. It was found that aligned MWCNTs were achieved from this study.

Catalyst supports that can easily be removed with water have been investigated for CNT synthesis. High yields of MWCNTs have been synthesized by cobalt metal using water soluble $CaCl_2$ as a support in the catalytic CVD method [83]. Chlorides such as NaCl have also been used as a catalyst support in the presence of cobalt metal to prepare other forms of nanostructured carbon materials [84].

The hollow and bamboo-structured MWCNTs were grown by hot filament chemical vapour depososition (HFCVD) using nickel as a catalyst and different reaction gases with or without ammonia [85]. It was found that hollow CNTs formed when methane and hydrogen were used as reaction gases, while bamboo-structured CNTs were grown when ammonia was added into the reaction gases. MWCNTs have been prepared on Au/Ni films covered by a mask using the HFCVD method which uses methane and hydrogen as reaction gases [86]. The various thickness ratios of Ni and Au layers in Au/Ni films were deposited on Si substrates by a magnetic sputtering method. Acetylene was used as a carrier gas and carbon source while ammonia and hydrogen were used for either dilution or etching. Park et al. reported on the growth of carbon nanostructures such as a carbon nanoparticle (CNP), CNTs and CNFs by HFCVD using various catalysts [87]. It was

shown from the study above that aligned MWCNTs were synthesized using H_2-plasma treated Fe and Fe-impregnated silica or alumina as catalysts. The growth of coiled MWCNT films using the decomposition of acetylene-hydrogen mixture over an Fe catalyst in a PECVD system have been studied by Jiang et al. [88].

Synthesis of Carbon nanofibers (CNFs)

Carbon nanofibers (CNFs) i.e. tubular materials without an inner hollow cavity were initially investigated a long time ago by Baker [23a,c]. CNFs are readily synthesized at low temperatures by a catalytic method using an alumina supported nickel as catalyst and acetylene as carbon source [89]. It was found that the Ni/alumina catalyst exhibited a large catalytic effect on the growth of carbon nanofibers at low temperatures. A nickel-alumina catalyst prepared from a Feitknecht compound was used in the catalytic growth of carbon fibers from methane [90]. Carbon fibers with a diameter of approximately 1-2 μm were synthesized by thermal CVD with a mixture of nitrogen and acetylene on nickel-coated silicon substrates in a horizontal furnace [91]. CNFs were synthesized on sintered metal fibers filters of nickel and nickel containing alloys by thermal CVD of ethane in the presence of hydrogen at low temperature [92]. Carbon fibers with different shapes and lengths were synthesized by decomposition of methane over a Ni/Silica supported catalyst under argon atmosphere [93]. Micro-coiled CNFs have been prepared by a CVD method with nickel as catalyst and powders of metal carbides using mixtures of acetylene, argon and hydrogen [94]. Vertically aligned CNFs have been grown from low pressure, plasma-enhanced CVD process in a hydrogen atmosphere using nickel as a catalyst and acetylene as a carbon source [95].

Synthesis of Carbon spheres

Carbon spheres have been produced by catalytic processes, similar to those used to produce nanotubes or filaments, i.e., by catalytic decomposition of a hydrocarbon at high temperatures. Carbon spheres can be synthesized in large quantities by a CVD method using Kaolin supported transition metal salts (Fe, Co, Ni etc.) as catalysts [96]. Porous carbon spheres of macroscopic shape and pore structure have been synthesized using zeolite Beta beads as support by decomposition of propylene without any catalyst [97].

1.2.3.2 Unsupported/ Floating catalyst method

The CVD method is a seeded method that uses a supported catalyst, while in the floating catalyst method the catalyst is floating in the reactor. Many studies have been performed on the CVD formation of CNTs by using the floating catalyst method. The main advantage of this method is that removal of nanotubes from the substrate (as a support) and the preparation of the substrate are not required. Further, it is a continuous process and therefore could be used in industry to produce CNTs once reaction conditions have been optimized. The amount of catalytic metal particles exposed to the gas is much higher than that found using a substrate method.

All various one dimensional carbon materials, such as SWCNTs, DWCNTs, MWCNTs, carbon nanofibers (CNFs), as well as aligned CNTs have been synthesized by the floating catalyst method. In general there are two kinds of reactors that can be used for the floating catalyst method: the first one is the vertical reactor [98], in which the liquid carbon source and catalyst precursor are injected into the chamber from the top (or bottom) of the reactor in the presence of a carrier gas such as Ar. The carbonaceous products are collected at the bottom (or top) of the reactor. The second one is the horizontal reactor [99], in which liquid or gaseous reactants and the vapour of the catalyst are carried into the reaction chamber by carrier gases such as H_2 and/or Ar. The most commonly used reactor is the two-furnace reactor. In the first furnace, vaporization of catalyst precursor is maintained at a relatively low temperature (Figure 1.5). The fine catalytic particles are formed from the catalyst precursor and carried into the second furnace by the carrier gas. The synthesis of aligned CNT arrays are mostly produced in horizontal reactors while all the reported carbonaceous products produced in vertical reactors are randomly arranged (MWCNTs, CNFs including SWCNTs bundles). This method is commonly known to be used for the bulk production of CNTs/CNFs.

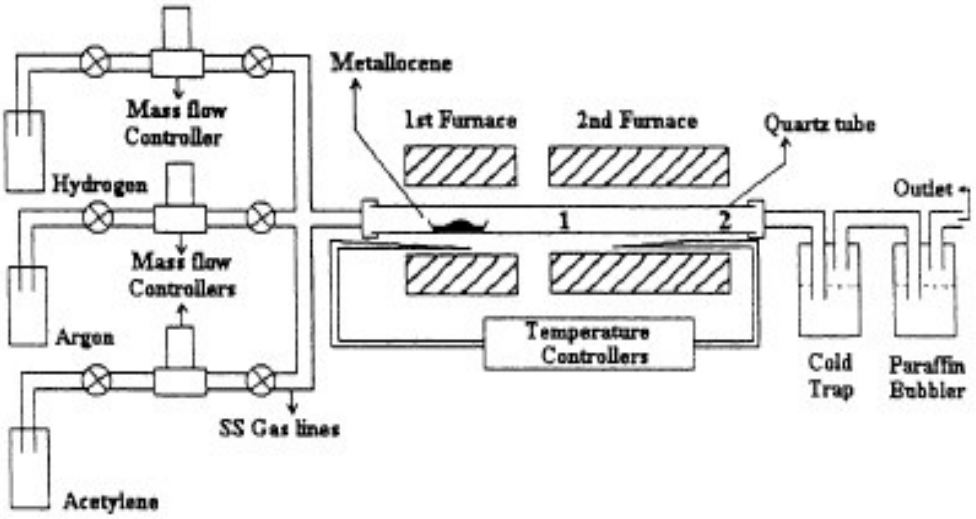

Figure 1.5: Schematic diagram of two-furnace horizontal reactor [100].

A double stage furnace is required because of the different temperatures needed for catalyst sublimation and CNT growth. Liquid precursors are introduced into the reactor as vapour obtained by bubbling a carrier gas (which can be either the carbon precursor or an additive gas such as hydrogen, nitrogen or argon) through the liquid [101]. Injectors have also been used to deliver liquid droplets directly to a hot reactor [102], while solid precursors are heated to their vaporization temperature and the vapour is transported to the furnace with the carrier gas [100]. Furthermore, spraying of a solution consisting of a catalyst and a solvent has been used to produce gas-phase catalyst particles [103]. Both the solvent and the catalyst vaporise in the first zone furnace and a carrier gas carries the vapours into the second zone, where the catalyst (typically an organometallic compound) decomposes to yield nanoparticles of the metal catalyst. Solvent and ligand molecules act as the carbon source for nanotube growth at the catalyst sites. Several metal-containing compounds such as chlorides, carbonyls, acetylacetones or metallocenes, have been applied as the catalyst precursors. The organometallic compounds that are commonly used are metallocenes (Fe, Co, Ni or Ru) [99, 104] and iron pentacarbonyl, [$Fe(CO)_5$] [105].

The vertical furnace has also been used for the production of CNTs and CNFs. This process, as shown in Figure 1.6, can be employed for the continuous production of carbon fibers and nanotubes [23d, 27d, 106].

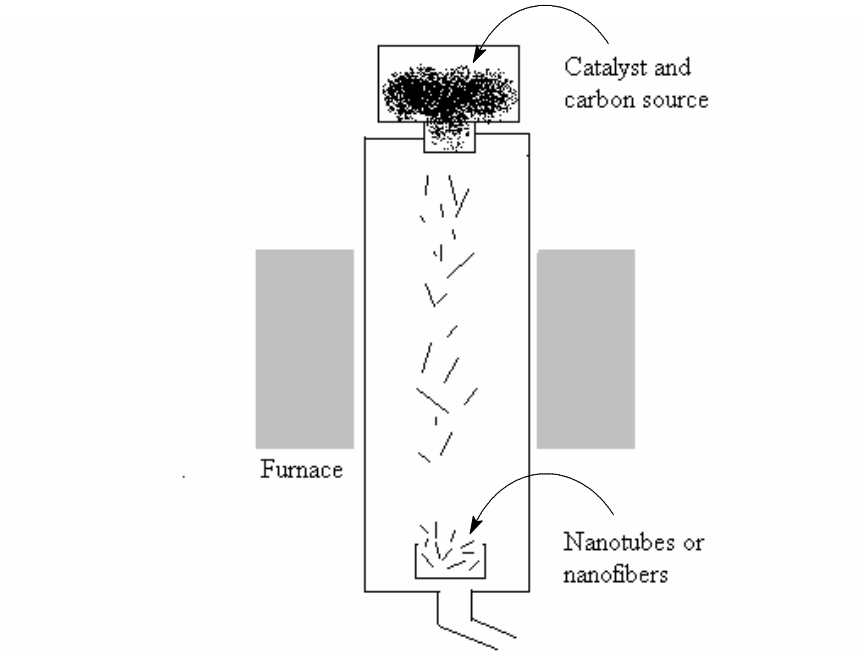

Figure 1.6: The vertical furnace used to synthesize CNTs and CNFs in CCVD method [24a]

The catalyst and catalyst source are injected into the reactor at the top of the furnace and the resultant filaments grow in the passage down the tube and are collected at the bottom of the chamber. The furnace can be run continuously for the mass production of CNTs and CNFs. The metal particles are either introduced into the reactor directly or formed in situ using precursors such as metallocenes. The residence time in the vertical furnace is short relative to the residence time in the horizontal furnace. The main advantage of a vertical furnace is that there is continuous production of CNTs/CNFs. A high purity product is formed, thus removing the need for the purification of the substrate. The vertical furnace technique has been used for the production of MWCNTs and CNFs in quantities of tons per year. Most of these materials are used as electrodes in lithium-ion batteries [107] and as fillers in conductive polymers [108].

In the sub-sections below we summarize the synthesis of various carbon nanostructures reported in the literature, grown from various unsupported-transition metal catalysts in the presence of different carbon source. This section shows that some carbon nanostructures could be formed without the presence of metal catalyst.

Synthesis of Single-wall carbon nanotubes (SWCNTs)

SWCNTs with rope like bundles, similar to those obtained by laser and arc techniques have been synthesized on a large scale and at a low cost by the catalytic decomposition of hydrocarbons (ferrocene and benzene) at high temperatures using the floating catalyst method using thiophene as a promoter [109]. SWCNTs without amorphous carbon have been prepared by thermally decomposing acetylene in a floating iron catalyst method at various temperatures, with the SWCNT growth rate limiting step controlled by adjusting the acetylene partial pressure and the reaction temperature [110]. Pyrolytic synthesis of long strands of large diameter SWCNTs by thermolysis of ferrocene-alcohol solutions under an argon atmosphere have been reported by Lupo and co-workers [111]. The synthesis of SWCNTs with controlled tube diameter, by adjusting or setting the gas pressure of an alcohol-ferrocene system, has also been reported [112]. SWCNTs have grown among vertically aligned MWCNTs by the catalytic pyrolysis of ferrocene and xylene using MWCNTs as support [113]. Synthesis of long strands of ordered SWCNTs have been accomplished by catalytic CVD technique using a vertical furnace where n-hexane is catalytically pyrolyzed when sulphur-containing compound and hydrogen are added to the process [114]. SWCNTs with coiled ring shapes have been synthesized in high yield through a floating CVD method using ferrocene and small amount of sulphur as a catalyst and promoter respectively [115]. SWCNTs were synthesized by vertical gas phase method from toluene colloidal solutions of Co and Mo nanoparticles as carbon source and catalyst, in the presence small amount of thiophene [116].

The high pressure CO disproportionation (HiPCO) process is a technique for the catalytic production of CNTs in a continuous flow gas phase using CO as the carbon feedstock and $Fe(CO)_5$ as the iron-containing catalyst precursor at high pressures and temperatures [105]. CNTs are formed by flowing CO mixed with small amount of $Fe(CO)_5$ through a heated reactor. The size and distribution of the nanotubes can be roughly selected by controlling the pressure of CO. This process has been shown to form SWCNTs of high purity. A gas process of SWCNT formation based on thermal decomposition of $Fe(CO)_5$ or ferrocene in the presence of CO was investigated in ambient pressure laminar flow

reactors at wide temperature range [117]. Isolated SWCNTs were grown by disproportionation of CO at high temperatures catalyzed by molybdenum particles [118]. SWCNTs were prepared in a horizontal reactor system using coal gas as a carbon source and ferrocene as a catalyst [119].

Synthesis of double wall carbon nanotubes (DWCNTs)

DWCNTs consisting of two concentric cylindrical graphene layers have been attracting increasing attention [120], mostly due to their ability to promote insight into the interaction between graphene layers in MWCNTs. It appears that DWCNTs were first prepared by Hutchison et al. [120d] as a dominant product in the arc discharge method using catalyst mixtures of Ni, Co, Fe and S. The floating catalyst method has since been demonstrated to be the ideal way to grow DWCNTs in bulk quantities [121]. DWCNTs were prepared using a floating CVD by adding a small amount thiophene as a promoter to ferrocene (acting as a catalyst) and methane as a carbon source in hydrogen atmosphere [122]. DWCNTs have also been prepared by thermally decomposing ferrocene mixed with sulphur powder in mixed flows of argon and acetylene at elevated temperatures [121b]. Xie and co-workers reported on the synthesis of SWCNTs and DWCNTs using different catalysts by a floating catalyst CVD method [121a]. It was found from this study that DWCNTs could be mass produced by thermally decomposing acetylene at elevated temperatures, on a floating iron catalyst in the presence of sulphur powder, while SWCNTs without amorphous carbon were produced in the absence of sulphur powder. DWCNTs have been synthesized by pyrolyzing C_2H_2 on the sulphur promoted floating iron catalyst [123]. Long DWCNTs were synthesized in a production rate of 0.5 g/h by the catalytic CVD method using xylene as carbon feedstock, ferrocene as a catalyst and sulphur as a promoter [124].

Synthesis of multi-wall carbon nanotubes (MWCNTs)

It has been reported in the literature that solutions containing both the hydrocarbon source and the metal catalyst precursor can be injected into a furnace with a syringe and subsequently pyrolyzed, producing aligned CNTs. The synthesis of aligned MWCNTs on quartz substrates by injection of a ferrocene-toluene solution into a CVD furnace have

been reported by Singh et al. [104d]. In a similar manner, Mayne et al. [104e] have prepared high yields of aligned MWCNTs by pyrolysing homogenously dispersed aerosols generated from benzene/ferrocene solutions using Ar as a carrier gas. Aligned MWCNTs of high purity were synthesized through the catalytic decomposition of a ferrocene-xylene mixture in a quartz tube reactor using an injection method [99]. Aligned MWCNT arrays were synthesized in an Ar/H_2 atmosphere by injecting a solution of ferrocene dissolved in xylene into a reaction furnace with the assistance of cobalt powder [125]. Aligned MWCNT bundles have been obtained by the pyrolysis of ferrocene along with methane, acetylene or butane as carbon sources and the quality of alignment was affected by the hydrocarbon used along with ferrocene [126]. The study of the controlled growth of large areas of aligned MWCNTs arrays, from a ferrocene-benzene precursor, and of nanotube junctions from ferrocene-thiophene precursors without hydrogen addition have been reported [127]. A wide variety of transition metals in the form of metallocenes and chlorides, dissolved in either benzene or methanol, were used as potential growth catalysts [128]. It was observed that when iron, nickel and cobalt were used as catalysts, well aligned MWCNTs were produced. There was no formation of CNTs when Cr, Mn, Zn, Cd, Ti, Zr, La, Cu, V and Gd were used as catalysts. Kamalakaran et al. produced thick aligned MWCNT arrays by pyrolysing a jet sprayed solution of ferrocene and benzene in an argon atmosphere at relatively low temperatures [104a]. Vertically aligned MWCNTs were grown by pyrolyzing camphor with ferrocene in an argon atmosphere [129].

By varying the pressure, a MWCNT powder has been synthesized using the floating catalyst method using ferrocene as a catalyst precursor, xylene or cyclohexane as carbon feedstock, H_2 as a carrier gas and thiophene as a promoter [130]. Liu and co-workers reported on the synthesis of MWCNTs and carbon spheres from the thermal decomposition of $Fe(CO)_5$ and acetylene [131]. They have also studied the effect of ferrocene dissolved in toluene as carbon source and catalyst on MWCNTs formation [132]. The applicability of several liquid hydrocarbons and various metallocenes on CNT formation has been reported [133]. It was found from this study that pure MWCNTs could be grown by the injection CVD method using solutions of metallocenes (ferrocene,

cobaltocene, nickelocene and their mixtures) in a range of liquid hydrocarbons (benzene, toluene, xylene, cyclohexane, cyclohexanone, n-hexane, n-pentane, n-octane, and n-pentane). A maximum yield of MWCNTs was produced when a ferrocene-nickelocene catalyst mixture was used with xylene as a carbon source. Similarly, Smith and co-workers [134] synthesized MWCNTs in supercritical toluene using ferrocene, cobaltocene and nickelocene nanocrystals as catalysts. Cobaltocene was found to be the best catalyst in terms of both purity of the nanotubes and the conversion of toluene to nanotubes formed. MWCNTs with different diameters and structures were obtained by controlling the ferrocene and benzene mole ratio [109]. It was found that the diameters of CNTs increased with decreasing ferrocene/benzene molar ratio. MWCNTs with high purity have been synthesized by a floating catalyst technique using ferrocene as a catalyst precursor, ethanol as a carbon source and thiophene as a promoter [135]. Large scale synthesis of MWCNTs with uniform diameter distribution have been synthesized by a spray pyrolysis method during the decomposition of toluene and precursor catalyst of iron: $[(Pentyl)_4N]_3FeBr_3Cl_3$, which was prepared from an aqueous solution of $FeCl_3$ and $(pentyl)_4NBr$ [136]. The effect of feedstock and process conditions on the synthesis of high purity MWCNTs from aromatic hydrocarbons (benzene, toluene, xylene and trimethyl benzene) and ferrocene as the source of Fe catalyst has been investigated [137]. Among the four feedstocks used, toluene proved to be the most effective in terms of total carbon conversion and CNT yield.

The growth of MWCNTs has been achieved over a nano-MgNi alloy using the CVD method with the pyrolysis of CH_4 in the presence of hydrogen in the reaction stream [138]. Synthesis of magnetic iron carbide-oxide filled MWCNTs with well ordered carbon layers using coal gas as carbon source and ferrocene as a catalyst have been reported [139]. MWCNTs have been synthesized by employing a $Cr_{2-x}Fe_xO_3$ solid solution as a catalyst under a mixture of natural gas (NG) and hydrogen [140]. It was observed from this study that the catalyst performed better in H_2/NG than in Ar/NG atmospheres. MWCNTs have been formed from the decomposition of acetylene using a Ni-Pd co-catalyst [141]. The synthesis of large areas and dense CNTs were achieved by using Ni-Pd co-catalysts, while when only Ni was used, carbon clusters and carbon fibers

were formed. A mixture of MWCNTs and SWCNTs has been synthesized by the floating catalytic reaction using colloidal solutions of metal particles in a vertical flow reactor [142]. Co-Mo served as the catalyst and toluene as a carbon source.

Branched MWCNTs have been synthesized by a combination of a dense fluidized bed and the floating CVD method with CNTs serving as support, using propylene as a gas carrier and ferrocene as a catalyst [143]. The floating catalyst method has been shown to yield Y-junction MWCNTs using a vertical electric furnace with iron as a catalyst, hexane as a carbon source and a small amount of thiophene as promoter [144]. Pyrolysis of thiophene with Fe- or Ni-phthalocyanines or $Fe(CO)_5$ that yield MWCNTs with Y-junctions have been reported by Deepak et al. [145]. Y-junction MWCNTs have been produced in relatively large quantities by vapour phase pyrolysis of a mixture of cobaltocene or ferrocene with thiophene in a hydrogen atmosphere [146]. Dillon and co-workers have employed HWCVD for the continuous production of MWCNTs on thin nickel films using methane as a carbon source without any support [147].

Synthesis of Carbon nanofibers (CNFs)

Besides CNTs, CNFs are also made by floating CVD procedures. CNFs prepared by the floating catalyst method using catalysts floating in a vertical reactor have the advantage of providing higher yields because of continuous production. It was found that the addition of an optimal amount of sulphur can activate the catalysts and promote growth of CNFs [148].

Vapour grown carbon fibers (VGCFs) have been synthesized by floating method using ferrocene as catalyst and ammonia as co-catalyst in the presence of hydrogen sulphide [149]. VGCFs with high purity have been prepared from thermal cracking of deoiled asphalt with ferrocene as a catalyst by the CVD method in an argon atmosphere [150]. VGCFs with a maximum length of 2 cm and a diameter of a few micrometers have been fabricated by a conventional thermal deposition at high temperatures using ferric sulphate or ferrous sulphate as catalyst precursors, nitrogen as a carrier gas and benzene as the source of carbon [151]. Benzene and several light paraffins were used as the initial

carbon source for VGCF production to clarify which of the hydrocarbons contributes more to fiber growth [152]. It was found that benzene was the actual contributor to fiber growth relative to methane and ethylene. Long bundles of aligned CNFs up to several millimetres in length were prepared by pyrolysis of a mixture of acetylene and ferrocene in a vertically installed quartz tube reactor using a floating catalyst [153]. Microcoiled fibers were synthesized by nickel powder in the presence of acetylene and thiophene under nitrogen atmosphere [154]. Ci et al. reported on high productivity of CNFs by decomposition of benzene using ferrocene as a catalyst and thiophene as a sulphur additive [98]. Martin-Gullon et al. [155] studied the synthesis of CNFs by decomposition of xylene or natural gas in a vertical tube reactor at high temperatures using Fe and Ni catalysts in the presence of sulphur. Pure VGCFs have been synthesized by floating catalyst method in a horizontal reactor using benzene as a carbon source, ferrocene as a catalyst and hydrogen as a carrier gas [156]. Two dimensional arrays of aligned CNFs have been prepared by pyrolyzing mixtures of ferrocene and melamine at elevated temperatures under an argon atmosphere [157]. The synthesis of herringbone-stacked carbon fibers by the floating catalyst method using cobaltocene and ferrocene as catalyst precursors, acetylene as a carbon source and thiophene as a promoter, have been reported by Singh et al. [158]. Herringbone-type CNFs with very small diameters and a large hollow core were synthesized by the catalytic decomposition of methane in the presence of Fe catalyst and thiophene as a promoter [159].

Phosphorous has been reported in the literature for its promoting effect in the formation of CNFs. Ci et al. [160] reported on the growth of CNFs using benzene solution with ferrocene as a catalyst precursor and triphenyl phosphine as a phosphorous source. Good yields of vapour grown carbon fibers (VGCFs) have been achieved by the catalytic decomposition of methane over particles obtained from $Fe_3(CO)_{12}$ with addition of small amount of phosphorous to the substrate [161]. The presence of a small amount of phosphorous was found to have a positive effect on the yield of VGCFs, while increasing the amount of phosphorous had an inhibiting effect on the growth of carbon fibers. Coiled CNFs have been formed by pyrolysis of acetylene activated using Ni catalyst and

a small amount of sulphur and phosphorous [162]. Thiophene and phosphorous trichloride were used as a sulphur and phosphorous additive respectively.

Synthesis of Carbon Spheres

Carbon spheres have also been synthesised by the CVD method without the presence of a catalyst. The controlled growth of carbon spheres with relatively uniform diameters was synthesized by pyrolysis of toluene using floating CVD method [163]. The diameters of these spheres were tailored by simply controlling the composition of the carrier gas. The floating CVD method has been shown to be an efficient method for production of carbon spheres by direct pyrolysis of a diverse range of hydrocarbons including styrene, toluene, benzene, hexane, cyclohexane and ethene in the absence of a catalyst [164]. Rao et al. reported on mono dispersed nanospheres synthesized by pyrolysis of benzene in the absence of a metal catalyst [100a].

1.3 Synthesis of Nitrogen and Boron-doped CNTs

In the literature it is suggested that by introducing dopants or by creating heterojunctions between nanotubes, chemically and electronically more stable electronic devices may be realized [165]. It has been reported that the incorporation of nitrogen in CNTs results in the enhancement of the conductivity of CNTs and improvement of the transport and field emission properties of the CNTs, due to the electron donor ability of the nitrogen atom [166]. Various routes have evolved for the synthesis of the heteroatom-doped nanotubes including arc discharge [167], laser ablation [168], substitution [169], pyrolysis [170] and various CVD methods [171].

The routine method for the synthesis of CN_x nanotubes is the chemical vapour deposition method of nitrogen containing compounds. Most previous results using the CVD method showed that the vertically aligned CNTs were formed in nitrogen or ammonia gas environments, which reveals the key role of nitrogen in CNT growth. Ammonia or any volatile nitrogen-compounds containing organics are generally used as a nitrogen source. Large quatities of CNx nanotubes have been synthesized on a silicon substrate via CVD

by pyrolysis of ferrocene and melamine [172]. CNTs synthesized from above have two different sections, one made of carbon with an empty hollow cylinder structure, and the other made of carbon nitride with a bamboo-like structure. Yudasaka et al. used nickel phthalocyanine as a starting material to synthesize CN_x nanotubes by a CVD method at the growth temperature of 700 and 800°C [173]. CN_x nanotubes obtained by pyrolysis of acetonitrile over catalytic nanoparticles formed by the thermal decomposition of Co and Ni bimaleates were reported by Kudashov et al. [174]. Pyrolysis of polyvinyl pyrrolidone on an alumina membrane template has been reported to be effective for the synthesis of well-aligned CN_x nanotubes [175]. Jung at al. [176] reported that activated nitrogen can enhance CNT growth and they compared the deposition behaviour in an NH_3 atmosphere with a mixed atmosphere of H_2 and N_2 (atomic ratio of H/N = 3) as in NH_3. Vertically aligned CNTs were obtained in the NH_3 atmosphere, in which the activated nitrogen was generated by thermal decomposition of NH_3. In the mixed atmosphere, N_2 acted like an inert gas and only amorphous carbon was obtained with no formation of CNTs. Nitrogen-doped SWCNTs that agglomerate in bundles and form long strands were synthesized from the thermal decomposition of ferrocene/ethanol/benzylamine solutions in an argon atmosphere [177]. Carbon nanotubes doped with a range of nitrogen contents were prepared by floating CVD method using ferrocene, NH_3 and xylene or pyridine [178]. Aligned bamboo-shaped CN_x have been produced by the pyrolysis of $Fe(CO)_5$ and acetylene mixtures with ammonia used as the source of nitrogen [179].

The effect of boron nitride (B-N) [167c, 180] and boron carbide nitrides (B-C-N) dopants [181] on carbon nanotubes heterojunctions have been discussed in various studies. The presence of the boron atom has been reported to increase the conductivity of CNTs and the graphitization of CNTs [182]. Boron containing nanotubes are predicted to behave as semiconductors over a large range of diameters and chiralities [182]. Terrones et al. [167a] have pyrolyzed the precursor addition compound, $CH_3CN.BCl_3$ in the temperature range of 900-1000°C over Co powder to produce graphitic boron nitride carbon nanotubes and carbon nanofibers. B-C-N, C-N and B-N nanotubes have been prepared by pyrolysis of pyridine over a Co catalyst at 1000°C in an argon atmosphere [170b]. B-N

nanotubes have been synthesized by heating boric acid, activated carbon, MWCNTs and catalytic iron particles in the presence of NH_3 [183].

1.4 Catalysts used for CNT growth

In the above sections the growth of SWCNTs, DWCNTs and MWCNTs were reviewed. From the above it is apparent that the catalysts used have mainly been transition metals such as iron, cobalt, nickel and the bimetallic catalysts.

Nanosized transition metal particles, in metallic forms particularly iron, cobalt, molybdenum and nickel have been used to catalyze CNT formation. The most important property of the metals with regard to the CNT growth is their ability to catalytically decompose gaseous carbon-containing molecules. Many papers in the literature, have reported the growth of CNTs using iron based catalysts and it was found that both the growth of MWCNTs [27b, 29a, 101a, 105, 184] and SWCNTs [100, 101c, 185] were obtained from Fe. Most of the CNTs formed using nickel based catalysts are MWCNTs [29b, 186] with few reports on the synthesis of SWCNTs [27c, 33b, 187]. Cobalt based catalysts can produce MWCNTs [27a, 29b, 184e, 186c, 188] and SWCNTs [27c, 33b, 100, 189]. Besides the commonly used metals (Fe, Co and Ni) other metals such as Mo, Cu or metal mixtures (Fe-Ni, Fe-Mo, Fe-Co, Co-Ni and Co-Mo) have been used for CNT growth [26b, 27b, 27c, 28, 44, 49, 50, 54, 190]. Mixtures of transition metals have been shown to be more effective for CNT growth than single metals and the yield of CNTs have been observed to increase with the use of bimetallic catalysts e.g Co-Mo [54], Fe-Mo [191] and Fe-Co [36]. Iron-cobalt alloys have been shown to produce SWCNTs [55, 192], with iron-nickel forming mainly MWCNTs [193]. Dai et al. have produced SWCNTs from nickel-cobalt alloys [26b]. Several alloy catalysts reported by other authors mostly produced SWCNTs [27c, 33b, 39, 194]. Addition of molybdenum to iron and cobalt has been shown to improve the performance of the "classical" catalysts. When Mo metal is added to Fe or Co catalysts, generally SWCNTs are obtained in high yield [28, 44, 49, 50, 54, 190b] compared to when single metal catalyst is used [27c]. Using thermal CVD, Co and Fe catalysts generally tend to form hollow and graphitized

nanotubes, whereas Ni and Cu produced structures which were not as well as graphitized [29b]. It can be noted that different metal catalysts will have their optimum catalytic activity at different temperatures.

1.5 Carbon sources used for CNTs growth

From the previous summary of CNT synthesis some general comments can be made about the carbon source used to form CNTs. Different carbon sources have been reported in the literature and play a crucial role in CNT synthesis using the supported CVD method and unsupported/floating CVD method. It has been shown in the literature that pyrolysis of carbon-containing molecules over supported nanometer sized metal particles using CVD method can be a promising way to scale up the production of SWCNTs. It appears that almost any hydrocarbon that contains C-H, C-C, and C-O bonds will produce CNTs by bond cleavage reactions. In case of the injection method, metal-hydrocarbon solutions have been shown to yield a high quality of nanotubes as well as aligned nanotubes. The liquid hydrocarbon solution provides a high precursor concentration and a homogenous reaction environment with growth on dispersed catalyst particles. The hydrocarbons that have been reported include: xylene, benzene, toluene, hexane, pentane, heptane, octane and cyclohexane. Other carbon containing compounds that have been exclusively used include cyclohexanone, CO and ethanol. Amongst these hydrocarbons toluene [34, 137], xylene [99, 195] and benzene [104e, 109] are the most effective for the preparation of high quality CNTs.

1.6 Growth mechanisms of CNTs

In general, CNT growth requires catalyst nanoparticles (usually Fe, Co, or Ni), a carbon feedstock (e.g., hydrocarbon or CO) and heat. Research on the growth of CNTs has been primarily carried out using the following two methods. In the first approach, a growth process mechanism of CNT is investigated based on the morphological characteristics of CNTs obtained from an experiment. In the second approach, a molecular reaction dynamic principle is adopted to simulate the microscopic growth process of CNTs [23a].

The growth of CNTs involves a very complicated series of steps and many researchers have suggested different mechanistic models to interpret CNT growth with results dependant on the experimental methods used and observations made.

1.6.1 Growth stages of MWCNTs by floating catalyst method

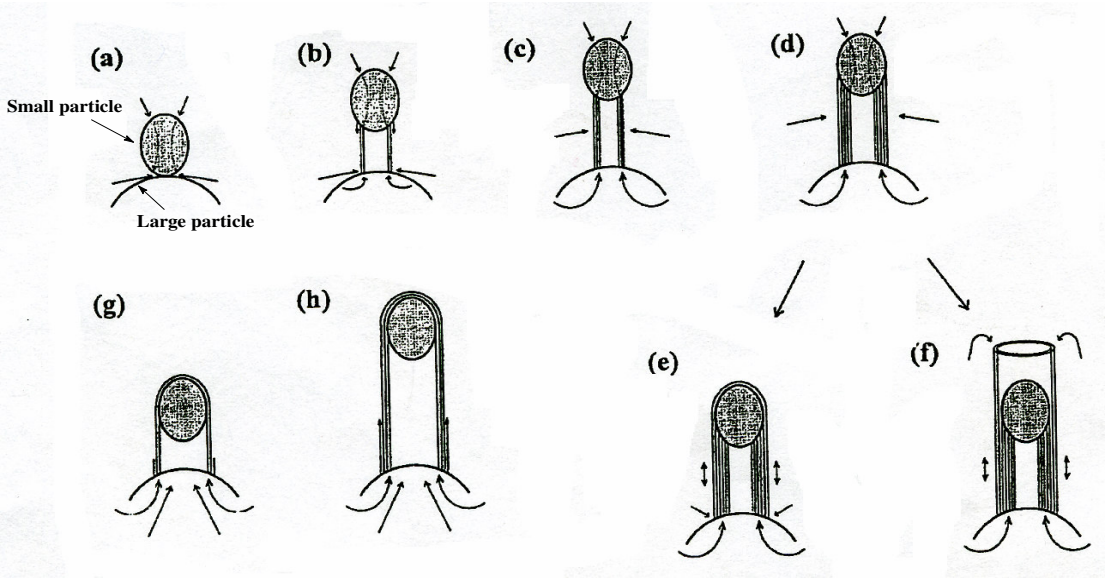

Figure 1.7: Schematic diagram of growth stages of MWCNTs by floating catalyst method [196].

According to Amelinckx et al., Figure 1.7 above illustrates the growth of MWCNTs by the floating catalyst method. A small metal particle rests on a larger metal particle that acts as a support (Figure 1.7a) and the small metal particle is lifted away from the support by the deposition of graphene sheets, formed from carbon diffusion through the catalyst and/or through the support (Figure 1.7b and 1.7c). The outer diameter of the tube increases in the process and eventually is found to be equal to the particle size (Figure 1.7d). This eventually causes the graphite layer to cover the small particle, which inhibits further growth. If the particle is already covered by a graphite sheet during the initial reaction stages (Figure 1.7g), further growth occurs by extrusion through the support and the diffusion occurs along the graphite surface (Figure 1.7h).

1.6.2 Growth stages of CNTs by CVD supported catalyst method

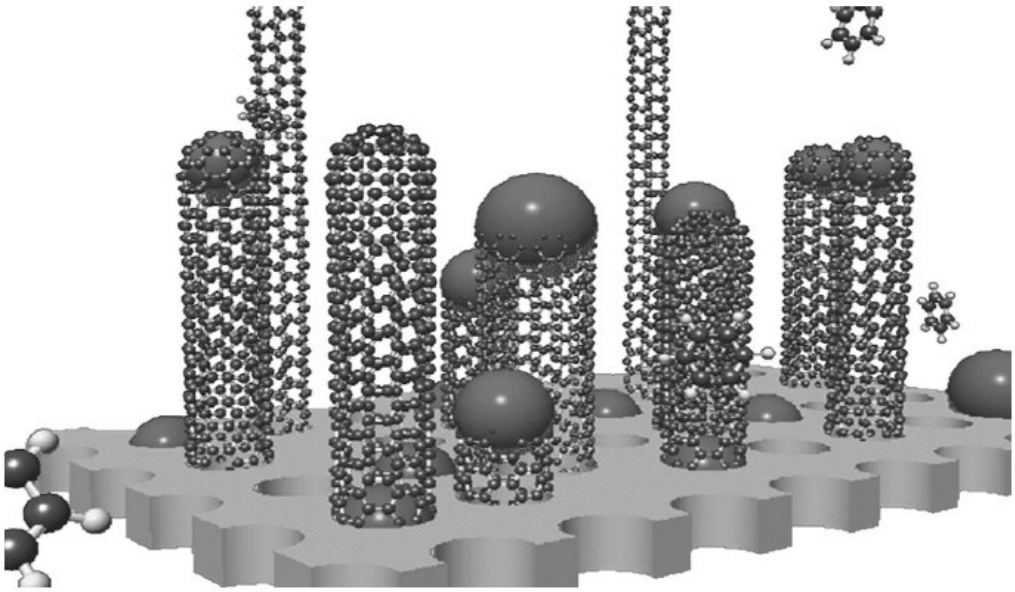

Figure 1.8: Growth mechanism of the tip growth and base growth nanotube models by supported CVD method [197]

Figure 1.8 is another representation of the process involved in CVD over supported catalyst and shows the two major mechanisms for the catalytic growth of CNTs depending on the position of the catalyst with respect to the substrate. The figure shows both the tip growth and base (root) growth mechanisms. The tip growth mechanism is one in which a catalyst particle is always located at the tip of the growing tube, and in the base growth mechanism, the catalytic particle is positioned at the bottom of the tube, fixed on the substrate [197]. It is believed that both the mechanisms occur simultaneously and they depend on the interaction of the catalytic particle with the surface. If the interaction is strong, base growth occurs and if the interaction is weak, then tip growth occurs.

1.7 Morphological and structural characterization of CNTs

In order to investigate the morphological and structural analysis of nanotubes, a number of techniques can be used. However, very few techniques are able to characterize CNTs at the atomic level. These techniques include, scanning electron microscopy (SEM), scanning tunnelling microscopy (STM) and transmission electron microscopy (TEM). X-ray photoelectron spectroscopy (XPS) is useful for determining the chemical structure of nanotubes, while neutron and X-ray diffraction (XRD), as well as infrared and Raman spectroscopy are mostly global characterization techniques. In this introduction, only four techniques (SEM, TEM, XRD and Raman spectroscopy) will be discussed briefly since they were the main characterization techniques used in this thesis study. These techniques have been discussed in more detail together with other techniques by Belin et al. [198].

1.7.1 Scanning electron microscopy (SEM)

SEM is one of the most widely used techniques used for characterizing nanostructures and nanomaterials. This method of characterization produces topographical information and provides chemical composition information for atoms near the surface. It does not show in detail the number of graphene layers (intershell spacing) in the tube but does show whether the CNTs are aligned or are randomly arranged.

1.7.2 Transmission electron microscopy (TEM)

TEM is useful in determining the quality of the CNT structure, the existence of amorphous material in and around the CNT structure and the type of contact between the support and the CNT. It also gives data on parameters such as length, diameter, the number of walls and the nature of the apex, i.e., whether the CNTs are open or closed. The advantages of TEM are the high magnification ranging from 50 to 10^6 and its ability to provide both image and diffraction information from a single sample. For example, the intershell spacing of MWCNTs were studied by Kaing et al. [199] using high resolution TEM (HRTEM) images and the intershell spacing was found to range from 0.34 to 0.39

nm values which are greater than the interplanar distance of graphite (0.336 nm). HRTEM-energy dispersive spectroscopy (EDS) is used to identify the composition of the material inside a CNT. For example, it can used to identify the nature of the metal particles encapsulated inside the tube.

1.7.3 X-ray diffraction (XRD)

XRD is a very important technique that has long been used to address all issues related to the crystal structure of solids. The intensity of the diffracted X-rays is measured as a function of the diffraction angle 2θ and the specimen's orientation. XRD is non-destructive and does not require sample preparation, which partly explains the wide usage of XRD to characterize materials. In the case of CNTs, it is used to obtain information on the CNT interlayer spacing, structural strain and the presence of impurities. Nanotubes posses multiple orientations compared to the X-ray incident beam and this leads to a statistical characterization of CNTs. The main feature of an XRD pattern of CNTs is the appearance of a peak similar to that of graphite (a peak at around 26.5° in 2θ). For MWCNTs, the peak can shift slightly, broaden or weaken compared to the graphite peak. This is due to the presence of different crystalline species. The mean diameter of CNTs can be calculated through the use of the Debye-Scherrer relation on the 26.5° 2θ peak.

1.7.4 Raman spectroscopy

This technique is one of the important tools used to analyse CNTs. Raman spectroscopy is very sensitive to the lengths, strengths and arrangements of chemical bonds in a material, but it is less sensitive to the chemical composition. Raman spectroscopy is more of a structural characterization technique than a chemical analysis. All allotropic forms of carbon (fullerenes, CNTs, amorphous carbon, polycrystalline carbon, etc) can be characterized by Raman spectroscopy. The position, width and relative intensity of the bands are modified according to the carbon forms. The most significant peaks have been summarised by Belin et al [198]. as follows: (a) low frequency peaks at about 200 cm^{-1}, which are characteristic of SWCNTs assigned to A_{1g} "breathing" mode of the tubes,

whose frequency depends on the diameter of the tube (RBM: radial breathing mode); (b) a large peak at 1340 cm^{-1}, assigned to residual ill-organized graphite (D-line: disorder); (c) a high frequency peaks between 1500 and 1600 cm^{-1} called the G band, which is also characteristic of CNTs. The G-line corresponds to the E_{2g} stretching mode of graphite [200]. (d) a second order mode between 2450 and 2650 cm^{-1} assigned to the first overtone of the D mode, often called the G' mode; (e) a combination mode of the D and G modes between 2775 and 2950 cm^{-1}.

1.8 Properties of CNTs

The discovery of CNTs has initiated numerous studies in order to understand their unique properties as well as to develop their future industrial applications [201]. Theoretical and experimental work has been focused on the relationship between the nanotube atomic structures and electronic structures, transport properties, electron-electron and electron-phonon interaction effects. An extensive effort has been made to investigate the mechanical, electronical, electrochemical properties and many other properties of CNTs. A brief summary of some of the properties is given below.

1.8.1 Electronic properties

Studies have shown that SWCNTs behave like pure quantum wires (1D-system) where the electrons are confined along the tube axis. The main scientific and technological interests in CNTs are the expected electronic properties which are directly related to the geometrical parameters (diameter and helicity) of CNTs [14]. SWCNTs exhibit both metallic and semi-conducting properties, depending on the diameter and the helicity, which is defined by the way in which the graphene sheet is rolled up [14] (armchair, zigzag or chiral). In particular, armchair SWCNTs are metallic while zigzag ones display semi-conductor behaviour. Tans et al. [202], Martel et al. [203] and Zhou et al. [204] carried out the measurements of individual semiconducting SWCNTs. The nanotubes exhibited transistor like behaviour at room temperature. Thus, their conductance can be changed dramatically (by orders of magnitude) by gate voltages. Electron transport from

metallic to metallic, metallic to semiconducting and semiconducting to semiconducting tubes was investigated [205].

Studies on the electronic properties of MWCNTs have revealed that they behave like an ultimate carbon fiber. Thus, at high temperature, their electrical conductivity may be described by semi-classical models already used for graphite, whereas at low temperature they reveal 2D-quantum transport features. A fine prediction of the electronic properties is even more difficult than in the case of SWCNTs due to two main factors: the rolling up of the graphene layers can vary along the different walls of a single MWCNT and the higher complexity of the structure will increase the possibility of the presence of defects. In MWCNTs, substitutional doping can be done to the lattice of the nanotubes. Studies have shown that the addition of boron and nitrogen in these structures create metallic features in the electronic density of states [206]. When SWCNT ropes were doped with alkali and halogen dopants, the dopants produced an order of magnitude increase in the electrical conductivity [206].

1.8.2 Mechanical properties

Nanotubes are made exclusively of covalently bonded carbon atoms (as in graphite). The strength of the carbon bonds in nanotubes makes them to be amongst the strongest and most resilient materials known to exist in nature. CNTs are very resistant with a Young modulus of the order of a tera-Pascal [207] and a resistance to traction of 250 GPa [208] which would be one hundred times higher than that displayed by steel but weighing six time less. It has been shown that CNTs are flexible and can be bent several times at 90° without undergoing structural changes. These values are theoretical and the presence of defects will reduce them, but their resistance will still be very high. The structure is not easily changed by pressure, and it has been demonstrated [209] that CNTs only undergo permanent structure changes at very high pressures (over 1.5 GPa) and below that value the deformations are totally elastic.

1.8.3 Adsorption properties

Different studies of the adsorption of nitrogen on MWCNTs [210] and SWCNTs [211] have shown that they have a porous nature. In MWCNTs, pores can be divided into inner hollow cavities of small diameter (mainly 3-6 nm) and aggregated pores (20-40 nm) formed by interaction of isolated MWCNTs, the latter being more important for adsorption. Acid-treated and as-prepared SWCNTs have been shown to have a microporous nature by N_2 adsorption which is opposite to the mesoporous nature of MWCNTs. The interaction of CNTs with gases or doping species adsorbed either on their internal or external surfaces of the CNTs attracts increasing attention due to the possible use of these materials for efficient gas storage. Adsorption by SWCNTs and MWCNTs bundles can occur either inside the tube or between the tubes.

1.8.4 Thermal Properties

Another important feature that has to be taken into consideration is the thermal stability of CNTs under different reaction conditions. The most common and simple way to study the resistance of the carbonaceous material towards temperature is thermogravimetric analysis (TGA). CNTs are more stable to oxidation than activated carbon but more reactive than graphite [212]. The studies conducted on CNT thermal behaviour have shown different behaviours for SWCNTs and MWCNTs. SWCNTs were found to be more stable than MWCNTs [213].

1.8.5 The catalytic properties of CNTs

Nhut et al. [214] studied the selectivity of CNTs and charcoal towards the C=C bond hydrogenation in α,β–unsaturated cinnamaldehyde. It was shown from this study that the CNTs exhibited an interesting behaviour towards selective carbon–carbon double bond hydrogenation as compared to that obtained from a commercial activated charcoal catalyst. The high selectivity obtained using a CNT-based catalyst was attributed to the complete absence of micropores and residual acidic sites in the support matrix.

1.8.6 CNTs as catalysts supports

Catalytic activity of a Rh/MWCNT catalyst for the hydrogenation of cinnamaldehyde to hydrocinnamaldehyde was found to be three times higher than the corresponding Rh/activated carbon (C*) reaction [215]. Selective dehydrogenation of cyclohexanol to cyclohexanone was studied with a Co/MWCNT and Co/C* based catalysts [216]. Co/MWCNT showed a slightly higher selectivity to cyclohexanone relative to Co/C*.
A series of studies have been reported by Vannice in the 1980s using organometallic iron complexes supported on graphitic carbon supports for the Fischer-Tropsch (FT) reaction [217]. Since these studies, very little work was reported in literature on the use of carbon supported metals in FT reaction. This is surprising since carbon supported iron catalysts have shown to give high selectivities to olefins in the FT reaction [218]. Recently, preliminary investigations into the use of CNTs as a carbon support for FT reactions [219] have been reported. The effect of catalyst promotion on the FT synthesis activity, stability and product selectivity of a series of Fe/CNT catalysts was reported by Bahome et al. [81] and the iron supported catalyst was found to be very stable and active.

1.9 References

[1] Tibbetts, G. G. *J. Cryst. Growth* **1984**, *66*, 632.

[2] Iijima, S. *Nature* **1991**, *354*, 56.

[3] Endo, M.; Hayashi, T.; Kim, Y. A.; Terrones, M.; Dresselhaus, M. S. *Phil Trans. R. Soc. Lond. A* **2004**, *362*, 2223.

[4] Dresselhaus, M. S. *J. Mater. Res*. **1998**, *13*, 2355.

[5] Huczko, A. *Appl. Phys. A* **2002**, *74*, 617.

[6] Ebessen, T. W.; Ajayan, P. M. *Nature* **1992**, *358*, 220.

[7] Kiang, C. H.; Goddard, W. A; Beyers, R.; Salem, J. R.; Bethune, D. *J. Phys. Chem. Solids* **1996**, *57*, 35.

[8] Ebbesen, T. W. *Annu. Rev. Mater. Sci*. **1994**, *24,* 235.

[9] Krätschmer, W.; Lamb, L. D.; Fostiropoulos, K.; Huffman, D. R. *Nature* **1990**, *347*, 354.

[10] (a) Botton, G. A.; Burnell, G.; Humphreys, C. J.; Yadav, T.; Withers, J. C. *J. Phys. Chem. Solids* **1997**, *58*, 1091. (b) Takizawa, M.; Bandow, S.; Torii, T.; Iijima, S.; Chem. *Phys. Lett.* **1999**, *302*, 146. (c) Shi, Z.; Lian, Y.; Liao, F. H.; Zhou, X.; Gu, Z.; Zhang, Y.; Iijima, S.; Li, H.; Yue, K.T.; Zhang, S. L.; *J. Phys. Chem. Solids* **2000**, *61*, 1031. (d) Sugai, T.; Omote, H.; Bandow, S.; Tanaka, N.; Shinohara, H. *J. Appl. Phys*. **1999**, *38*, L477.

[11] Liu, C.; Cong, H. T.; Li, F.; Tan, P. H.; Cheng, H. M.; Lu, K.; Zhou, B. L. *Carbon* **1999**, *37*, 1865.

[12] Sun, L. F.; Xie, S. S.; Liu, W.; Zhou, W. Y.; Liu, Z. Q.; Tang, D. S.; Wang, G.; Qian, L. X. *Nature* **2000**, *403*, 384.

[13] Iijima, S.; Ichihashi, T. *Nature* **1993**, *363*, 603.

[14] Bethune, D. S.; Kiang, C. H.; de Vries, M. S.; Gorman, G.; Savoy, R.; Vazquez, J.; Beyers, R. *Nature* **1993**, *363*, 605.

[15] Zhou, D.; Seraphin, S.; Wang, S. *Mater. Res. Soc. Symp. Proc.* **1994**, *349*, 257.

[16] Journet, C.; Bernier, P. *Appl. Phys. A* **1998**, *67*, 1.

[17] Kroto, H. W.; Heath, J. R.; O'Brien, S. C.; Curl, R. F.; Smalley, R. E. *Nature* **1985**, *318*, 162.

[18] Guo, T.; Nikolaev, P.; Rinzler, A. G.; Tomanek, D.; Colbert, D. T.; Smalley, R. E. *J Phys. Chem*. **1995**, *99*, 10964.

[19] (a) Guo, T.; Nikolaev, P.; Thess, A.; Colbert, D. T.; Smalley, R. E. *Chem. Phys. Lett*. **1995**, *243*, 49. (b) Rinzler, A. G.; Liu, J.; Dai, H.; Nikolaev, P.; Huffman, C. B.; Rodriguez-Macias, F. J.; Boul, P. J.; Lu, A. H.; Heymann, D.; Colbert, D. T.; Lee, R. S.; Fischer, J. E.; Rao, A. M.; Eklund, P. C.; Smalley, R. E. *Appl. Phys. A* **1998**, *67*, 29. (c) Yudasaka, M.; Komatsu, T.; Ichihashi, T.; Iijima, S. *Chem. Phys. Lett*. **1997**, *278*, 102. (d) Yudasaka, M.; Kokai, F.; Takahashi, K.; Yamada, R.; Sensui, N.; Ichihashi, T.; Iijima, S. *J. Phys. Chem. B* **1999**, *103*, 3576. (e) Yudasaka, M.; Ichihashi, T.; Komatsu, T.; Iijima, S. *Chem. Phys. Lett*. **1999**, *299*, 91. (f) Bandow, S.; Asaka, S.; Saito, Y.; Rao, A. M.; Grigorian, L.; Richter, E.; Eklund, P. C. *Phys. Rev. Lett.* **1998**, *80*, 3779.

[20] Kataura, H.; Kimura, A.; Ohtsuka, Y.; Suzuli, S.; Maniwa, Y. *J. Appl. Phys*. **1998**, *37*, L616.

[21] Zhang, Y.; Iijima, S.; *Appl. Phys. Lett*. **1999**, *75*, 3087.

[22] Guo, T.; Nikolaev, P.; Thess, A.; Colbert, D. T.; Smalley, R. E. *Chem. Phys. Lett.* **1996**, *260*, 471.

[23] (a) Baker, R. T. K.; Barber, P. S.; Harris, P. S.; Feates, F. S.; Waite, R. J. *J. Catal.* **1972**, *26*, 51. (b) Baker, R. T. K.; Harris, P. S.; Thomas, R. B.; Waite, R. F. *J. Catal.* **1973**, *30*, 86. (c) Baker, R. T. K. *Carbon* **1989**, *27*, 315. (d) Endo, M. *Chemtech* **1988**, *18*, 568. (e) Rodriguez, N. M.; Chambers, A.; Baker, R. T. K. *Langmuir* **1995**; *11*, 3862. (f) Gavillet, J.; Loiseau, A.; Journet, C.; Willaime, F.; Ducastelle, F.; Charlier, J. C. *Phys. Rev. Lett*. **2001**, *8727*, 275504.

[24] (a) Teo, K. B. K.; Singh, C.; Chhowalla, M.; Milne, W. I. *Encyclopedia of Nanoscience and Nanotechnology* **2003**, *X*, 1. (b) Dupuis, A. C. *Progress in Materials Science* **2005**, *50*, 929.

[25] Pan, S. S.; Xie, Z. W.; Chang, B. H.; Wang, C. Y.; Lu, L.; Liu, W.; Zhou, W. Y.; Li, W. Z.; Qian, L. X. *Nature* **1998**, *394*, 631.

[26] (a) Rodriguez, N. M. *J. Mater. Res*. **1993**, *8*, 3233. (b) Dai, H. J.; Rinzler, A. G.; Nikolaev, P.; Thess, A.; Colbert, D. T.; Smalley, R. E. *Chem. Phys. Lett*. **1996**, *260*, 471. (c) Joseyacaman, M.; Mikiyoshida, M.; Rendon, L.; Santiesteban, J. G. *Appl. Phys. Lett*. **1993**, *62*, 657.

[27] (a) Terrones, M.; Grobert, N.; Olivares, J.; Zhang, J. P.; Terrones, H.; Kordatos, K.; Hsu, W. K.; Hare, J. P.; Townsend, P. D.; Prassides, K.; Cheetham, A. K.; Kroto, H. W.; Walton, D. R. M. *Nature* **1997**, *388*, 52. (b) Kukovecz, A.; Konya, Z.; Nagaraju, N.; Willems, I.; Tamasi, A.; Fonseca, A.; Nagy, J. B.; Kiricsi, I. *Phys. Chem.* **2000**, *2*, 3071. (c) Colomer , J. F.; Bister, G.; Willems, I.; Konya, Z.; Fonseca, A.; Van Tendeloo, G.; Nagy, J. B. *Chem. Commun*. **1999**, *14*, 1343. (d) Zhu, H. W.; Xu, C. L.; Wu, D. H.; Wei, B. Q.; Vatjai, R.; Ajayan, P. M. *Science* **2002**, *296*, 884.

[28] Kong, J.; Soh, H. T.; Cassell, A. M.; Quate, C. F. Dai, H. J. *Nature* **1998**, *395*, 878.

[29] (a) Piedigrosso, P.; Konya, Z.; Colomer, J. F.; Fonseca, A.; Van Tendeloo, G.; Nagy, J. B. *Phys. Chem*. **2000**, *2*, 163. (b) Ivanov, V.; Nagy, J. B.; Lambin, P.; Lucas, A.; Zhang, X. B.; Zhang, X. F.; Bernaerts, D.; Van Tendeloo, G.; Amelinckx, S.; Van Landuyt, J. *Chem. Phys. Lett*. **1994**, *223*, 329. (c) Ivanov, V.; Fonseca, A.; Nagy, J. B.; Lucas, A.; Lambin, P.; Bernaerts, D.; Zhang, X. B. *Carbon* **1995**, *33*, 1727.

[30] (a) Nolan, P. E.; Lynch, D. C.; Cutler, A. H. *J. Phys. Chem. B* **1998**, *102*, 4165. (b) Gonser, U.; Mooradian, A.; Muller, K. A.; Panish, M. B.; Sakaki, H. *in Graphite Fibers and filaments, Springer-Verlag Berlin* **1988**, *5*, 382.

[31] Matsumoto, S.; Sato, Y.; Kamo, M.; Setaka, N.; *J. Appl. Phys*. **1982**, *21*, L183.

[32] Tsai, S. H.; Chao, C. W.; Lee, C. L.; Shih, H. C. *Appl. Phys. Lett*. **1999**, *74*, 3462.

[33] (a) Casell, A. M.; Raymakers, J. A.; Kong, J.; Dai, H. J.; *J. Phys. Chem. B* **1999**, *103*, 6484. (b) Colomer, J. F.; Stephan, C.; Lefrant, S.; Van Tendeloo, G.; Willems, I.; Konya, Z.; Fonseca, A.; Laurent, Ch.; Nagy, J.B. *Chem. Phys. Lett.* **2000**, *317*, 83.

[34] Liang, Q.; Gao, L. Z.; Li, Q.; Tang, S. H.; Liu, B. C.; Yu, Z. L. *Carbon* **2001**, *39*, 897.

[35] Jeong, H. J.; An, K. H.; Lim, S. C.; Park, M. S.; Chang, J. S.; Park, S. E.; Eum, S. J.; Yang, C. W.; Park, C. Y.; Lee, Y. H. *Chem. Phys. Lett.* **2003**, *380*, 263.

[36] Flahaut, E.; Govindaraj, A.; Peigney, A.; Laurent, Ch.; Rousset, A.; Rao, C. N. R. *Chem. Phys. Lett.* **1999**, *300*, 236.

[37] Liu, B. C.; Lyu, S. C.; Jung, S. I.; Kang, H. K.; Yang, C. W.; Park, J. W.; Park, C. Y.; Lee, C. J. *Chem. Phys. Lett.* **2004**, *383*, 104.

[38] Lyu, S. C.; Liu, B. C.; Lee, S. H.; Park, C. Y.; Kang, H. K.; Yang, C. W.; Lee, C. J. *J. Phys. Lett. B*. **2004**, *108*, 1613.

[39] Kong, J.; Cassell, A. M.; Dai, H. *Chem. Phys. Lett.* **1998**, *292*, 567.

[40] Ago, H.; Uehara, N.; Yoshihara, N.; Tsuji, M.; Yumura, M.; Tomonaga, N.; Setoguchi, T. *Carbon* **2006,** *44*, 2912.

[41] Yu, H.; Zhang, Q.; Zhang, Q.; Wang, Q.; Ning, G.; Luo, G.; Wei, F. *Carbon* **2006**, *44*, 1706.

[42] Liu, Q.X.; Fang, Y. *Spectrochimica Acta A* **2006,** *64,* 296.

[43] Wang, W. L.; Bai, X. D.; Xu, Z.; Liu, S.; Wang, E. G. *Chem. Phys. Lett*. **2006,** *419,* 81.

[44] Hafner, J. H.; Bronikowski, M. J.; Azamian, B. R.; Nikolaev, P.; Rinzler, A. G.; Colbert, D. T.; Smith, K. A.; Smalley, R. E. *Chem. Phys. Lett.* **1998,** *296*, 195.

[45] Chiu, C. C.; Chen, C. Y.; Tai, N. H.; Tsai, C. H. *Surface and Coatings Technology* **2006**, *200*, 3199.

[46] Liu, B. C.; Lyu, S. C.; Lee, T. J.; Choi, S. K.; Eum, S. J.; Yang, C. W.; Park, C. Y.; Lee, C. J. *Chem. Phys. Lett.* **2003**, *373*, 475.

[47] Ward, J. W.; Wei, B.Q.; Ajayan, P. M. *Chem. Phys. Lett*. **2003**, *376*, 717.

[48] Lamouroux, E.; Serp, P.; Kihn, Y.; Kalck, P. *Catal. Commun*. **2006**, *7*, 604

[49] Su, M.; Zheng, B.; Liu, J. *Chem. Phys. Lett*. **2000**, *322*, 321.

[50] Kitiyanan, B.; Alvarez, W.E.; Harwell, J.H.; Resasco, D.E. *Chem. Phys. Lett.* **2000**, *317*, 497.

[51] Herrera, J. E.; Balzano, L.; Borgna, A.; Alvarez, W. E.; Resasco, D. E. *J. Catal. 2001*, **204**, 129.

[52] Chaisitsak, S.; Yamada, A.; Konagai, M. *Diamond and related Materials* **2004**, *13*, 438.

[53] Geng, J.; Li, H.; Zhou, D.; Huck, W. T. S.; Johnson, B. F. G. *Polyhedron* **2006**, *25*, 585.

[54] Alvarez, W. E.; Kitiyanan, B.; Borgna, A.; Resasco, D. E. *Carbon* **2001,** *39,* 547.

[55] Maruyama, S.; Kojima, R.; Miyauchi, Y.; Chiashi, S.; Kohno, M. *Chem. Phys. Lett.* **2002**, *360,* 229.

[56] Hiraoka, T.; Kawakubo, T.; Kimura, J.; Taniguchi, R.; Okamoto, A.; Okazaki, T.; Sugai, T.; Ozeki, Y.; Yoshikawa, M.; Shinohara, H.; *Chem. Phys. Lett.,* **2003**, *382*, 679.

[57] Kawasaki, S.; Shinoda, M.; Shimada, T.; Okino, F.; Touhara, H. *Carbon* **2006**, *44,* 2139.

[58] Okazaki, T.; Shinohara, H. *Chem. Phys. Lett.* **2003**, *376*, 606.

[59] Xu, J.M.; Zhang, X.B.; Li, Y.; Tao, X.Y.; Chen, F.; Li, T.; Bao, Y.; Geise, H.J. *Diamond and related Materials* **2004**, *13*, 1807.

[60] Peréz-Mendoza, M.; Vallés, C.; Maser, W.K.; Martínez, M.T.; Langlois, S.; Sauvajol, J.L.; Benito, A.M. *Carbon* **2005**, *43*, 3002.

[61] Singh, B.K.; Ryu, H.; Chikate, R.C.; Hoa, N.D.; Park, S.J.; Kim, S.; Lee, J.R. *Solid State Commun.* **2006,** *139*, 102.

[62] Mauron, Ph.; Emmenegger, Ch.; Sudan, P.; Wenger, P.; Rentsch, S.; Züttel, A.; *Diamond and Related Materials* **2003**, *12*, 780.

[63] Zheng, L.; Liao, X.; Zhu, Y. T.; *Mater. Lett*., **2006**, *60*, 1968.

[64] Wang, Y.; Wei, F.; Luo, G.; Yu, H.; Gu, G. *Chem. Phys. Lett.* **2002**, *364*, 568.

[65] Zhao, N. Q.; He, C. N.; Du, X. W.; Shi, C. S.; Li, J. J.; Cui, L. *Carbon* **2006,** *44*, 1859.

[66] Eswaramoorthi, I.; Hwang, L. P. *Carbon* **2006**, *44*, 2330.

[67] Wang, S. D.; Chen, W. L.; Chang, M. H.; Chueh, Y. L. *J. Cryst. Growth* **2006**, *291,* 218.

[68] Kim, N. S.; Lee, Y. T.; Park, J.; Han, J. B.; Chi, Y. S.; Choi, S.Y.; Choo, J.; Lee, G.H. *J. Phys. Chem. B* **2003**, *107*, 9249.

[69] Terrado, E.; Redrado, M.; Munoz, E.; Maser, W. K.; Benito, A. M.; Martinez, M. T. *Diamond and Related Materials* **2006**, *15*, 1059.

[70] Zhao, N. Q.; He, C. N.; Ding, J.; Zou, T. C.; Qiao, Z. J.; Shi, C. S.; Du, X. W.; Li, J. J.; Li, Y. D. *J. Alloys Compd.* **2006,** *In Press.*

[71] Xu, J.; Zhang, X.; Chen, F.; Li, T.; Li, Y.; Tao, X.; Wang, Y.; Wu, X. *Appl. Surf. Sci.* **2005**, *239*, 320.

[72] Cao, J. M. *Appl. Surf. Sci*. **2006**, *253*, 2460.

[73] Kozhuharova, R.; Ritschel, M.; Elefant, D.; Graff, A.; Mönch, I.; Mühl, T.; Schneider, C.M.; Leonhardt, A. *J. Magnetism and Magnetic Mater*. **2005**, *290*, 250.

[74] Seelan, S.; Hwang, D. W.; Hwang, L. P.; Sinha, A. K. *Vacuum* **2004**, *75*, 105.

[75] Yu, G. Y.; Gong, J. L.; Zhu, D. Z.; He, S. X.; Cao, J. Q.; Zhu, Z. Y. *Diamond and Related Materials* **2005**, *15*, 1261.

[76] Katok, K. V.; Tertykh, V. A.; Brichka, S. Y.; Prekhod'ko, G. P. *Mater. Chem. Phys.* **2006**, *96,* 396.

[77] Somanathan, T.; Pandurangan, A.; Sathiyamoorthy, D. *J. Mol. Catal. A* **2006**, *256*, 193.

[78] Wang, X. Q.; Wang, M.; Jin, H. X.; Li, Z. H.; He, P. M. *Appl. Surf. Sci.* **2005**, *243*, 151.

[79] Couteau, E.; Hernadi, K.; Seo, J.W.; Thiên-Nga, L.; Mikó, Cs.; Gaál, R.; Forró, L. *Chem. Phys. Lett.***2003**, *378*, 9.

[80] Cheng, J.; Zhang, X.; Luo, Z.; Liu, F.; Ye, Y.; Yin, W.; Liu, W.; Han, Y. *Mat. Chem. Phys.* **2006**, *95*, 5.

[81] Bahome, M. C.; Jewell, L. L.; Hildebrandt, D.; Glasser, D.; Coville, N. J. *Appl. Catal. A* **2005**, *287*, 60.

[82] Terrado, E.; Redrado, M.; Muňoz, E.; Maser, W. K.; Benito, A. M.; Martínez, M. T. *Mater. Scie. Eng.* **2006**, *26*, 1185.

[83] Eftekhari, A; Jafarkhani, P.; Moztarzadeh, F. *Carbon*, **2006**, *44*, 1343.

[84] (a) Liu, B. H.; Ding J.; Zhong, Z. Y.; Dong, D. L.; White, T.; Lin, J. Y. *Chem. Phys. Lett*. **2002**, *358*, 96. (b) Sazbo, A.; Mehn, A.; Konya, Z.; Fonseca, A.; Nagy, J. B. *Phys. Chem. Commun*. **2003**, *6*, 40.

[85] Wang, T.; Wang, B. *Appl. Surf. Sci*. **2006**, *253*, 1606.

[86] Sun, Y.; Gu, C. Z.; Liu, W.; Jin, Z. S. *Diamond and related Materials* **2004**, 13, 1187.

[87] Park, K. H.; Yim, J. H.; Lee, S.; Koh, K. H. *Thin Solid Films* **2006**, *501*, 233.

[88] Jiang, J.; Feng, T.; Cheng, X. H.; Dai, L. J.; Cao, G. B.; Zhang, J. H.; Jiang B. Y.; Wang, X.; Liu, X. H.; Zou, S. C. *Mater. Lett*. **2006**, *60*, 1085.

[89] Zheng, G. B.; Kouda, K.; Sano, H.; Uchiyama, Y.; Shi, Y. F.; Quan, H. J. *Carbon* **2004**, *42*, 635.

[90] Li, Y.; Chen, J.; Chang, L. *Appl. Catal. A* **1997**, *163*, 45.

[91] Li, Y. J.; Lau, S. P.; Tay, B. K.; Chen, G. Y.; Sun, Z.; Chen, J. S.; You, G. F.; Sheeja, D. *Diamond and Related Mater.* **2001**, 10, 878.

[92] Tribolet, P.; Kiwi-Minsker, L. Catal. Today **2005**, 102, 15.

[93] Wei, B. Q.; Vajtai, R.; Ajayan, P.M. Carbon **2003**, 41, 179.

[94] Motojima, S.; Asakura, S.; Kasemura, T.; Takeuchi, S.; Iwanaga, H. Carbon **1996**, 34, 289.

[95] Cantoro, M.; Dolovko, V. B.; Hofmann, S.; Williams, D. R.; Ducati, C.; Geng, J.; Boskovic, B. O.; Kleinsorge, B.; Jefferson, D. A.; Ferrari, A. C.; Johnson, B. F. G.; Robertson, J. *Diamond and Related Materials* **2005**, 14, 733.

[96] Miao, J. Y.; Hwang, D. W.; Narasimhulu, K. V.; Lin, P. I.; Chen, Y. T.; Lin, S. H.; Hwang, L. P. Carbon **2004**, 42, 813.

[97] Tosheva, L.; Parmentier, J.; Valtchev, V.; Vix-Guterl, C.; Patarin, J. Carbon **2005**, 43, 2474.

[98] Ci, L.; Li, Y.; Wei, B.; Liang, J.; Xu, C.; Wu, D. Carbon **2000**, 38, 1933.

[99] Andrews, R.; Jacques, D.; Rao, A. M.; Derbyshire, F.; Qian, D.; Fan, X.; Dickey, E. C.; Chen, J. *Chem. Phys. Lett*. **1999**, *303*, 467.

[100] Satishkumar, B. C.; Govindaraj, A.; Sen, R.; Rao, C. N. R. *Chem. Phys. Lett.* **1998**, *293*, 47.

[101] (a) Sen, R.; Govindaraj, A.; Rao, C. N. R. *Chem. Phys. Lett.* **1997**, *267*, 276. (b) Cheng, H. M.; Li, F.; Sun, X.; Brown, S. D. M.; Pimenta, M. A.; Marucci, A.; Dresselhaus, G.; Dresselhaus, M. S. *Chem. Phys. Lett*. **1998**, *289*, 602. (c) Cheng, H. M.; Li, F.; Su, G.; Pan, H. Y.; He, L. L.; Sun, X.; Dresselhaus, M. S. *App. Phys. Lett*. **1998**, *72*, 3282.

[102] Benito, A. M.; Maniette, Y.; Munoz, E.; Martinez, M. *Carbon* **1998**, *36*, 681.

[103] Jeong, H. J.; Choi, H. K.; Kim, G. Y.; Song, Y. I.; Tong, Y.; Lim, S. C.; Lee, Y. H. *Carbon* **2006**, *44*, 2689.

[104] (a) Kamalakaran, R.; Terrones, M.; Seeger, T.; Kohler-Redlich, Ph.; Rűhle, M. *Appl. Phys. Lett*. **2000**, *77*, 3385. (b) Cao, A.; Ci, L.; Wu, G.; Wei, B.; Xu, C.; Liang, J.; Wu, D. *Carbon* **2001**, *39*, 152. (c) Dickey, E. C.; Grimes, C. A.; Jain, M. K.; Ong, K. G.; Qian, D.; Kichambare, P. D.; Andrews, R.; Jacques, D. *Appl. Phys. Lett*. **2001**, *79*, 4022. (d) Singh, C.; Shaffer, M. S. P.; Windle, A. H. *Carbon* **2003**, *41*, 359. (e) Mayne, M.; Grobert, N.; Terrones, M.; Kamalakaran, R.; Rühle, M.; Krato, H. W.; Walton, D. R. M. *Chem. Phys. Lett.* **2001**, *338*, 101. (f) Wei, B.; Vajtai, R.; Choi, Y. Y.; Ajayan, P. M. *Nano Lett.* **2002**, *2*, 1105. (g) Singh, C.; Shaffer, M.; Kinloch, I.; Windle, A. *Physica B* **2002**, *323*, 339.

[105] Nikolaev, P.; Bronikowski, J.; Bradley, R. K.; Rohmund, F.; Colbert, D. T.; Smith, K.A.; Smalley, R.E. *Chem. Phys. Lett.* **1999**, *313*, 91

[106] (a) Tennent, H. G.; Barber, J. J.; Hoch, R. *Hyperion Catalysis, Cambridge, MA* **1996.** (b) Kato, T.; Kusakabe, K.; Morooka, S. *J. Mater. Sci. Lett*. **1992**, *11*, 674. (c) Ohshima, S.; Ago, H.; Inoue, H.; Yumara, M. *New Diam. Front. Carbon Technol*. **2001,** *11*, 437.

[107] Endo, M.; Kim, Y. A.; Hayashi, T.; Nishimura, K.; Matusita, T.; Miyashita, K.; Dresselhaus, M. S. *Carbon* **2001**, *39*, 1287.

[108] Baughman, R. H.; Zakhidov, A. A.; de Heer, W A. *Science* **2002**, *297*, 787.

[109] Bai, S.; Li, F.; Yang, Q. H.; Cheng, H. M.; Bai, J. B. *Chem. Phys. Lett*. **2003**, *376,* 83.

[110] Ci, L.; Xie, S.; Tang, D.; Yan, X.; Li, Y.; Liu, Z.; Zou, X.; Zhou, W.; Wang, G. *Chem. Phys. Lett.* **2001**, *349*, 191.

[111] Lupo, F.; Rodriguez-Manzo, J.A.; Zamudio, A.; Elias, A.L.; Kim, Y.A.; Hayashi, T.; Muramatsu, M.; Kamalakaran, R.; Terrones, H.; Endo, M.; Rűhle, M.; Terrones, M.; *Chem. Phys. Lett.,***2005**, *410*, 384.

[112] Hiraoka. T.; Bandow, S.; Shinohara, H.; Iijima, S.; *Carbon*, **2006**, *44*, 1845.

[113] Cao, A.; Zhang, X.; Xu, C.; Liang, J.; Wu, D.; Chen, X.; Wei, B.; Ajayan, P. M. *Appl. Phys. Lett*. **2001**, *79*, 1252.

[114] Wei, B.; Vajtai, R.; Choi, Y. Y.; Ajayan, P. M. Zhu, H.; Xu, C.; Wu, D. *Nano Lett.* **2002**, *2*, 1105.

[115] Zhou, Z.;Wan, D.; Bai, Y.; Dou, X.; Song, L.; Zhou, W.; Mo, Y.; Xie, S.; *Physica E*, **2006,** *33*, 24.

[116] Ago, H.; Ohshima, S.; Uchida, K.; Yumura, M.; *J. Phys. Chem*., **2001**, *105*, 10453.

[117] Moisala, A.; Nasibulin, A. G.; Brown, D. P.; Jiang, H.; Khriachtchev, L.; Kauppinen, E. I. *Chem. Eng. Sci*. **2006**, *61*, 4393.

[118] Dai, H.; Rinzler, A. G.; Nikolaev, P.; Thess, A.; Colbert, D. T.; Smalley, R.E.; *Chem. Phys. Lett*. **1996**, *260*, 471.

[119] Qiu, J.; An, Y.; Zhao, Z.; Li, Y.; Zhou, Y. *Fuel Processing Technology*, **2004**, *85*, 913.

[120] (a) Bandow, S.; Chen, G.; Sumanasekera, G. U.; Gupta, R.; Yudasaka, M.; Iijima, S.; Eklund, P. C. *Phys. Rev. B* **2002**, *66*, 075426. (b) Kwon, Y. K.; Tomanek, D.; *Phys. Rev. B* **1998**, *58*, R16001. (c) Tanaka, K.; Aoki, H.; Ago, H.; Yamabe, T.; Okahara, K. *Carbon* **1997**, *35*, 121. (d) Hutchison, J. L.; Kiselev, N. A.; Krinichnaya, E. P. Krestinin, A. V.; Loutfy, R. O.; Morawsky, A. P. et al. *Carbon*, **2001**, *39*, 761. (e) Bandow, S.; Takizawa, M.; Hirahara, K.; Yudasaka, M.; Iijima, S. *Chem. Phys. Lett.* **2001**, *337*, 48.

[121] (a) Ci, L.; Rao, Z., Zhou, Z.; Tang, D.; Yan, X.; Liang, Y.; Liu, D.; Yuan, H.; Zhou, W.; Wang, G.; Liu, W.; Xie, S. *Chem. Phys. Lett.* **2002**, *359*, 63. (b) Zhou, Z.; Ci, L.; Chen, X.; Tang, D.; Yan, X.; Liu, D.; Liang, Y.; Yuan, H.; Zhou, W.; Wang, G.; Xie, S. *Carbon* **2003**, *41*, 337.

[122] Ren, W.; Li, F.; Chen, J.; Bai, S.; Cheng, H. M. *Chem. Phys. Lett*. **2002**, *359*, 196.

[123] Ci, L.; Zhou, Z.; Yan, X.; Liu, D.; Yuan, H.; Song, L.; Wang, J.; Gao, Y.; Zhou, J.; Zhou, W.; Wang, G.; Xie, S. *J. Phys. Chem. B* **2003**, *107*, 8760.

[124] Wei, J.; Jiang, B.; Wu, D.; Wei, B. *J. Phys. Chem. B* **2004**, *108*, 8844.

[125] Zhang, H.; Liang, E.; Ding, P.; Chao, M. *Physica B* **2003**, *337*, 10.

[126] Satishkumar, B.C.; Govindaraj, A.; Rao, C.N.R. *Chem. Phys. Lett.* **1999**, *307*, 158.

[127] Tapasztó, L.; Kertész, K.; Vértesy, Z.; Horváth, Z. E.; Koós, A. A.; Osváth, Z.; Sárközi, Zs.; Darabont, Al.; Biró, L. P. *Carbon* **2005**, *43*, 970.

[128] Deck, C.P.; Vecchio, K. *Carbon* **2006**, *44*, 267.

[129] Kumar, M.; Ando, Y. *Chem. Phys. Lett*. **2003**, *374*, 521.

[130] Chen, Y.; Sun, Z.; Li, Y.N.; Tay, B.K. *Mater. Chem. Phys.* **2006**, *98*, 256.

[131] Liu, X. Y.; Huang, B. C.; Coville, N. J. *Carbon* **2002**, *40*, 2799.

[132] Liu, X. Y.; Huang, B. C.; Coville, N.J. *Fullerenes Nanotubes Carbon Nanostruct* **2002**, *10*, 339.

[133] Horváth, Z. E.; Kertész, K.; Pethő, L.; Koós, A. A.; Tapasztó, L.; Vértesy, Z.; Osváth, Z.; Darabont, Al. Nemes-Incze, P.; Sárközi, Zs; Biró, L. P. *Curr. Appl. Phys.* **2006**, *6*, 135.

[134] Smith, D.K.; Lee, D.C.; Korgel, B.A. *Chem. Mater.* **2006**, *18*, 3356.

[135] Niu, J. J.; Wang, J. N.; Jiang, Y.; Su, L. F.; Ma, J. *Microporous and Mesoporous Materials* **2006**, *100*, 1.

[136] Alonso-Nuñez, G.; Valenzuela-Muñiz, A.M.; Paraguay-Delgado, F.; Aguilar, A.; Verde, Y. *Optical Mater*. **2006**, *29*, 134.

[137] Das, N.; Dalai, A.; Mohammadzadeh, J.S.S.; Adjaye, J. *Carbon* **2006**, *44*, 2236.

[138] Chen, C.M.; Dai, Y.M.;Huang, J.G.; Jehng, J.M.; *Carbon* **2006** *44*, 1808.

[139] Qiu, J.; Li, Q.; Wang, Z.; Sun, Y.; Zhang, H.; *Carbon* **2006**, 44, 2565.

[140] Lima, M. D.; Bonadiman, R.; de Andrade, M. J.; Toniolo, J.; Bergmann, C. P. *Diamond and Related Materials* **2006,** *15*, 1708.

[141] Chen, T. T.; Liu, Y. M.; Sung, Y.; Wang, H. T.; Ger, M. D. *Mater. Chem. Phys*. **2006**, *97*, 511.

[142] Ago, H.; Ohshima, S.; Tsukuagoshi, K.; Tsuji, M.; Yumura, M. *Curr. Appl. Phys*. **2005**, *5*, 128.

[143] Yu, H.; Li, Z.; Luo, G.; Wei, F. *Diamond and Related Materials* **2005**, *15*, 1447.

[144] Zhu, H.; Ci, L.; Xu, C.; Liang, J.; Wu, D. *Diamond and Related Materials* **2002**, *11*, 1349.

[145] Deepak, F. L.; Govindaraj, A.; Rao, C. N. R. *Chem. Phys. Lett,* **2001**, *345*, 5.

[146] Govindaraj, A.; Rao, C. N. R. *Pure Appl. Chem.* **2002**, *74*, 1571.

[147] Dillon, A. C.; Mahan, A. H.; Deshpande, R.; Alleman, J. L.; Blackburn, J. L.; Parillia, P. A.; Heben, M. J.; Engtrakul, C.; Gilbert, K. E. H.; Jones, K. M.; To, R.; Lee, S. H.; Lehman, J. H. *Thin Solid Films* **2006**, *501*, 216.

[148] Ci, L. J.; Wei, B. Q.; Liang, J.; Xu, C. L.; Wu, B. H. *J. Mater. Sci. Lett*. **1999**, *18*, 797.

[149] Collins, S.; Brydson, R.; Rand, B. *Carbon* **2002**, *40*, 1089.

[150] Yang, Y.; Liu, X.; Xu, B.; Li, T. *Carbon* **2006**, *44*, 1661.

[151] Li, Y. Y.; Bae, S. D.; Sakoda, A.; Suzuki, M. *Carbon* **2001**, *39,* 91.

[152] Mukai, S. R.; Masuda, T.; Harada, T.; Hashimoto, K. *Carbon* **1996**, *34*, 645.

[153] Cheng, J.; Zhang, X.; Liu, F.; Tu, J.; Lu, H.; Sun, Y.; Chen, F. *Mater. Chem. Phys*. **2004**, *87*, 241.

[154] Mukhopadhyay, K.; Ram, K.; Lal, D.; Mathur, G.N.; Rao, K. U. B. *Carbon* **2003,** *43*, 2397.

[155] Martin-Gullon, I.; Vera, J.; Conesa, J.A.; González, J. L.; Merino, C. *Carbon*, **2006,** *44*, 1572.

[156]Fan, Y. Y.; Cheng, H. M.; Wei, Y. L.; Su, G.; Shen, Z. H. *Carbon* **2000**, *38*, 789.

[157] Terrones, M.; Terrones, H.; Grobert, N.; Hsu, W. K.; Zhu, Y.Q.; Hare, J. P.; Kroto, H. W.; Walton, D. R. M.; Kohler-Redlich, Ph.; Rűhle, M.; Zhang, J. P.; Cheetham, A.K. *Appl. Phys. Lett.* **1999**, *75,* 3932.

[158] Singh, C.; Quested, T.; Boothroyd, C. B.; Thomas, P.; Kinloch, I. A.; Abou-Kandil, A. I.; Windle, A. H. *J. Phys. Chem. B* **2002**, *106*, 10915.

[159] Ren, W. C.; Cheng, H. M. *Carbon* **2003**, *41*, 1657.

[160] Ci, L.; Zhu, H.; Wei, B.; Liang, J.; Xu, C; Wu, D. *Carbon* **1999**, *37*, 1652.

[161] Benissad-Aissani, F.; Aït-Amar, H.; Schouler, M. C.; Gadelle, P. *Carbon* **2004**, *42*, 2163.

[162] Motojima, S.; Hasegawa, I.; Kagiya, S.; Momiyama, M.; Kawaguchi, M.; Iwanaga, H.; *Appl. Phys. Lett*., **1993,** *62,* 2322.

[163] Qian, H. S.; Han, F. M.; Zhang, B.; Guo, Y. C.; Yue, J.; Peng, B. X. *Carbon*, **2004**, *42*, 761

[164]. Jin, Y. Z.; Gao, C.; Hsu, W. K.; Zhu, Y.; Huczko, A.; Bystrzejewski, M.; Roe, M.; Lee, C. Y.; Acquah, S.; Kroto, H.; Walton, D. R. M. *Carbon* **2005**, *43*, 1944.

[165] (a) Kim, D. P.; Lin, C.L. Mihalisin, T.; Heiney, P. Labes M. M. *Chem. Mater.* **1991**, *3*, 686. (b) Nevidomskyy, A. H.; Csanyi, G.; Payne, M. C. *Phys. Rev. Lett*. **2003**, *9*, 1055021. (c) dos Santos, M. C. Alvares, F. *Phys. Rev. B* **1998**, *58*, 13918.

[166] Terrones, M.; Ajayan, P. M.; Banhart, F.; Blasé, X.; Carroll, D. L.; Charlier, J. C.; Czerw, R.; Foley, B.; Grobert, N.; Kamalakaran, R.; Kohler-Redlich, Ph.; Rühle, M.; Seeger, T.; Terrones, H. *Appl. Phys. A* **2002**, *74*, 355.

[167] (a) Terrones, M., Grobert, N.; Terrones, H. *Carbon* **2002**, *40*, 1665. (b) Bill, J.; Riedel, R. *Mater. Res. Soc. Symp. Proc*. **1992**, *271*, 839. (c) Suenaga, K.; Colliex, C.; Demoncy, N.; Loiseau, A.; Pascard, H.; Willaime, F. *Science* **1997**, *278*, 653. (d) Zhang, Y.; Gu, H.; Suenaga, K.; Iijima, S.; *Chem. Phys. Lett*. **1997**, *279,* 264.

[168] (a) Glenis, S.; Cooke, S.; Chen, X.; Labes, M. M. *Chem. Mater*. **1994**, *6*, 1850. (b) Ying, Z. C.; Hettich, R. L.; Compton, R. N.; Haufler, R. E. *J. Phys. B At. Mol. Opt. Phys.* **1996**, *29*, 4935.

[169] Han, W.; Bando, Y.; Kurashima, K.; Sato, T. *Chem. Phys. Lett.* **1999**, 299, 368.

[170] (a) Sen, R.; Satishkumar, B. C.; Govindaraj, A.; Harikumar, K. R.; Renganathan, M. K.; Rao, C. N. R. *J. Mater. Chem*. **1997**, *7*, 2335. (b) Sen, R.; Satishkumar, B. C.; Govindaraj, A.; Harikumar, K. R.; Raina, G.; Zhang, J. P.; Cheethan, A. K.; Rao, C. N. R. *Chem. Phys. Lett*. **1998**, *287*, 671.

[171] (a) Glerup, M.; Castignolles, M.; Holzinger, M.; Hug, G.; Loiseau, A.; Bernier, P. *Chem. Commun.* **2003**, *20*, 2542. (b) Tang, C.; Bando, Y.; Golberg, D.; Xu, F. *Carbon* **2004**, *42*, 2625.

[172] Chai, Y.; Zhang, Q.F.; Wu, J.L. *Carbon* **2006**, *44*, 687.

[173] Suenaga, K.; Yudasaka, M.; Colliex, C.; Iijima, S. *Chem. Phys. Lett.* **2000**, *316*, 365.

[174] Kudashov, A. G.; Okotrub, A.V.; Bulusheva, L. G.; Asanov, I. P.; Shubin, Y. V.; Yudanov, N. F.; Yudanova, L. I.; Danilovich, V. S.; Abrosimov, O. G. *J. Phys. Chem. B* **2004**, *108*, 9048.

[175] Maiyalagan, T.; Viswanathan, B. *Mater. Chem. Phys*. **2005**, *93*, 291.

[176] Jung, M.; Eun, K. Y.; Lee, J. K.; Baik, Y. J.; Lee, K. R.; Park, J. W. *Diamond and Related Materials* **2001**, *10*, 1235.

[177] Villalpando-Paez, F.; Zamudio, A.; Elias, A. L.; Son, H.; Barros, E. B.; Chou, S. G.; Kim, Y. A.; Muramatsu, H.; Hayashi, T.; Kong, J.; Terrones, H.; Dresselhaus, G.; Endo, M.; Terrones, M.; Dresselhaus, M. S. *Chem. Phys. Lett*. **2006**, *424*, 345.

[178] Maldonado, S.; Morin, S.; Stevenson, K.J.; *Carbon,* **2006**, *44*, 1429.

[179] Lee, C. J.; Lyu, S. C.; Kim, H. W.; Lee, J. H.; Cho, K. I. *Chem. Phys. Lett.* **2002**, *359*, 115.

[180] Chopra, N. G.; Luyken, R. J.; Cherry, K.; Crespi, V. H.; Cohen, M. L.; Louie, S. G.; Zettl, A. *Science* **1995**, *269*, 966.

[181] (a) Stéphan, O.; Ajayan, P. M.; Colliex, C.; Redlich, Ph.; Lambert, J. M.; Bernier, P.; Lefin, P. *Science* **1994**, *266*, 1683. (b) Wengsieh, Z.; Cherry, K.; Chopra, N. G.; Blasé, X.; Miyamato, Y.; Rubio, A.; Cohen, M. L.; Louie, S. G.; Zettl, A.; Gronsky, R. *Phys. Rev. B* **1995**, *51*, 11229. (c) Redlich, Ph.; Loeffler, J.; Ajayan, P. M.; Aldinger, Ruhle, M. *Chem. Phys. Lett.* **1996**, *260*, 465.

[182] Malcioğlu, O B.; Taşci, E.; Erkoç, S. *Physica E* **2005,** *28*, 296.

[183] Deepak, F. L.; Vinod, C. P.; Mukhopadhyay, K.; Govindaraj, A.; Rao, C. N. R. *Chem. Phys. Lett.* **2002**, *353*, 345.

[184] (a) Pérez-Cabero, M.; Rodríguez-Ramos, I.; Guerrero-Ruiz, A. *J. Catal*. **2003**, *215*, 305. (b) Ermakova, M.A.; Ermakov, D. Y.; Chuvilin, A. L.; Kuvshinov, G. G. *J. Catal*. **2001**, *201*, 183. (c) Pan, S. S.; Xie, Z. W.; Chang, B. H.; Sun, L. F.; Zhou, W. Y.; Wang, G. *Chem. Phys. Lett*. **1999**, *299*, 97. (d) Venegoni, D.; Serp, P.; Feurer, R.; Kihn, Y.; Vahlas, C.; Kalck, P. *Carbon* **2002**, *40*, 1799. (e) Hernadi, K.; Fonseca, A.; Nagy, J. B.; Bernaerts, D.; Fudala, A.; Lucas, A. A. *Zeolites* **1996**, *17*, 416. (f) Fonseca, A.; Hernadi, K.; Nagy, J. B.; Bernaerts, D.; Lucas, A. A. *J. Mol. Catal. A* **1996**, *107*, 159. (g) Cui, H.; Zhou, O.; Stoner, B. R. *J. Appl. Phys*. **2000**, *88*, 6072. (h) Wang, Y. H.; Lin, J.; Huan, C. H. A.; Chen, G. S. *Appl. Phys. Lett*. **2001**, *79*, 680. (i) Cho, Y. S.; Choi, G. S.; Hong, S. Y.; Kim, D. *J. Cryst. Growth* **2002**, *243*, 224. (j) Duesberg, G. S.; Graham, A. P.; Liebau, M.; Seidel, R.; Unger, E.; Kreupl, F. *Nano Lett.* **2003**, *3*, 257. (k) Fan, S.; Chapline, M. G.; Franklin, N. R.; Tombler, T. W.;

Cassell, A. M.; Dai, H. *Science* **1999**, *283*, 512. (l) Fan S.; Liang, W.; Dang, H.; Franklin, N. R.; Tombler, M. G.; Chapline, T. W. *Physica E* **2000**, *8*, 179. (m) Hernadi, A.; Fonseca, K.; Nagy. J. B.; Bernaerts, D.; Lucas, A. A. *Carbon* **1996**, *34*, 1249. (n) Sacco, A.; Thacker, P.; Chang, T. N.; Chiang, A. T. S. *J. Catal*. **1984**, *85*, 224.

[185] (a) Li, Y.; Kim, W.; Zhang, Y.; Rolandi, M.; Wang, D.; Dai, H. *J. Phys. Chem. B* **2001**, *105*, 11424. (b) Cheung, C. L.; Kurtz, A.; Park, H.; Lieber, C. M. *J. Phys. Chem. B* **2002**, *106*, 2429. (c) Zhu, S.; Su, C. H.; Cochrane, J. C.; Lehoczky, S.; Cui, Y.; Burger, A. *J. Cryst. Growth* **2002**, *234*, 584. (d) Hongo, H.; Yudasaka, M.; Ichihashi, T.; Nihey, F.; Iijima, S. *Chem. Phys. Lett*. **2002**, *361*, 349. (e) Kim, W.; Choi, H. C.; Shim, M.; Li, Y.; Wang, D.; Dai, H. Nano Lett. 2002, 2, 703. (f) Zhang, Y.; Li, Y.; Kim, W.; Wang, D.; Dai, H. *Appl. Phys. A* **2002**, *74*, 325.

[186] (a) Yudasaka, M.; Kikuchi, R.; Matsui, T.; Yoshimasa, O.; Yoshimura, S. *Appl. Phys*. *Lett*. **1995**, *67*, 2477. (b) Teo, K. B. K.; Chhowalla, M.; Amaratunga, G. A. J.; Milne, W. I.; Hasko, D. G.; Pirio, G. *Appl. Phys. Lett*. **2001**, *79*, 1534. (c) Klinke, C.; Bonard, J. M.; Kern, K. *Surf. Sci*. **2001**, *492,* 195. (d) Choi, Y. C.; Shin, Y. M.; Lee, Y. H.; Lee, B. S.; Park, G. S.; Choi, W. B. *Appl. Phys. Lett*. **2000**, *76*, 2367. (e) Huang, Z. P.; Xu, J. W.; Ren, Z. F.; Wang, J. H.; Siegal, M. P.; Provencio, P. N. *Appl. Phys. Lett*. **1998**, *73*, 3845. (f) Jiao, J.; Seraphin, S. *J. Phys. Chem. Solids* **2000**, *61*, 1055. (g) Kukovitsky, E. F.; L'vov, S. G.; Sainov, N. A.; Shustov, V. A.; Chernozatonkii, L. A. *Chem. Phys. Lett.* **2002**, *355*, 497. (h) Siegal, M. P.; Overmyer, D. L.; Provencio, P. P. Appl. Phys. Lett. 2002, 80, 2171. (i) Teo, K. B. K.; Chhowalla, M.; Amaratunga, G. A. J.; Milne, W. I.; Pirio, G.; Legagneux, P. et al. *J. Vac. Sci. Technol. B* **2002**, *20*, 116. (j) Yudasa, M.; Kikuchi, R.; Ohki, Y.; Ota, E.; Yoshimura, S. *Appl. Phys. Lett*. **1997**, *70*, 1817. (k) Zhang, W. D.; Wen, Y.; Tjiu, W. C.; Xu, G. Q.; Gan, L. M. *Appl. Phys. A* **2002**, *74*, 419.

[187] Seidel, R.; Duesberg, G. S.; Unger, E.; Graham, A. P.; Liebau, M.; Kreupl, F. J. *Phys. Chem. B* **2004**, *108*, 1888.

[188] (a) Ago, H.; Komatsu, T.; Oshima, S.; Kuriki, Y.; Yumura, M. *Appl. Phys. Lett.* **2000**,*77*, 79. (b) Hsu, C. M.; Lin, H. L.; Cgabg, C. H.; Kuo, C. T. *Thin Solid Films* **2002**, *420-421*, 225. (c) Hernadi, K.; Fonseca, A.; Nagy, J. B.; Siska, A.; Kisicsi, I.

Appl. Catal. A **2000**, *199*, 245. (d) Ago, Murata, K. Yumura, M.; Yotani, J. Uemura, S. *Appl. Phys. Lett.* **2003**, *82*, 811. (e) Bower, C.; Zhu, W.; Jin, S.; Zhou, O.; *Appl. Phys. Lett.* **2000**, *77*, 830. (f) Terrones, M.; Grobert, N.; Zhang, J. P.; Terrones, H.; Olivares, J.; Hsu, W. K. et al. *Chem. Phys. Lett*. **1998**, *285*, 299.

[189] Marty, L. Bouchiat, V.; Bannot, A. M.; Chaumont, M.; Fournier, T.; Decossas, S. et al. *Microelectron Eng*. **2002**, *61*, 485.

[190] (a) Ren, Z. F.; Huang, Z. P.; Xu, J. W.; Wang, J. H.; Bush, P.; Siegal, M. P.; Provencio, P. N. *Science* **1998**, *282*, 1105. (b) Dai, H. J.; Kong, J.; Zhou, C. W.; Franklin, N.;Tombler, T.; Cassell, A.; Fan, S. S.; Chapline, M. *J Phys. Chem. B* **1999**, *103*, 11246. (c) Fonseca, A.; Hernadi, K.; Piedigrosso, P.; Colomer, J. F.; Mukhopadhyay, K.; Doome, R.; Lazarescu, S.; Biro, L. P.; Lambin, P.; Thiry, P. A.; Bernaerts, D.; Nagy, J. B. *Appl. Phys. A* **1998**, *67*, 11. (d) Cassell, A. M.; Raymakers, J. A.; Kong, J.; Dai, H. J. *J Phys. Chem. B* **1999**, *103*, 6484. (e) Geng, J.; Singh, C.; Sherpard, D.; Shaffer, M.; Johnson, B. F. G.; Windle, A. H. *Chem. Commun*. **2002**, 2666.

[191] Harutyunyan, A. R.; Pradhan, B. K.; Kim, U. J.; Chen, G.; Eklund, P. E. *Nano Lett*. **2002**, *2*, 525.

[192] (a) Cassell, A. M.; Mc Cool, G. C.; Tee, Ng. H.; Koehne, J. E.; Chen, B.; Li, J. et al. *Appl. Phys. Lett*. **2003**, *82*, 817. (b) Chen, B.; Parker, H. G.; Han, J.; Meyyappan, M.; Cassell, A. M. *Chem. Mater*. **2002,** *14*, 1891. (c) Murakami, Y.; Miyauchi, Y.; Chiashi, S.; Maruyama, S. *Chem. Phys. Lett*, **2003**, *374*, 53. (d) Willems, I.; Konya, Z.; Colomer, J. F.; Van Tendeloo, G.; Nagaraju, N.; Fonseca, A. et al. *Chem Phys. Lett*. **2000**, *317*, 71.

[193] (a) Baek, Y. G.; Honda, S. I.; Ikuno, T.; Ohkura, S.; Katayama, M.; Hirao, T. et al. *J. Appl. Phys.* **2003**, *42*, 579. (b) Yang, Y.; Hu, Z.; Tian, Y. J.; Lü, Y. N.; Wang, X. Z.; Chen, Y. *Nanotechnology* **2003**, *14*, 733.

[194] Thess, A. Lee, R.; Nikolaev, P.; Dai, H.; Petit, P.; Robert, J. et al. *Science* **1996**, *273*, 483.

[195] Horvath, Z. E.; Kertesz, K.; Petho, L.; Koos, A. A.; Tapaszto, L.; Vertesy, Z.; Osvath, Z.; Darabont, Al.; Nemes-Incze, P.; Sarkozi, Zs.; Biro, L P. *Curr. Appl. Phys*. **2006**, *6*, 135.

[196] Amelinckx, S.; Zhang, X. B.; Bernaerts, X. F.; Zhang, X. F.; Ivanov, V.; Nagy, J. B. *Science* **1995**, *267*, 635.

[197] Hayashi, T.; Kim, Y. A.; Matoba, T.; Ezaka, M.; Nishimura, K.; Tsukada, T.; Endo, M.; Dresselhaus, M. S. *Nano Lett*. **2003**, *3*, 887.

[198] Belin, T.; Epron, F. *Mater. Sci. Eng.B* **2005,** *119*, 105.

[199] Kiang, C.; Endo, M.; Ajayan, P.; Dresselhaus, G.; Dresselhaus, M. *Phys. Rev. Lett*. **1998**, *81*, 1869.

[200] Mamedov, A. A.; Kotov, N. A.; Prato, M.; Guldi, D. M.; Wicksted, J. P.; Hirsch, A. *Nat. Mater.* **2002**, *1*, 190.

[201] (a) Ebbesen, T. W. "Carbon nanotubes: Preparation and properties", Ed. Boca Raton Press: CRC, **1997**. (b) Dresselhaus, M. S.; Dresselhaus, G.; Avouris, Ph. "Carbon nanotubes: Synthesis, structure, properties and applications", Heidelberg Press: Springer, **2001**. (c) Terrones, M. *Rev. Mater. Res*. **2003**, *33*, 419.

[202] Tans, S.; Verschueren, A.; Dekker, C. *Nature* **1998**, *393*, 49.

[203] Martel, R.; Schmidt, T.; Shea, H. R.; Hertel, T.; Avouris, P. *Appl. Phys. Lett.* **1998**, *73*, 2447.

[204] Zhou, C.; Kong, J.; Dai, H. *Appl. Phys. Lett*. **1999,** *76*, 1597.

[205] Fuhrer, M. S.; Nygard, J.; Shih, L.; Forero, M.; Yoon, Y.; Mazzoni, M.; Joon, H.; Choi, J.; Loui, S.; Zettl, A. McEuen, P. *Science* **2000**, *288*, 494.

[206] Ewels, C. P.; Glerup, M. J. *Nano Sci. Nanotech*. **2005**, *5*, 1345.

[207] Pagani, R. *C&EN* **1999**, *1*, 31.

[208] Treacy, M. M. J.; Ebbesen, T. W.; Gibson, J. M. *Nature* **1996**, *381*, 678.

[209] Tang, J.; Matsushita, A.; Tikegawa, T.; Yudusaka, M.; Bandow, S.; Iijima, S. *Mater. Rec. Soc. Symp. Proc*. **2000**, 593.

[210] (a) Yang, Q. H.; Hou, P. X.; Bai, S.; Wang, M. Z.; Cheng, H. M. *Chem. Phys. Lett*. **2001**, *345*, 18. (b) Inoue, S.; Ichikuni, N.; Suzuki, T.; Uematsu, T.; Kaneko, K. *J. Phys. Chem.* **1998**, *102*, 4689.

[211] Eswaramoorthy, M.; Sen, R.; Rao, C. N. R. *Chem. Phys. Lett.* **1999**, *304*, 207.

[212] Serp, P.; Corrias, M.; Kalck, P. *Appl. Catal. A* **2003**, *253*, 337.

[213] Moon, J. M.; An, K. H.; Lee, Y. H.; Park, Y. S.; Bae, D. J.; Park, D. S. *J. Phys. Chem. B* **2001**, *105*, 5677.

[214] Nhut, J. M.; Vieira, R.; Pesant, L.; Tessonnier, J. P.; Keller, N.; Ehret, G.; Huu, C. P.; Ledoux, M. J. *Catal. Today* **2002**, *76*, 11.

[215] Giordano, R.; Serp, P.; Kalck, P.; Kihn, Y.; Schereiber, J.; Marhic, C.; Duvail, J. L. *Eur. J. Inorg. Chem*. **2003**, 610.

[216] Liu, Z. J.; Xu, Z.; Yuan, Z. Y.; Lu, D.; Chen, W.; Zhou, W. *Catal. Lett*. **2001**, *72*, 203.

[217] (a) Jung, H. J.; Walter Jr., J. P.; Vannice, M. A. *J. Catal*. **1982**, *75*, 416. (b) Jung, H. J.; Vannice, M. A.; Mulay, L. N.; Stanfield, R. M.; Delgass, W. N. *J. Catal*. **1982**, *76*, 208. (c) Venter, J.; Kaminsky, M.; Geoffroy, M.; Vannice, M. A. *J. Catal*. **1987**, *103*, 450. (d) Venter, J.; Kaminsky, M.; Geoffroy, M.; Vannice, M. A. *J. Catal*. **1987**, *105*, 155. (e) Venter, J.; Chen, A. A.; Phillips, J.; Vannice, M. A. *J. Catal*. **1989**, *119*, 451.

[218] Dry, M.E. in: Anderson, J. R.; Boudart, M. (Eds); "Catalysis Science Technology", Springer Press: New York, **1981**, *1*, 159.

[219] (a) Van Steen, E.; Prinsloo, F. F.; *Catal. Today* **2002**, *71*, 327. (b) Moy, D.; Hoch, R. Hyperion Catalysis international Inc. US Patent 5,569,635, **1996**.

CHAPTER 2

Experimental Section

2.1 Introduction

Three main generic synthesis methods have been used to make CNTs namely: arc-discharge [1], laser ablation [2], and chemical vapor deposition (CVD) methods [3]. All three methods can produce SWCNTs and MWCNTs. The CVD method requires the use of both a catalyst (typically Fe, Co or Ni) and a carbon source to produce CNTs and other novel carbon 'shaped' materials. Two of the most promising methods for depositing commercial quantities of CNTs are the floating catalyst CVD method [4] and the injection CVD method [5]. For the injection method an organic solvent containing a dissolved organometallic compound that decomposes to form the catalyst is injected into a two-zone furnace. The solvent and the catalyst vaporize into the first zone, and the carrier gas pushes the vapour into the second zone where the organometallic compound decomposes to yield nanoparticles. Solvent and the ligand molecules serve as the carbon source for nanotube synthesis at the catalyst sites. Organometallic compounds that are generally used are metallocenes (Fe, Co, Ni or Ru) [6] and iron pentacarbonyl [7]. In this research report, a wide range of organometallic compounds as catalysts for CNT growth using the injection CVD method have been investigated.

2.2 Carbon nanotube preparation

Multiwalled carbon nanotubes were deposited using a single furnace system in which a quartz tube reactor (800 × 28 mm i.d.) was inserted horizontally into an electrical furnace with the outlet of the tube connected to a gas bubbler similar to studies reported by other workers [8]. The temperature inside the quartz tube was determined by means of a thermocouple placed in the middle of the furnace. A second moveable thermocouple was used to establish the profile of the temperature in the reactor.

CNTs were produced from toluene solutions of iron complexes or mixtures of iron complexes and other transition metals using the injection CVD method. Toluene solutions of the catalyst precursors were placed in a 10 ml syringe driven by a SAGE syringe pump. The solutions were injected into the quartz tube reactor via a special designed quartz tube (2 mm i.d., 200 mm in length), cooled by water, similar to that described in the literature [8b]. Solutions were injected into the high temperature zone at injection rates ranging from 0.2-3.3 ml/min with typically 7 ml being delivered. Synthesis of CNTs was carried out in the temperature range 800-1000 °C, under 5% H_2 in argon (v/v) (AFROX) at atmospheric pressure. The flow rate of H_2 in argon was kept constant at 100 ml/min for all reactions. CNTs were deposited on the walls of the quartz tube reactor. Synthesized CNTs were characterized by scanning electron microscopy (SEM), transition electron microscopy (TEM), thermal gravimetric analysis (TGA) and Raman spectroscopy.

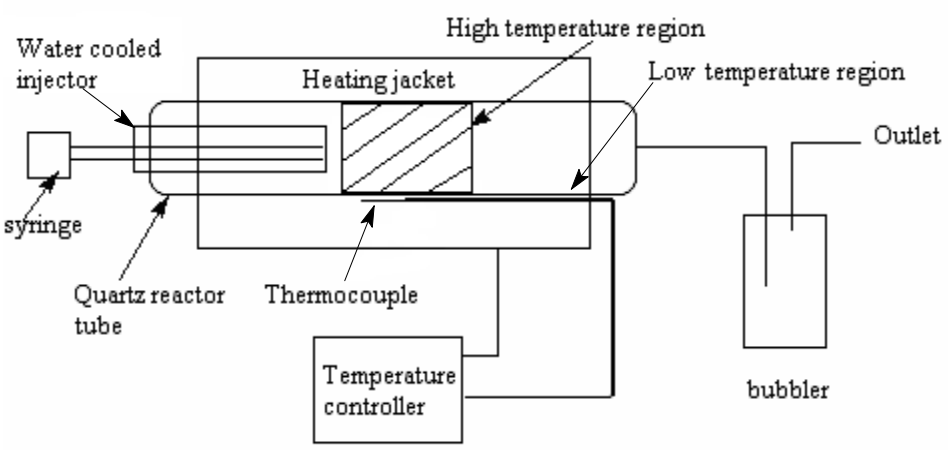

Figure 2.1: Thermal pyrolysis apparatus used to synthesize CNTs.

2.3 TEM analysis

Low magnification transmission electron microscope analysis of the CNTs was performed with a JEM 100S microscope and high magnification transmission electron microscopy (HMTEM) was performed with Philips CM200 microscope. Samples for

TEM analysis were prepared by sonication of the carbonaceous material in methanol and a few drops of the resulting suspension were placed onto a holey copper TEM grid for analysis.

2.4 SEM analysis

Scanning electron microscopy results were performed on Jeol JSM 840 microscope. Prior to analysis, the samples were mounted onto an aluminium stub using colloidal graphite and finally coated with carbon and gold-palladium.

2.5 TGA analysis

Thermal gravimetric analysis data were collected with a Perkin Elmer TGA 7 analyzer. Samples sizes (5-10 mg) of CNTs were loaded into platinum pans and heated to 1000°C in flowing air at 10 ml/min heating rate.

2.6 Raman analysis

Raman spectra were obtained with a Jobin-Yvon T64000 Raman spectrometer operated in single spectrograph mode with either a 600 lines/mm grating or an 1800 lines/mm grating. The 514.5 nm line of an argon ion laser was used as the excitation source. The laser light was focused onto the sample using the 20x objective of an Olympus microscope, and the scattered light was collected in a backscattering configuration. Laser power at the sample was kept at 1.2 mW or less to minimize local heating. Laser plasma lines were removed from the incident beam using a narrow bandpass interference filter and a Kaiser Optics holographic notch filter was used to remove the Rayleigh scattered light from the backscattered beam. Spectra accumulation time was 120 seconds and was collected using a liquid nitrogen-cooled CCD detector. Data was collected and analyzed using Jobin-Yvon's Labspec software.

2.7. References

[1] Ebbesen, T. W.; Ajayan, P. M. Nature, **1992**, *358*, 220.

[2] Liu, J.; Rinzler, A. G.; Dai, H.; Hafner, J. H.; Bradley, R. K.; Boul, P. J.; Lu, A.; Iverson, T.; Shelimov, K.; Huffman, C. B.; Rodriguez-Macias, F.; Shon, Y.; Lee, T. R.; Colbert, D. T.; Smalley, R. E. *Science* **1998,** *101*, 1253.

[3] (a) Amelinckx, S.; Zhang, X. B.; Bernaerts, D.; Zhang, X. F.; Ivanov, V.; Nagy, J. B. *Science* **1994**, *265*, 635. (b) Dupuis, A. C. *Progress in Materials Science* **2005**, *50*, 929.

[4] Satishkumar, B. C.; Govindaraj, A.; Sen, R.; Rao, C. N. R. *Chem. Phys. Lett.* **1998**, *293*, 47.

[5] Andrews, R.; Jacques, D.; Rao, A. M.; Derbyshire, F.; Qian, D.; Fan, X.; Dickey, E. C.; Chen, J. *Chem. Phys. Lett*. **1999**, *303*, 467.

[6] (a) Satishkumar, B.C.; Govindaraj, A.; Rao, C.N.R. *Chem. Phys. Lett.* **1999**, *307*, 158. (b) Mayne, M.; Grobert, N.; Terrones, M.; Kamalakaran, R.; Rühle, M.; Krato, H. W.; Walton, D. R. M. *Chem. Phys. Lett.* **2001**, *338*, 101. (c) Wei, B.; Vajtai, R.; Choi, Y. Y.; Ajayan, P. M. *Nano Lett.* **2002**, *2*, 1105. (d) Singh, C.; Shaffer, M.; Kinloch, I.; Windle, A. *Physica B* **2002**, *323*, 339.

[7] (a) Nikolaev, P.; Bronikowski, J.; Bradley, R. K.; Rohmund, F.; Colbert, D. T.; Smith, K. A.; Smalley, R. E. *Chem. Phys. Lett.* **1999**, *313*, 91 (b) Lee, C. J.; Lyu, S. C.; Kim, H. W.; Park, C. Y.; Yang, C. W. *Chem Phys. Lett*. **2002**, *359*, 109.

[8] (a) Nerushev, O. A.; Sveningsson, M.; Falk, L. K. L.; Rohmund, F. *J. Mater. Chem*. **2001**, *11*, 1122. (b) Liu, X.Y.; Huang, B. C.; Coville, N. J. *Fullerenes nanotubes and carbon nanostructure* **2002**, *10*, 339.

CHAPTER 3

Carbon nanotube synthesis from Fe-Mo bimetallic catalysts[1]

3.1 Introduction

CVD synthesis of CNTs requires the presence of a catalyst. Most of the catalysts employed are related to Co, Ni, Fe and other transition metals (or combination of the transition metals) dispersed on different supports such as SiO_2, Al_2O_3 or MgO [1]. Bimetallic catalysts have been found to be effective in producing CNTs from hydrocarbons [2] and CO [3]. The composition of a bimetallic catalyst has been found to affect CNT growth significantly.

Examples of the effect of bimetallic catalysts on CNT production include:
(i) MWCNTs were grown by catalytic decomposition of CO over a Co-Mo/SiO_2 supported catalyst [4]. SWCNTs and MWCNTs were synthesized by the gas phase catalytic reaction over a precipitate formed from colloidal solutions of Co-Mo nanoparticles dissolved in toluene, using a vertical flow reactor in the presence of thiophene as sulphur additive [5]. Co-W/SiO_2 and Co-Mo/SiO_2 bimetallic catalysts have been employed to produce SWCNTs by CO decomposition at various temperatures and the selectivity of the Co-W towards SWCNTs was found to strongly depend on the stabilization of Co species in a nonmetallic state before exposure to CO [6]. Co alone was not selective for the production of SWCNTs and generated mainly graphitic carbon and MWCNTs.

(ii) High quality MWCNT bundles that are hair-like fibers were efficiently synthesized by catalytic decomposition of methane in hydrogen with a higher yield over Ni-Mo/MgO catalyst than over Fe-Mo/MgO [7]. The arrangement and shape of these MWCNT bundles were different from MWCNTs synthesized over monometallic Ni/MgO system

[1] Mohlala M. S.; Liu, X. Y.; Robinson, J. M.; Coville, N. J. *Organometallics,* **2005***, 24,* 972.

[8] and the yield of nanotubes produced with Ni-Mo/MgO catalyst system was found to be higher than over Ni/MgO or Mo/MgO catalysts [7].

(iii) Thin MWCNTs with tube walls of between 2 to 6 nm have been synthesized from a Fe-Mo/MgO bimetallic catalyst by decomposition of methane and ethylene [9]. DWCNT bundles without amorphous carbon covering the surface have been produced by catalytic decomposition of benzene over a Fe-Mo/Al_2O_3 catalyst [10]. The Fe-Mo/Al_2O_3 catalyst has successfully been applied in the methane decomposition reaction to produce SWCNTs using a vertical flow reactor [11]. It was found from the above study that under the same reaction conditions, monometallic catalysts, Fe/Al_2O_3 and Mo/Al_2O_3 were not active for the production of SWCNTs. A mixture of DWCNTs and SWCNTs with high graphitic structure has been synthesized from catalytic decomposition of methane over a Fe-Mo/Al_2O_3 catalyst using a horizontal reactor [12]. SWCNTs have been synthesized at milligram per hour rates by catalytic decomposition of both carbon monoxide and ethylene over Fe-Mo/alumina catalyst [13]. DWCNTs with small amounts of amorphous carbon have been synthesized by catalytic decomposition of n-hexane over Fe-Mo/MgO catalysts [14]. SWCNTs have been prepared over Fe-Mo/MgO supported catalyst by catalytic decomposition of ethylene but when Fe or Mo single catalysts were used with the same reaction conditions less yield of SWCNTs was produced [15]. Therefore it is clear that bimetallic catalysts show promise in CNT growth. SWCNTs have been synthesized by decomposition of methane catalyzed by Fe-Mo/MgO catalyst [16].

We have commenced a study to systematically explore the use of organometallic complexes in CNT synthesis [17] and herein we report our studies on the use of mixed ferrocene/$Mo(CO)_6$ and ferrocene/$M(CO)_5(^tBuNC)$ (M = Mo, W) mixtures, together with a carbon source, to make CNTs using an injection CVD method. The $M(CO)_5(^tBuNC)$ catalysts were chosen so as to enhance the solubility, and hence the gas phase concentration, of the Mo and W precursors. The Fe/M (M = Mo, W) mixture has been chosen since reports on supported Fe/Mo catalysts have revealed that the Mo enhances the activity and selectivity of the Fe catalyst and the process selectively produces

SWCNTs in good yield [10, 12, 18]. The results from our study have been compared with literature reports on supported Fe/Mo catalysts.

3.2 Experimental

Ferrocene and $M(CO)_6$ (M = Mo, W) were purchased from Strem Chemicals and used as received**.** The preparation of $M(CO)_5(^tBuNC)$ catalysts were carried out as described elsewhere (see Appendix at the end of the Chapter) [19]. Reactions were performed in the apparatus shown in Chapter 2 (Figure 2.1). Synthesis of CNTs was carried out in the temperature range 700-900 °C, under 5% H_2 in argon (v/v) (AFROX) at atmospheric pressure. The flow rate of H_2 in argon was kept constant at 100 mL/min. Mixtures of ferrocene and $M(CO)_5RNC$ or $Mo(CO)_6$ at different weight ratios were dissolved in toluene (Merck chemicals). The catalyst solutions were placed in a 10 ml syringe driven by a SAGE syringe pump at ~0.80 ml/min rate. The solutions were injected into the quartz tube reactor via a special designed quartz tube (2 mm i.d., 200 mm in length), cooled by water, similar to that described in the literature [20]. This specially designed tube enabled the solution to be injected into the high temperature region of the large quartz tube reactor.

The method used in this study differed from our earlier procedure in that the solution was injected from the temperature reported into a 'hot' zone *(about 1.5 cm from the spray nozzle)* that was *ca.* 100 ^oC hotter than that reported [17b]. The carbon deposited materials formed were scraped from the walls of the quartz tube in both the high temperature region and low temperature region (temperature < 300 °C) of the tube (see Chapter 2, Figure. 1). The carbon materials were characterized by scanning electron microscopy (SEM) (Jeol JSM 840), low magnification transmission electron microscopy (TEM) (Jeol JEM 100S) high magnification transmission electron microscopy (HMTEM) (Philips CM200) and Raman spectroscopy (J-Y T64000). Thermal gravimetric analysis (TGA) measurements were performed in air using Perkin Elmer TGA 7 to determine the oxidizing characteristics of the nanotubes and the iron residue content. Samples for SEM analysis were prepared by placing the carbonaceous material on conductive tape. Samples

for TEM analysis were prepared by sonication of the carbonaceous material in methanol and a few drops of the resulting suspension were placed onto a holey carbon TEM grid for analysis. The number and size of the carbon tubes and spheres were obtained from the SEM/TEM images by counting procedures and represent average values.
The nanotube yield was calculated from the wt.% of the products obtained relative to the mass of solvent injected into the system.

3.3 Results

All CNT synthesis reactions were carried out in the apparatus shown in Figure 2.1 (Chapter 2). In these reactions the carbon source and the catalysts were injected into the hot quartz tube where the organometallic precursors instantly decomposed to form metal particles. These zero oxidation state metal particles either condense in the gas phase or on the quartz reactor walls to generate the small active metal particles used to synthesize the CNTs.

Reactions were performed under a standard set of conditions, so that the effect of the metals on the carbonaceous material produced in the reaction could be made. Variables that were investigated in the reaction were toluene injection rate, metal ratios, metal concentrations and reaction temperature. No attempt was made to optimize product yields. The yields of the carbonaceous materials relative to the carbon source (toluene) were found to range between 0.1 and 2%.

Thermal pyrolysis of toluene in the absence of a catalyst was first investigated. It was observed that at 700 ^{o}C no carbon deposit was observed, but at 800 °C (and higher) small amounts of carbon spheres (CSs) were observed (Figure 3.1). These were similar to the CSs previously observed by ourselves and others [18] with the diameters of the spheres formed by pyrolysis of toluene (no metal present) in the range 250-750 nm.

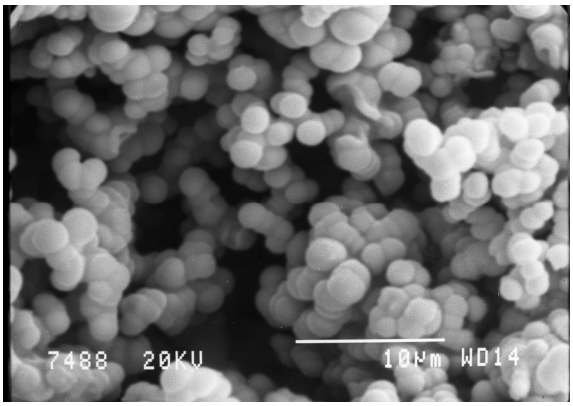

Figure 3.1: SEM image of CSs (800 °C, toluene)

Attempts were then made to use $Mo(CO)_6$/toluene to synthesize CNTs and CSs. The poor solubility of $Mo(CO)_6$ in toluene resulted in only low concentrations of $Mo(CO)_6$ being used in our studies. Consequently little carbon deposit due to the presence of the pure metal could be detected. To overcome this limitation, soluble Mo complexes were used in further studies. When single metal catalysts containing $Mo(CO)_5{}^tBuCN$ or $W(CO)_5{}^tBuCN$ in a weight ratio of 5.0 wt% (700–900 ^oC) were used, CSs and amorphous carbon were formed (Table 3.1). The amount and diameters of these CSs (diameter between 625 nm - 1µm) were generally found to be larger than those formed using only toluene.

Table 3.1: Effect of toluene and single metal catalysts on the synthesis of CNTs and CSs

Metal content	Temperature (°C)	Notes[a]	Mean diameter[b] (nm)
Toluene	700	No carbon deposit	
	800	Spheres	625
	900	Spheres	750
Ferrocene 5 wt.%	700	Spheres (40%), tubes (10%), a-C (50%)	500S, 167T
	800	Spheres (20%), tubes (60%), a-C (20%)	750S, 50T
	900	Spheres (30%), tubes (50%), a-C (20%)	800S, 160T

Table 3.1 Contd.

$Mo(CO)_5{}^tBuCN$	700	Spheres (60%), a-C (40%)	1µm
5 wt.%	800	Spheres (70%), a-C (30%)	625
	900	Spheres (80%), a-C (20%)	600
$W(CO)_5{}^tBuCN$	700	Spheres (50%), a-C (50%)	670
5 wt.%	800	Spheres (40%), a-C (60%)	690
	900	Spheres (60%), a-C (40%)	625

[a]a-C = amorphous carbon; [b]T = tubes, S = sphere; Injection flow rate = 0.8 ml/min, H_2 flow rate = 100 ml/min

Ferrocene has been reported to be a catalyst for the synthesis of CNTs [17a, 21] and blank runs were performed to determine the conditions for CNT synthesis in our apparatus. Conditions were chosen to limit tube formation such that the effect of the second metal (Mo, W) could be evaluated. It was established that ferrocene (5.0 wt.%) generated a maximum of 60 % CNTs, (as well as CSs) under our reaction conditions.

Table 3.2: Effect of Fc/Mo bimetallic catalyst on the synthesis of CNTs and CSs

Metal content[a]	Temperature (°C)	Notes[b]	Mean diameter[c] (nm)
$Fc:Mo(CO)_6$ (9:1)	800	Tubes (60%)	525
10 wt.%	900	Graphite	
$Fc:Mo(CO)_5{}^tBuCN$	700	Spheres (30%), a-C (70%)	600
(1:1) 5.0 wt.%	800	Spheres (40%), a-C (60%)	625
	900	Spheres (50%), tubes (10%), a-C (50%)	750S, 300T
$Fc:Mo(CO)_5{}^tBuCN$	700	No carbon deposit	
(1:2) 7.5 wt.%	800	Spheres (50%), tubes (10%), a-C (40%)	1.2 µmS, 250T
	900	Spheres (50%), tubes (20%), a-C (30%)	700S, 200T
$Fc:Mo(CO)_5{}^tBuCN$	700	No carbon deposit	

Table 3.2 Contd.

(2:1) 7.5 wt.%	800	Spheres (40%), tubes (20%), a-C (40%)	750S, 250T
	900	Spheres (50%), tubes (30%), a-C (20%)	475S, 250T
Fc:$Mo(CO)_5{}^tBuCN$	700	Tubes (60% , very low yield), a-C (40%)	50
(10:1) 5.0 wt.%	800	Spheres (30%), tubes (50%), a-C (20%)	500S, 300T
	900	Spheres (70%), tubes (20%), a-C (10%)	700S, 200T
Fc:$Mo(CO)_5{}^tBuCN$	700	Spheres (20%), tubes (40%), a-C (40%)	500S,
(50:1) 5.0 wt.%	800	Spheres (60%), tubes (30%), a-C (10%)	600S,
	900	Spheres (50%), tubes (40%), a-C (10%)	500S, 250T

[a]Fc = ferrocene; [b]a-C = amorphous carbon; [c]T = tubes, S = spheres; Injection flow rate = 0.8 ml/min, H_2 flow rate = 100 ml/min

Reactions were then performed at different metal ratios, flow rates and temperatures to evaluate the effect of Fe/Mo and Fe/W mixed metals on CNT and CS synthesis (Tables 3.2 and 3.3). Figure 3.2 shows a SEM image of a product revealing both CNTs and CSs. All the CNTs produced were MWCNTs (Figure 3.2 and 3.3). While the ratio, and size, of the CNTs/CSs varied, all reactions gave similar shaped products. The diameters of CNTs are widely distributed compared with the CNTs that have been reported using different heterogeneous Fe-Mo bimetallic catalysts and other synthetic techniques [18b, 22]. Further, the diameters of the CNTs and CSs have changed relative to the diameters of CNTs and CSs formed from Fc alone (800 ^oC and 900 ^oC, Tables 3.1 and 3.3). The inner diameters of these tubes ranged from 8 to 12 nm.

Table 3.3: Effect of Fc/W bimetallic catalyst on the synthesis of CNTs and CSs

Metal content[a]	Temperature (°C)	Notes[b]	Mean diameter[c] (nm)
Fc:$W(CO)_5{}^tBuCN$	700	Spheres (40%), a-C (60%)	800
(1:1) 5.0 wt.%	800	Spheres (40%), a-C (60%)	500
	900	Spheres (50%), a-C (60%)	750
Fc:$W(CO)_5{}^tBuCN$	700	No carbon deposit	
(1:2) 7.5 wt.%	800	Spheres (50%), a-C (50%)	500
	900	Spheres (40%), tubes (10%), a-C (50%)	650S, 500T
Fc:$W(CO)_5{}^tBuCN$	700	No carbon deposit	
(2:1) 7.5 wt.%	800	Spheres (30%), tubes (20%), a-C (50%)	500S, 167T
	900	Spheres (50%), tubes (10%), a-C (40%)	667S, 467T
Fc:$W(CO)_5{}^tBuCN$	700	Spheres (30%), a-C (70%)	500
(10:1) 5.0 wt.%	800	Spheres (30%), tubes (50%), a-C (20%)	500S, 200T
	900	Spheres (60%), tubes (30%), a-C (10%)	625S, 333T
Fc:$W(CO)_5{}^tBuCN$	700	Spheres (50%), tubes (20%), a-C (30%)	700S, 300T
(50:1) 5.0 wt.%	800	Spheres (60%), tubes (30%), a-C (10%)	333S, 300T
	900	Spheres (70%), tubes (30%)	375S, 250T

[a]Fc = ferrocene; [b]a-C = amorphous carbon; [c]T = tubes, S = spheres; Injection flow rate = 0.8 ml/min, H_2 flow rate = 100 ml/min

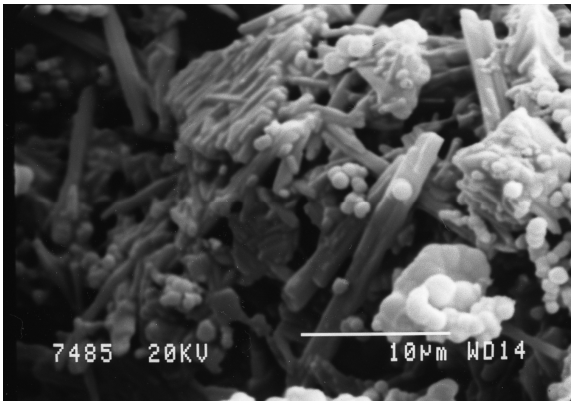

Figure 3.2: SEM image of CSs and CNTs (800 °C, Fc:$Mo(CO)_5$ ^{t}BuNC (2:1) 7.5 wt.%)

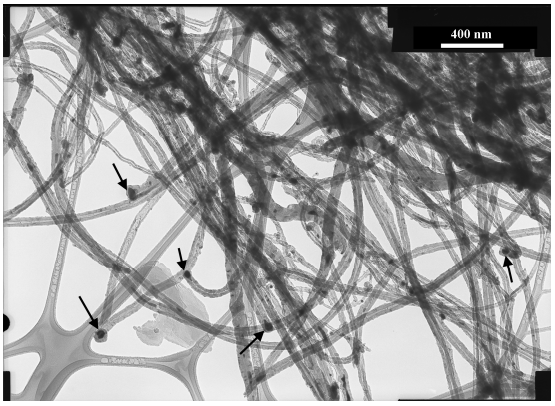

Figure 3.3: TEM image of CNTs (700 °C, Fc:$Mo(CO)_5$^{t}BuNC content: (10:1) 5 wt.%)

Figure 3.3 shows a TEM image of the 'spaghetti' like arrangement of the CNTs produced from Fc/Mo (10:1; 5%) at 700 ^{o}C. The metal particles (diameter range of 40-80 nm) are clearly seen both at the ends and in the tubes [23] (indicated by arrows). Similar TEM images are observed for the products produced at 800 ^{o}C (similar reaction conditions).

Toluene conversion catalysed by Fc:$W(CO)_5$^{t}BuNC gave a very low yield of tubes (700–900 ^{o}C; all ratios) and CSs. These results indicate that W metal is not a good catalyst for nanotube synthesis.

In the Fe/Mo catalysed reaction, variation of the product distribution was found as a function of position in the reactor. The products collected in the low temperature region of the reactor indicated the presence of more CNTs than CSs. The diameters of the CSs found in the high temperature region were found to be widely distributed compared to the diameter of the carbon spheres formed in the low temperature region. CSs in the high temperature region have diameters in the range of 250-3000 nm while CSs collected in the low temperature region have a diameter range of 250-700 nm. The diameters of CNTs collected from the high temperature region (17-500 nm) and the low temperature region (17-400 nm) are similar.

The yield of the carbon materials increased with increasing temperature. It was found that at 800 °C and 900 °C amorphous carbon and graphite were also formed in 20 and 40% relative yield respectively.

Figure 3.4 shows a TEM image of a single, closed, MWCNT (low magnification). The image clearly reveals an inner region (in this case not filled with metal catalyst) surrounded by a layered tube arrangement. A high magnification TEM image of a similar (filled) tube is shown in Figure 3.5, and the inner portion of the tube (dark colouration) was shown by EDS to correspond to the metal catalyst. The tube is made up of about 25 carbon layers.

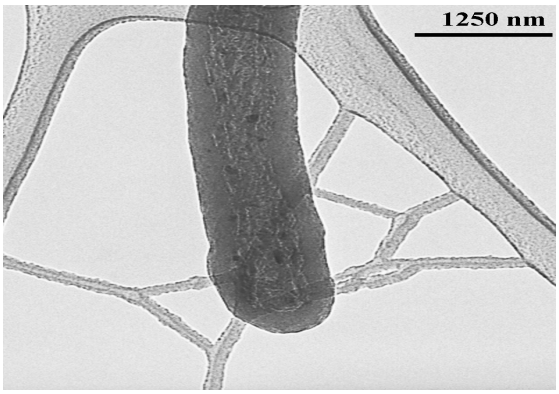

Figure 3.4: TEM image of MWCNT (900 °C, Fc:Mo(CO)$_5$^{t}BuNC content: (10:1) 5 wt.%)

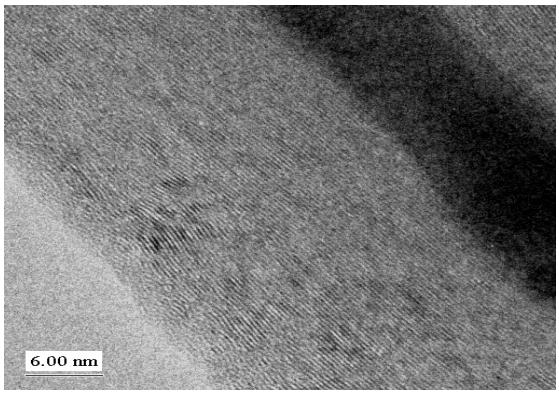

Figure 3.5: HMTEM of MWCNT showing metal particle in the middle of the tube (tube contains about 25 layers; metal completely fills the centre of the tube)

The identity of the metal particles was confirmed by EDS analysis performed by focusing the electron beam onto the individual metal particles. Most metal particles were identified to be Fe and no pure Mo metal particles were observed. However, many particles were shown by EDS to be Fe-Mo metal alloys. The elemental percentage ratio of Fe and Mo (by EDS) varied from 100:0 to 95:5 for the mixed catalyst systems (10:1; 50:1) indicating that the Mo and Fe did indeed interact in the gas phase in a ratio close to that used in the reaction.

Raman analysis

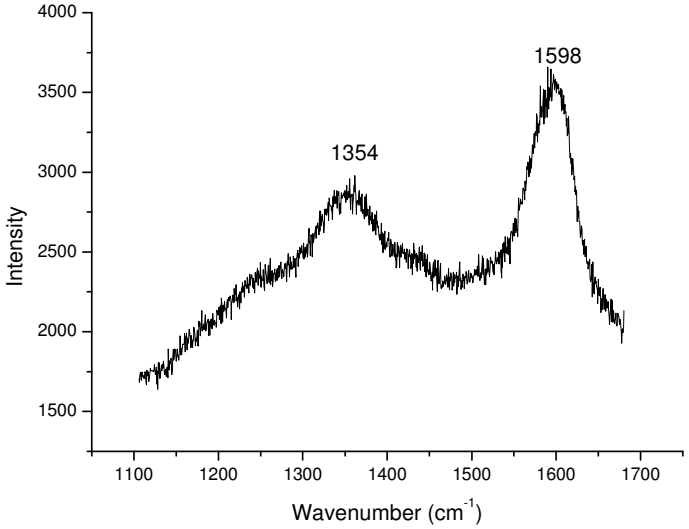

Figure 3.6: Raman spectra of MWCNTs synthesized from Fc:$Mo(CO)_5$^{t}BuCN(10:1); 5 wt%; at 800 °C.

To obtain the information about the disorder of the CNTs, Raman spectroscopy was used (Figure 3.6). The spectrum showed two bands at 1354 cm^{-1} (D band) and 1598 cm^{-1} (G band). The G band originated from the Raman active E_{2g} mode due to in plane atomic displacements. The D band has been explained as a disorder-induced feature due to the finite particle size effect or lattice distortion [24]. The I_D/I_G ratio indicates the degree of disorder of the tubes. Thus, if the ratio approaches 0 the tubes are less disordered but if the ratio value is closer to 1 then the tubes are more disordered. The I_D/I_G ratio of the synthesized CNTs from this study was found to be 0.55 which indicates there is moderate disorder in the tubes.

TGA analysis

Grown MWCNTs were also characterised by thermal gravimetric analysis (TGA) (Figure 3.7). The TGA data shows the decomposition of MWCNTs which occurs at 396 to 575 °C, which is lower than the decomposition of MWCNTs prepared from ferrocene (usually decompose from 410 to 620 °C). This lower decomposition rate could be attributed to the presence of nitrogen (from the ^{t}BuCN functional group) in the CNTs.

The weight loss between 338 and 396 °C indicates the decomposition of amorphous carbon. The remaining 3 wt% is the iron (and possibility of some Mo) catalyst that is in CNTs.

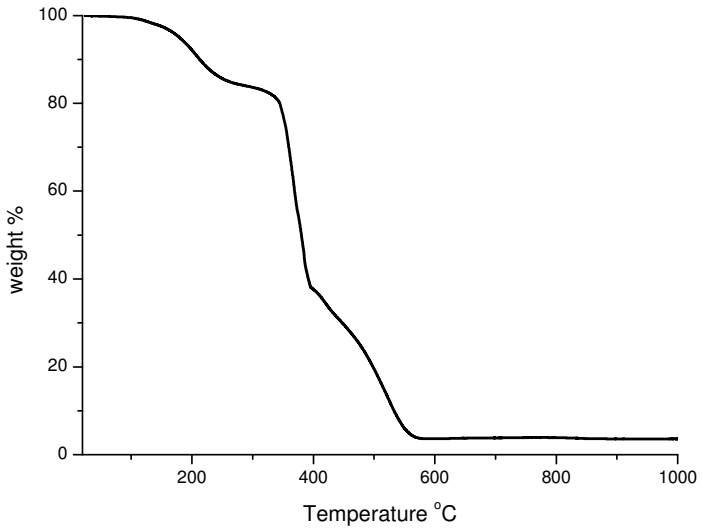

Figure 3.7: TGA of MWCNTs grown from Fc:$Mo(CO)_5{}^tBuCN$(10:1); 5 wt%; at 800 °C.

3.4 Discussion

The choice of reagents used in this study was determined by the following considerations: (i) the solubility of the organometallic complexes in appropriate solvents, (ii) the use of low oxidation state metals, as CNT formation is known to be generated by zerovalent metals (or metal carbides), (iii) the use of a reactive carbon source e.g. toluene to minimize the reaction temperature and (iv) the well known behaviour of the Mo/Fe system, produced by classical deposition methods, to produce SWCNTs.

When ferrocene was used as a catalyst, CNTs as expected were produced. However, no CNTs were produced by pure $M(CO)_5({}^tBuNC)$, and indeed high concentrations of Mo (or W) in ferrocene (1:1, 1:2) resulted in reduced CNT formation. However, when lower Fe/M ratios are used (1:10; 1:50), an increase in CNT production was noted. CSs were also produced in the catalysed reaction but presumably not via a metal catalysed route.

The results for the reactions carried out in this study have been collected together in Tables 3.1-3.3. The data indicate that a small temperature range is available for the maximization of tube formation, with maximum relative tube production generally occurring at 800-900 ^{o}C. There is no correlation between the size (diameter) of the CSs or the CNTs with temperature from our data set. The data do however indicate that a synergic effect exists when the two metals are in close contact with each other. This interaction is confirmed by the detection of Fe/Mo alloys by EDS.

A key difference between the CNTs produced in this study and those produced when heterogeneous supported Mo/Fe complexes are used as catalysts for CNT synthesis is that only MWCNTs were observed in this study. This may relate to the metal particle size produced in the reactor since it is well known that the metal particle size will influence both the internal tube diameter and the type of CNT produced (multi wall, single wall etc.). Large metal particles generate large tubes that tend to be multi-walled, and in the extreme, generate amorphous carbon materials [3a]. It appears that alloy formation in the gas phase results in the formation of larger metal particles than produced from ferrocene alone. This is substantiated by the smaller diameters of the CNTs produced from pure ferrocene (average diameter of 50 to 167 nm) relative to those produced from Fe/Mo or Fe/W mixtures (>150 nm). The mechanism for CNT production is known in some detail and in the case of CVD, Fe catalysts tube growth is anticipated to occur by both tip and base growth mechanisms [25].

While the effect of an alloy of Fe on the CNT formation mechanism is not known, the following is to be noted: (i) most metal particles were found at the tip of a tube and inside a tube (Figure 3.3) - this implies that the mechanism to produce CNTs from alloys is substantially the same as that to produce CNTs from Fe, and (ii) fewer tubes were formed from Fe-Mo metal alloys than produced from Fe metal particles. This must relate to an inhibiting effect that Mo has on CNT growth, an effect indicated by use of the pure metal. Our results thus reveal the impact that a Mo/Fe alloy has on CNT production. The Mo modifies the behaviour of the Fe to generate larger metal particles and hence larger tubes. The key to high CNT production with this system will thus entail better control of the

particle sizes and metal content ratios produced in the gas phase. This suggests that the use of gas phase organometallic metal clusters may be more appropriate catalysts for controlled CNT synthesis, and studies in this direction have been commenced.

3.5 Conclusion

A series of experiments were performed in which mixtures of ferrocene and $M(CO)_5{}^tBuNC$ (M = Mo, W) were decomposed in the presence of toluene at high temperature (700–900 ^oC). From the experiments the following conclusions can be drawn: (i) in the absence of metal, CSs were formed from toluene, (ii) the low solubility of $Mo(CO)_6$ prevented formation of any carbonaceous materials from this metal source in the temperature range 700-900 °C, (iii) the single metal catalysts, $M(CO)_5{}^tBuNC$, produced only CSs and (iv) CNTs were mainly synthesized by Fc or Fc-Mo bimetallic mixtures. TEM results revealed that metal particles, comprising of Fe or Fe-Mo alloys were present in the MWCNTs produced. The large size of the particles produced in this study is believed to be responsible for the limited formation of CNTs produced in the reaction.

3.6 References

[1] (a) Cassell, A. M.; Raymakers, J. A.; Kong, J.; Dai, H. J. *J. Phys. Chem. B* **1999**, *103*, 6484. (b) Colomer, J. F.; Stephan, C.; Lefrant, S.; Van Tendeloo, G.; Millems, I.; Konya, Z. et al. *Chem. Phys. Lett.* **2000**, *31*, 83.

[2] (a) Kiang, C. H.; Goddard III, W. A.; Beyers, R.; Salem, J. S.; Bethume, D. S. *J. Phys. Chem. Solids* **1996**, *57*, 35. (b) Flahaut, E.; Govindaraj, A.; Peigney, A.; Laurent, Ch.; Rousset, A.; Rao, C. N. R. *Chem. Phys. Lett.* **1999**, *300*, 236. (c) Cassell, A. M.; Raymakers, J. A.; Kong, J.; Dai, H. *J. Phys. Chem. B* **1999**, *103*, 6484. (d) Su, M.; Zheng, B.; Liu, J. *Chem. Phys. Lett.* **2000**, *322*, 321. (e) Peréz-Mendoza, M.; Vallés, C.; Maser, W. K.; Martínez, M. T.; Langlois, S.; Sauvajol, J. L.; Benito, A. M. *Carbon* **2005**, *43*, 3002.

[3] (a) Dai, H.; Rinzler, A. G.; Nikolaev, P.; Thess, A.; Colbert, D. T.; Smalley, R. E. *Chem. Phys. Lett*. **1996,** *260*, 471. (b) Rodriguez, N. M. *J. Mater. Res*. **1993**, *8*, 3233. (c) Kitiyanan, B.; Alvarez, W.E.; Harwell, J.H.; Resasco, D.E.; *Chem. Phys. Lett.,* **2000**, *317*, 497. (d) Lan, A.; Iqbal, Z.; Aitouchen, A.; Libera, M.; Grebel, H. *Appl. Phys. Lett*. **2002**, *81*, 433. (e) Alvarez, W. E.; Kitiyanan, B.; Borgna, A.; Resasco, D. E. *Carbon* **2001,** *39,* 447.

[4] Serquis, A.; Liao, X. Z.; Huang, J. Y.; Jia, Q. X.; Peterson, D. E.; Zhu, Y. T. *Carbon* **2003**, *41*, 2635.

[5] Ago, H.; Ohshima, S.; Tsukuagoshi, K.; Tsuji, M.; Yumura, M. *Curr. Appl. Phys*. **2005**, *5*, 128.

[6] Herrera, J. E.; Resasco, D. E. *J Phys. Chem. B* **2003**, *107*, 3738.

[7] Li, Y.; Zhang, X. B.; Tao, X. Y.; Xu, J. M.; Huang, W. Z.; Luo, J. H.; Luo, Z. Q. Li, T.; Liu, F.; Bao, Y.; Gise, H. J. *Carbon* **2005**, *43*, 295.

[8] (a) Soneda, Y.; Duclaux, L.; Béguin, F. *Carbon* **2002**, *40*, 965. (b) Chen, P.; Zhang, H. B.; Lin, G. D.; Hong, Q.; Tsai, K. R. *Carbon* **1997**, *35*, 1495.

[9] Jeong, H. J.; Kim, K. K.; Jeong, S. Y.; Park, M. H.; Yang, C. W.; Lee, Y. H. *J. Phys. Chem. B* **2004**, *108*, 17695.

[10] Lyu, S. C.; Liu, B. C.; Lee, C. J.; Kang, H. K.; Yang, C. W.; Park, C. Y. *Chem. Mater*. **2003**, *15*, 3951.

[11] Lamouroux, E.; Serp, P.; Kihn, Y.; Kalck, P. *Catal. Commun*. **2006**, *7*, 604.

[12] Liu B. C.; Lyu, S. C.; Lee, T. J.; Choi, S. K.; Eum, S. J.; Yang, C. W.; Park, C. Y.; Lee, C. J. *Chem. Phys. Lett.* **2003**, *373*, 475.

[13] Hafner, J. H.; Bronikowski, M. J.; Azamian, B. R.; Nikolaev, P.; Rinzler, A. G.; Colbert, D. T.; Smith, K. A.; Smalley, R. E. *Chem. Phys. Lett.* **1998,** *296*, 195.

[14] Lyu, S. C.; Liu, B. C.; Lee, S. H.; Park, C. Y;, Kang, H. K.; Yang, C. W.; Lee, C. J. *J. Phys. Chem. B.* **2004**, *108*, 2192.

[15] Lyu, S. C.; Liu, B. C.; Lee, S. H.; Park, C. Y.; Kang, H. K.; Yang, C. W.; Lee, C. J. *J. Phys. Chem. B*. **2004**, *108*, 1613.

[16] Yu, H.; Zhang, Q.; Zhang, Q.; Wang, Q.; Ning, G.; Luo, G.; Wei, F. *Carbon* **2006**, *44*, 1706.

[17] (a) Mabudafhasi, M. L.; Bodkin, R.; Nicolaides, C. P.; Liu, X. Y., Witcomb, M. J.; Coville, N. J. *Carbon* **2002**, *40*, 2737. (b) Liu, X.Y.; Huang, B. C.; Coville, N. J. *Fullerenes nanotubes and carbon nanostructure* **2002**, *10*, 339. (c) Liu, X. Y.; Huang, B. C. Coville, N. J. *Carbon* **2002**, *40*, 2791.

[18] (a) Qian, W.; Liu, T.; Wei, F.; Wang, Z.; Li, Y. *Appl. Catal. A* **2004**, *258*, 121. (b) Lacerda, R. G.; Teh, A. S.; Yang, M. H.; Teo, K. B. K.; Rupesinghe, N. L.; Dalal, S. H.; Koziol, K. K. K.; Roy, D.; Amaratunga, G. A. J.; Milne, W. I. *Appl. Phys. Lett*. **2004**, *84*, 269. (c) Cui, H.; Eres, G.; Howe, J. Y.; Puretkzy, A.; Varela, M.; Geohegan, D. B.; Lowndes, D. H. *Chem. Phys. Lett.* **2003**, *374,* 222.

[19] Albers, M. O.; Singleton, E.; Coville, N. J. *J. Chem. Edu*. **1986**, *63*, 444.

[20] Nerushev, O. A.; Sveningsson, M.; Falk, L. K. L.; Rohmund, F. *J. Mater. Chem*. **2001**, *11*, 1122.

[21] Cheng, H. M.; Li, F.; Su, G.; Pan, H. Y.; He, L. L.; Sun, X.; Dresselhaus, M. S. *Appl. Phys. Lett*. **1998**, *72*, 3282. (b) Zhu, H. W.; Xu, C. L.; Wu, D. H.; Wei, B. Q.; Vajtai, R.; Ajayan, P. M. *Science* **2002**, *296*, 884.

[22]. (a) Qian, W.; Liu, T.; Wei, F.; Wang, Z.; Yu, H.; *Carbon* **2003**, *CO1-848*, 846. (b) Seidel, R.; Duesberg, G. S.; Unger, E.; Graham, A. P.; Liebau, M.; Kreupl, F. *J. Phys. Chem. B*. **2004**, *108*, 1888. (c) Liu, B. C.; Lyu, S. C.; Jung, S. I.; Kang, H. K.; Yang, C. W.; Park, J. W.; Park, C. Y.; Lee, C. J. *Chem. Phys. Lett.* **2004**, *383*, 104.

[23] Ci, L.; Wei, B.; Liang, J.; Xu, C.; Wu, D. *J. Mat. Science Lett*. **1999**, *18*, 797.

[24] Dresselhaus, M. S.; Dresselhaus, G.; Jorio, A.; Souza, F. et al. *Carbon* **2002**, *40*, 2043.

[25] (a) Louchev, O. A.; Sato, Y.; Kanda, H. *Appl. Phys. Lett.* **2002,** *80*, 2772. (b) Louchev, O. A.; Laude, T.; Sato, Y.; Kanda, H. *J. Chem. Phys.* **2003,** *118*, 7622. (c) Endo, M.; Hayashi, T.; Kim, Y. A.; Terrones, M.; Dresselhaus, M. S. *Phil. Trans. R. Soc. Lond*. A **2004,** *362*, 2223.

3.7 Appendix

Synthesis of $M(CO)_5(^tBuNC)$ (M = Mo or W) [19]

The catalyst PdO (0.02 g, 0.16 mmol), $[M(CO)_6]$ (2.0 mmol) M = W (0.70 g) and Mo (0.53 g) and toluene (50 ml) were placed in 100 ml flask. The reaction mixture was stirred and refluxed at 125 °C for 5 min. The appropriate amount of t-butylisonitrile (230 µL, 2.05 mmol) was added to the reaction mixture by micro-syringe. The reaction mixture was heated under reflux until completion of the reaction (as monitored by IR spectroscopy or thin layer chromatography). The mixture was cooled and filtered, and the solvent was removed by rotary evaporator to give the crude product. The product was purified by chromatography using a hexane:CH_2Cl_2 (4:1) mixture to obtain over 70-85% yields for both metals.

$Mo(CO)_5(^tBuNC$)

^{1}H-NMR δ $CDCl_3$: 1.48 (s, 9H, CH_3); **IR** (CH_2Cl_2): ν(CO) = 1958 (s) and 2065 cm^{-1} (w), ν(CN) = 2150 cm^{-1}. **MP** = 115-116 °C.

$W(CO)_5(^tBuNC)$

^{1}H-NMR δ $CDCl_3$: 1.50 (s, 9H, CH_3); **IR** (CH_2Cl_2): ν(CO) = 1952 (s) and 2062 cm^{-1}(w), ν(CN) = 2155 cm^{-1}. **MP** = 131-132 °C.

CHAPTER 4

Carbon nanotube synthesis using ferrocene and ferrocenyl sulphide: The effect of sulphur[1]

4.1 Introduction

The synthesis of carbon nanostructures; whether SWCNTs, DWCNTs, MWCNTs, or CNFs depends on the carbon feedstock, type of metal catalyst, presence of additives as well as reaction temperature used to make the carbon materials. In general, high temperatures (≥ 1000 °C), a low supply of carbon and a small amount of sulphur additive such as thiophene, favour the formation of SWCNTs and DWCNTs, while higher amounts of sulphur favour the formation of MWCNTs and CNFs. Studies on the pyrolysis of various organometallic compounds with sulphur-containing compounds using the floating catalyst method have been widely reported [1]. Early work on the synthesis of carbon fibers revealed that the addition of sulphur enhanced the yield of carbon fibers [2]. The addition of sulphur to a catalyst anode in the arc discharge CNT process was also found to enhance both the yield and the quality of the CNTs produced [3]. Not long afterwards the sulphur addition approach was used in CVD CNT synthesis [1] and since then many studies have been reported on the effect of sulphur on CNT production.

DWCNTs were mass produced by pyrolysis of acetylene on a floating iron catalyst in the presence of sulphur powder as a promoter under an argon atmosphere [4]. DWCNTs were grown using a floating CVD method by adding a small amount of sulphur into ferrocene with methane used as a carbon source and argon as a carrier gas [5]. DWCNTs have been prepared by thermally decomposing ferrocene mixed with a small amount of sulphur in a mixture of argon and acetylene at high temperatures [6]. Long DWCNTs

[1] Mohlala M. S.; Liu, X. Y.; Witcomb, M. J. Coville, N. J. *Applied Organometallics,* **In Press.**

were synthesized by decomposition of ferrocene-xylene solution after the addition of a small amount of sulphur powder under an argon-hydrogen atmosphere [7]. DWCNTs were synthesized by pyrolyzing acetylene on a sulphur-promoted iron catalyst in an argon atmosphere [8].

The carbon nanostructures including SWCNTs, MWCNTs and CNFs were synthesized using a floating catalyst method in the presence of thiophene as a promoter by controlling the ferrocene and benzene mole ratio under hydrogen atmosphere [9]. SWCNTs and CNFs were grown in a floating catalyst method using ferrocene as a catalyst, benzene as a carbon source, hydrogen as a carrier gas and a small amount of thiophene [10]. SWCNTs and MWCNTs have been synthesized by gas phase catalytic reaction of colloidal solutions of Co-Mo nanoparticles in the presence of thiophene using a vertical flow reactor [11]. The reverse micelle solution of the Co-Mo nanoparticles were dissolved in toluene and injected into the reactor under a hydrogen atmosphere. It was observed from the above study that a small percentage of thiophene was effective for SWCNTs growth, while higher amounts favoured MWCNT growth.

MWCNTs have been synthesized by a floating catalyst method using ferrocene as a catalyst precursor, xylene or cyclohexane as carbon feedstocks, hydrogen as a carrier gas and thiophene as a promoter [12]. MWCNTs with junctions were grown from ferrocene-benzene solution in the presence of thiophene under an argon atmosphere using an injection CVD method [13]. Y-junction CNTs have been prepared by decomposition of ferrocene-hexane solution under hydrogen atmosphere with addition of small amount of thiophene [14]. Rao et al. reported on a large scale production of Y-juntion CNTs by the vapour phase pyrolysis of a mixture of cobaltocene or ferrocene with thiophene in an argon-hydrogen atmosphere [1c]. Pyrolysis of Ni- and Fe-phthalocyanines or $Fe(CO)_5$ with thiophene have been found to yield Y-junction nanotubes under an argon-hydrogen atmosphere [15].

While the addition of a low percentage of sulphur to a ‘floating catalyst’ has been shown to increase the yield of the CNTs, large amounts of sulphur reduces the CNT yield [16].

Thiophene [17] and sulphur powder [3b, 6, 8, 18] have been widely used as the sulphur sources. Thiophene has been found to influence the number of CNT walls and provide a means of controlling the formation of SWCNTs [1a, 10, 19] relative to MWCNTs. Indeed sulphur can also influence the number of internal tubes produced (SWCNT versus DWCNT) [1a, 3c, 10, 11] and sulphur powder was found to be essential in the formation of DWCNTs [4, 5, 7, 11]. In some cases, the addition of sulphur compounds can also affect the shape of the CNTs [16b]. Thiophene is also considered to play a key role in forming SWCNT bundles [20] and super long SWCNTs strands [21]. To date a number of mechanisms have been proposed to explain the effect of the sulphur on the reaction. Thus, sulphur is proposed to exert its influence by (i) blocking active sites on the catalyst [22] (ii) by lowering the melting point of the catalyst (a eutectic effect) [2b, 23] or (iii) by interacting with the growing tube/fiber [24]. However, there is no consensus yet on the mechanism of sulphur or other so called 'impurities' in influencing CNT formation.

In an attempt to evaluate the effect of sulphur on the catalytic growth of CNTs using the 'floating catalyst' approach, a study was carried out using ferrocene as a catalyst and sulphur-ring substituted ferrocene as the sulphur source for the reaction. In particular we have used $Fe(C_5H_4SMe)_2$ as our sulphur source since the material (i) can be readily synthesized [25], (ii) is volatile and (iii) is soluble in many CNT carbon sources. Further, it has been suggested that the weak effect of sulphur on CNT production in the floating catalyst method relative to the arc discharge method could be due to time for the benzene and thiophene to meet iron particles, and the contact time between reactants and iron particles is an important factor in fiber formation [26]. This methodology using $Fe(C_5H_4SMe)_2$ should overcome the contact time issue. Herein we report on the use of $Fe(C_5H_4SMe)_2$/ferrocene mixtures for the catalytic synthesis of CNTs (and fibers) from toluene as carbon source. This is a continuation of our attempt [27] and other authors [28] attempts to systematically explore the use of organometallic complexes in the synthesis of CNTs and other tubular, spherical and fiber-like materials.

4.2 Experimental

Ferrocene (Fc) was purchased from Strem Chemicals and used as received**.** The preparation of ferrocenyl sulphide catalyst was carried out as described elsewhere (see Appendix at the end of the Chapter) [25]. Synthesis of CNTs was carried out in the temperature range 800-1000 °C, in 5% H_2 in argon (v/v) (AFROX) at atmospheric pressure. The flow rate of H_2 in argon was kept constant at 100 ml/min. Mixtures of ferrocene and ferrocenyl sulphide with different weight ratios were dissolved in toluene (Merck Chemicals). The catalyst solutions were placed in a 10 ml syringe and injected into the heated tube by means of a SAGE syringe pump (at 0.8 and 0.2 ml/min injection rate). The solutions were injected into the tube reactor via a specially designed quartz tube (2 mm i.d., 200 mm in length), cooled by water, similar to that described in the literature (Figure 2.1, Chapter 2). The solution was injected directly into the high temperature region of the large quartz tube reactor.

The carbon deposited materials formed were scraped from the walls of the quartz tube in both the high temperature region and low temperature region (temperature < 300°C) in the tube. Carbon products were also collected at the rear end of the quartz tube; these products were carried away from the hot zone by the gas stream. The carbon materials were characterized by scanning electron microscopy (SEM) (Jeol JSM-840), low magnification transmission electron microscopy (TEM) (Jeol JEM-100S), high magnification transmission electron microscopy (HMTEM) (Philips CM200), XRD (Philips PW187020/00), Raman spectroscopy (J-Y T64000) and thermal gravimetric analysis (TGA) measurements were performed on a Perkin Elmer TGA 7. The number and size of the carbon materials were obtained from the SEM/TEM micrographs by counting procedures and represent average values. The nanotube yield was calculated from the wt. % of the products obtained relative to the mass of solvent injected into the system.

4.3 Results and discussion

Reference reactions: The reaction performed with ferrocene, Fc, (no S source) gave results consistent with data reported previously for the same system [27b], indicating that Fc/toluene mixtures produced CNTs and amorphous carbon in the temperature regime 800 – 1000 ^{o}C. Products obtained with toluene and no Fc gave only amorphous carbon and carbon microspheres [27c]. Reactions were also attempted with only 1,1'-bis(methylthio)ferrocene, FcS_2Me_2 (1-5 wt %), and in every instance no CNTs were produced. This result is consistent with the poisoning of the iron catalyst by excess sulphur [29].

Effect of Temperature: In a typical reaction, the carbon source (toluene) and the catalysts (mixture of Fc and FcS_2Me_2) were injected into the hot quartz tube reactor, where both carbon source and catalysts were decomposed immediately. The iron atoms were derived from thermal decomposition of ferrocene and 1,1'-bis(methylthio)ferrocene that formed catalyst particles by collision and coalescence. After that the precipitation of carbon begins and carbon nanotubes are formed.

A temperature study was undertaken on the reaction for a given set of reaction conditions (at constant flow rate; constant Fc:FcS_2Me_2 molar ratio). The reaction temperature played a crucial role in the growth of CNTs. The reactions were performed in the temperature range of 800 °C to 1000 °C, and the products formed at 800 °C and 900 °C were mainly amorphous carbon and fibers, while CNTs were formed at 1000 °C. The data indicated that both the quality and quantity of CNTs produced followed expected trends [1a, 4, 6, 10, 11] – the highest yields of CNTs were found at T = 1000 ^{o}C and this temperature was used in the later studies. Zhou et al. reported growth of DWCNTs prepared in a wide temperature range of 950-1150 °C with C_2H_4 as a carbon source by a floating iron catalyst system in the presence of sulphur as a promoter [18a]. They found that at the temperature below 950 °C, only a thin film was formed on the wall of the quartz, while at temperatures above 950 °C the yield as well as the quality of CNTs were enhanced.

Table 4.1: Effect of sulphur containing compounds on CNTs growth[a].

Metal[b]	Injection rate (ml/min)	Notes[c]	Mean diameter[d] (nm)
Fc:FcS_2Me_2	0.8	Tubes (60%), spheres (30%), a-C (10%)	68T (outer), 16 (inner), 120S
(6:1) 5 wt.%	0.2	Tubes (40%), a-C (60%)	44 (outer), 15 (inner)
Fc:FcS_2Me_2	0.8	Tubes (15%), spheres (5%), a-C (80%)	47T (outer), 12 (inner), 200S
(13:1) 5.0 wt.%	0.2	Tubes (30%), a-C (70%)	38 (outer), 13 (inner)
Fc:FcS_2Me_2	0.8	Tubes (20%), a-C (80%)	70T (outer), 30 (inner)
(36:1) 5.0 wt.%	0.2	Tubes- fibers (80%), a-C (20%)	61T (outer), 22(inner), 110F
Fc:FcS_2Me_2	0.8	Tubes (35%) and a-C (65%)	57 (outer), 30 (inner)
(73:1) 5.0 wt.%	0.2	Tubes (40%) and a-C (60%)	79 (outer), 34(inner)
Fc:FcS_2Me_2	0.8	Tubes-fibers (70%), a-C (30%)	80T (outer), 30(inner), 120F
(105:1) 5.0 wt.%	0.2	Tubes-fibers (80%), a-C (20%)	65T (outer), 22 (inner), 120F
Fc:FcS_2Me_2	0.8	Tubes-fibers (60%), a-C (20%), spheres (20%)	76T (outer), 32 (inner), 187F, 280S
(148:1) 5.0 wt.%	0.2	Tubes- fibers (80%), a-C (20%)	30T (outer), 22(inner), 100F
Fc:thiophene	0.8	Tubes-fibers (70%), a-C (30%)	54T (outer), 20 (inner), 130F
(4 :1) 5.0 wt.%	0.2	Tubes-fibers (80%), a-C (20%)	44T (outer), 20(inner), 100F
Fc:sulphur	0.8	Tubes-fibers (90%), a-C (10%)	74T (outer), 20(inner), 110F
(2:1) 5.0 wt.%	0.2	Tubes-fibers (80%), a-C (20%)	42T (outer), 22(inner), 100F

[a]Temperature = 1000 °C; [b]Fc = ferrocene, FcS_2Me_2 = 1,1'-bis(methylthio)ferrocene ; [c]a-C = amorphous carbon, [d]T = tubes, S = spheres, F = fibers ; H_2 flow rate = 100 ml/min

Effect of Fc:FcS_2Me_2 molar ratio: Sulphur has been found to be a key element in producing filamentous carbon by the floating catalyst method and in enhancing the productivity of carbon fibers [10]. The effect of Fc:FcS_2Me_2 molar ratio (6:1 up to 148:1) was investigated (1000 ^oC) at two different flow rates (Table 4.1). In general four types of carbonaceous products were obtained, namely fibers, amorphous carbon, MWCNTs and spheres. In contrast with other literature procedures used in studying sulphur effects, no SWCNTs or DWCNTs were formed in the reaction.

In the yield analysis (Table 4.1), the CNT and fiber yields have been combined. At the lower flow rate (0.2 ml/min) the total amount of carbonaceous material produced generally increased with the Fc:FcS_2Me_2 ratio (Figure 4.1). At the higher flow rate, the total yield of material was less affected by the ratio.

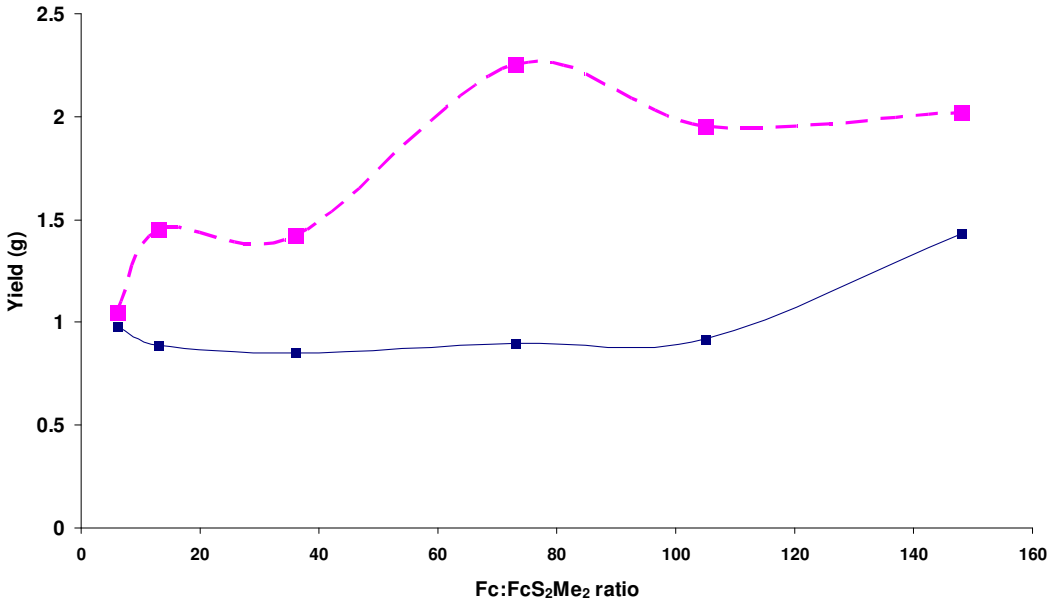

Figure 4.1: CNT/CNF yield versus Fc:FcS_2Me_2 (6:1-148:1) metal ratio, at 1000 °C and injection rate of 0.2 ml/min (- - -) and 0.8 ml/min (–).

More significant is the finding that the yield of fibers and MWCNTs is affected by the catalyst/S ratio (Figure 4.1). In general, at the lower flow rate (0.2 ml/min) the CNT formation remained constant, the amorphous C content decreased and the yield of

carbon fibers increased as the Fc:FcS_2Me_2 molar ratio increased. The optimal ratio appears to be about a 73:1 ratio of Fc:FcS_2Me_2 (Table 4.1) suggesting that the two effects, catalyst poisoning and catalyst activation, are in competition with each other. This is entirely consistent with published literature reports for related systems when S is used as an additive. For example, Ago et al. have studied the effect of thiophene concentration on the formation of CNTs using Co-Mo nanoparticles in a gas phase catalytic reaction [30]. They observed that when the thiophene concentration was low, (1 wt.%) SWCNTs were formed while MWCNTs were formed at high thiophene concentration (10 wt.%).

To further explore this issue, an analysis of the carbon materials was undertaken by TEM analysis (Table 4.1). The TEM analysis visually reveals that the Fc:FcS_2Me_2 molar ratios (and flow rates) influences the width of the CNTs.

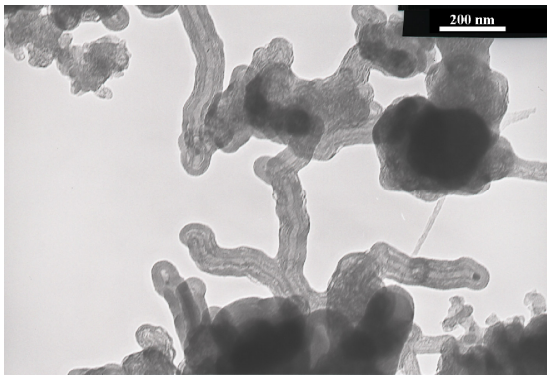

Figure 4.2a: TEM image of CNTs (1000 °C; Fc:FcS_2Me_2: (36:1); 0.8 ml/min; 5 wt.%)

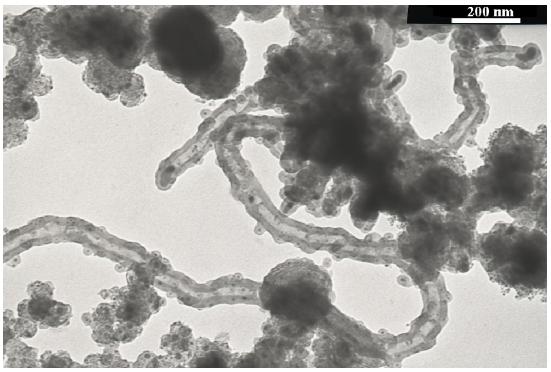

Figure 4.2b: TEM image of CNTs (1000 °C; Fc:FcS_2Me_2: (36:1); 0.2 ml/min; 5 wt.%)

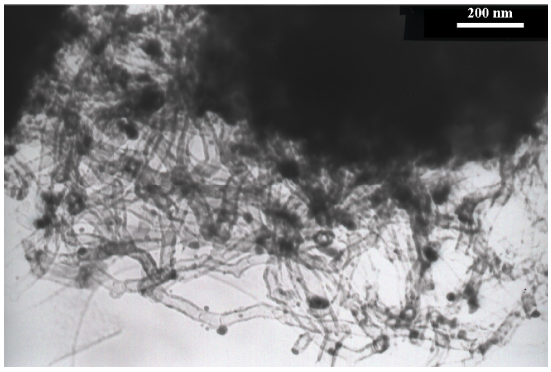

Figure 4.2c: TEM image of CNTs (1000 °C; Fc:FcS_2Me_2: (73:1); 0.8 ml/min; 5 wt.%)

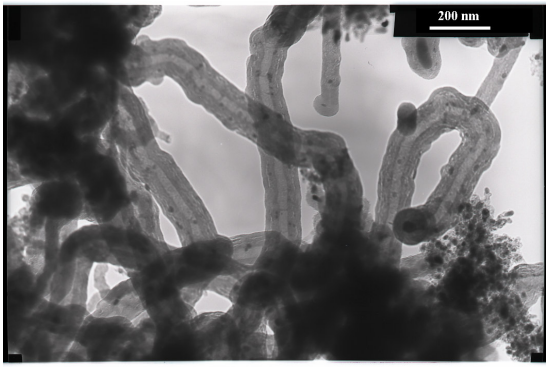

Figure 4.2d: TEM image of CNTs (1000 °C; Fc:FcS_2Me_2: (73:1); 0.2 ml/min; 5 wt.%)

Some examples are shown in Figure 4.2. The mean outer diameters and inner diameters of the CNTs were measured as a function of Fc:FcS_2Me_2 molar ratio (and flow rate). The data obtained with lower flow rate reveal that the diameters of the tubes increase to a maximum and then decrease with Fc:FcS_2Me_2 molar ratio (Figure 4.3). The CNT wall thickness is also influenced by the Fc:FcS_2Me_2 molar ratio and follows the same trend as for the CNT diameters (Figure 4.4). The solid fibers have a larger diameter than the CNTs (100-130 nm) and have no hollow core typical of CNTs.

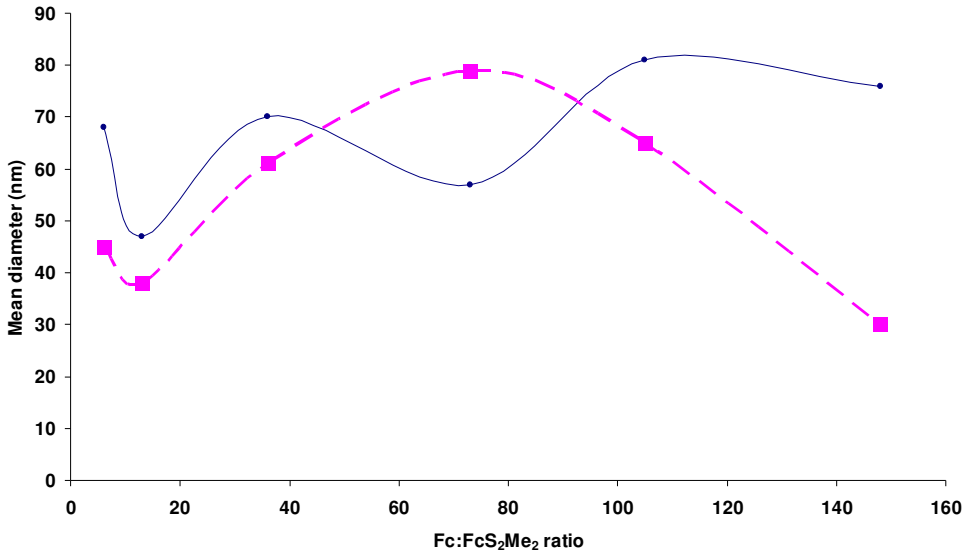

Figure 4.3: Mean diameter of the CNTs versus Fc:FcS_2Me_2 metal ratio (6:1-148:1), at 1000 °C and injection rate of 0.2 ml/min (- - -) and 0.8 ml/min (–).

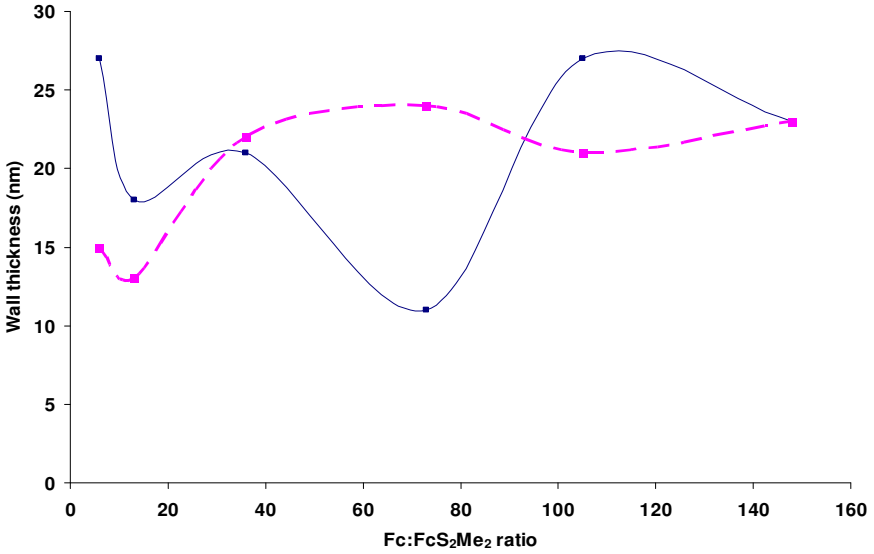

Figure 4.4: Wall thickness of the CNTs versus Fc:FcS_2Me_2 (6:1-148:1) metal ratio, at 1000 °C and injection rate of 0.2 ml/min (- - -) and 0.8 ml/min (–).

The data further reveal that the CNT inner channel, which reflects the size of the catalyst particle, also increases and then decreases in size as the Fc:FcS_2Me_2 molar ratio varies.

EDX analysis of the metal catalyst particles in the tubes only revealed the presence of Fe but not S, showing that the S content of the particles was low. XRD analysis confirmed only the presence of graphitic carbon but not the presence of S or Fe. Fiber formation occurs at the expense of the amorphous carbon, suggesting that the S content reduces the fiber content.

HMTEM analysis of a typical CNT is shown in Figure 4.5. The metal particles were observed at the tip of the tube (and/or in the middle of the tube). Most of the tubes were closed. It can be seen that the material is not well graphitized. The metal particle is surrounded by graphitic material, but the outer layers show the well known 'wavy' behaviour seen in many CNTs.

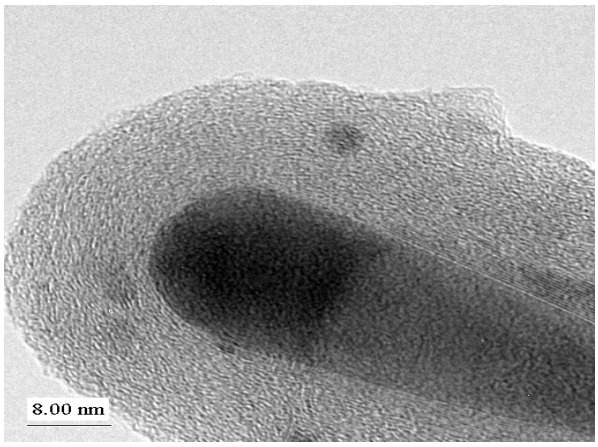

Figure 4.5: HMTEM image of a MWCNT (1000 °C; Fc:FcS_2Me_2: (73:1); 0.8 ml/min; 5 wt.%).

Comparison of different sulphur sources: A comparison of data obtained with different sulphur sources (sulphur source = FcS_2Me_2, S_8, thiophene) at different Fc:S ratios was perfomed (see Figure 4.6 and Table 4.1). The data reveal that when the S source = thiophene (Fc:S = 4:1) or S_8 (Fc:S = 2:1), the carbon products produced are similar (mixture of fibers, amorphous C and MWCNTs). Furthermore, the iron particles that produce the CNTs are both about 20 nm (average) in diameter.

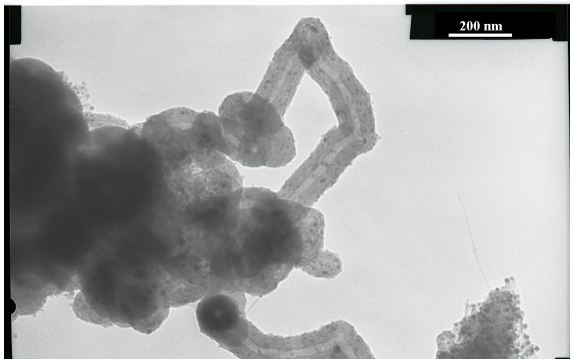

Figure 4.6a: TEM image of CNTs (1000 °C; Fc:thiophene: (4:1); 0.2 ml/min; 5 wt.%)

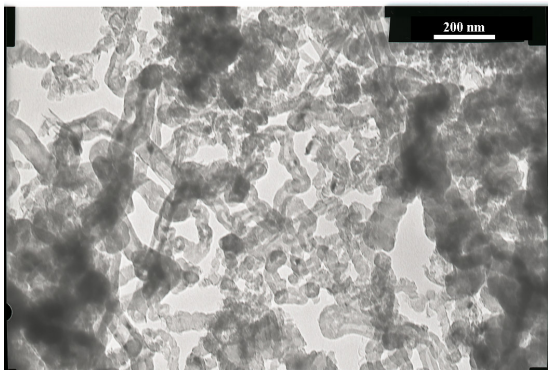

Figure 4.6b: TEM image of CNTs (1000 °C; Fc:sulphur: (2:1); 0.2 ml/min; 5 wt.%)

In contrast, when FcS_2Me_2 is used as the S source at about the same Fc:S ratio (Fc:S = 6:1 and 13:1), the yield of tubes is much lower and no fibrous material is produced. A similar product distribution to that achieved with S = S_8 or thiophene was also obtained *at a lower Fc:S ratio*. Thus, the data for Fc:S ratios of 105:1 and 148:1 (for S = FcS_2Me_2) give carbon deposits similar to that with the 2:1 and 4:1 ratio when the S

source is thiophene or sulphur. Further, TEM analysis showed that the size of iron particle is similar for the 3 different S sources at these differing Fc:S ratios. This confirms that the proximity of the Fe and S in the FcS_2Me_2 modifies the catalyst behaviour. The proximity leads to a better interaction between the Fe and S and thus *much less sulphur is needed to produce the enhanced effects of S on the CNT synthesis.*

Raman analysis

Figure 4.7 shows the Raman spectrum of the synthesized MWCNTs. The tangential stretching mode G band which is the stronger peak in the Raman spectrum is located at 1598 cm^{-1}. The D band of the MWCNTs is located at 1354 cm^{-1}. The ratio between the intensity of the D band and G band (I_D/I_G) can be used to show the degree of crystallization of the carbon materials. In our samples, the I_D/I_G = 0.67, indicating a low crystallization of the grown CNTs, which is consistent with HMTEM image showing less graphitization (Figure 4.5).

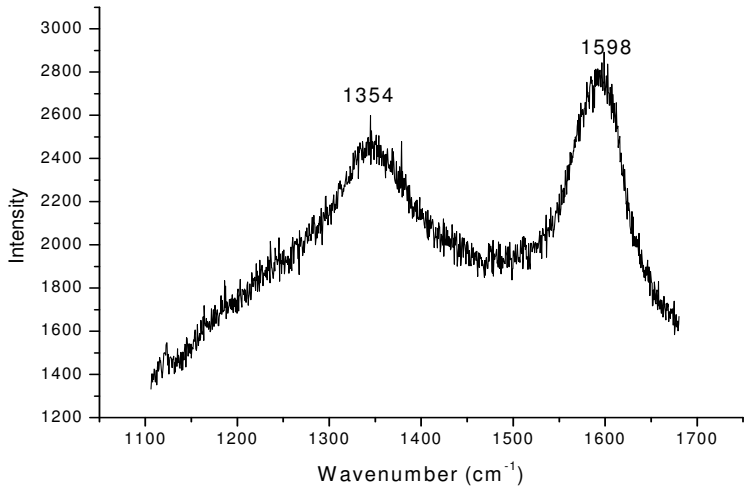

Figure 4.7: Raman spectra of CNTs grown using Fc:FcS_2Me_2: (73:1); 5 wt% , 0.8 ml/min; at 1000 °C.

TGA analysis

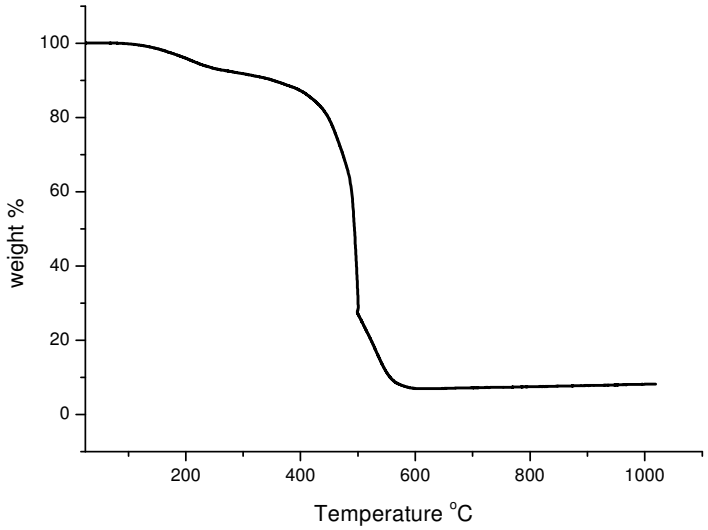

Figure 4.8: TGA of CNTs grown using Fc:FcS_2Me_2: (73:1); 5 wt% , 0.8 ml/min; at 1000 °C.

TGA data were recorded on the unpurified CNTs under oxygen. The TGA profile shows the major weight loss occurs in the temperature ranges of 260-496 °C and 496-577 °C. The weight loss in the 260-496 °C range is due to oxidation of amorphous carbon [31] and the weight loss in the 496-577 °C range is due to the oxidation of CNTs. The residue left after complete carbon oxidation was 7 wt% of the original mass and was due to the iron that was used as catalyst.

4.4 Conclusion

The synthesis of ferrocene moieties that are covalently bound to elements that can influence the synthesis of CNTs provides a route to the control of CNT morphology. In this instance sulphur has been incorporated into a catalyst for CNT synthesis. The sulphur as expected did modify both the tube diameter and the CNT product yield. In our studies, the presence of sulphur gave MWCNTs instead of DWCNTs or SWCNTs [1a, 4, 5, 6, 10, 19]. It has also been shown from the literature that the presence of a sulphur additive increases the diameter of the fibers or carbon nanotubes [3c, 4, 6, 10, 19] and this agrees with our data. It is believed that sulphur enhances the growth of graphitic carbon and thus assists in the synthesis of wide (many layered) CNTs. More importantly it was observed that *less* sulphur was required to induce the changes when compared to using sulphur added from an external source (S_8, thiophene).

4.5 References

[1] (a) Cheng, H. M.; Li, F.; Su, G.; Pan, H. Y.; He, L. L.; Sun, X.; Dresselhaus, M. S. *App. Phys. Lett*. **1998**, *72*, 3282. (b) Ci, L.; Wei, B.; Liang, J.; Xu, C.; Wu, D.; *J. Mater. Science Lett.,* **1999**, *18*, 797. (c) Govindaraj, A.; Rao, C. N. R. *Pure Appl. Chem.* **2002**, *74*, 1571.

[2] Katsuki, K.; Matsunaga, K.; Egashira, M.; Kawasumi, S. *Carbon* **1981**, *19*, 148. (b) Tibbetts, G. G.; Bernado, C. A.; Gorkiewicz, D. W.; Alig, R. L. *Carbon* **1994**, *32*, 569.

[3] (a) Kiang, C.H.; Dresselhaus, M.S.; Beyers, R.; Bethune, D.S. *Chem. Phys. Lett.* **1996,** *259*, 41. (b) Bethune, D. S. *Physica B* **2002**, *323*, 90. (c) Saito, Y.; Nakahira, T.; Uemura, S. *J. Phys. Chem. B.* **2003**, *107*, 931.

[4] Ci, L.; Rao, Z.; Zhou, Z.; Tang, D.; Yan, X.; Liang, Y.; Liu, D.; Yuan, H.; Zhou, W.; Wang, G.; Liu, W.; Xie, S. *Chem. Phys. Lett.* **2002**, *359*, 63.

[5] Wei, J.; Ci, L.; Jiang, B.; Li, Y.; Zhang, X.; Zhu, H.; Xu, C.; Wu, D. *J. Mater. Chem*. **2003**, *13*, 1340.

[6] Zhou, Z.; Ci, L. Chen, X.; Tang, D.; Yan, X.; Liu, D.; Liang, Y.; Yuan, H.; Zhou, W.; Wang, G.; Xie, S. *Carbon* **2003**, *41*, 337.

[7] Wei, J.; Jiang, B.; Wu, D.; Wei, B. *J. Phys. Chem. B* **2004**, *108*, 8844.

[8] Ci, L.; Zhou, Z.; Yan, X.; Liu, D.; Yuan, H.; Song, L.; Wang, J.; Gao, Y.; Zhou, J.; Zhou, W.; Wang, G.; Xie, S. *J. Phys. Chem. B* **2003**, *107*, 8760.

[9] Bai, S.; Li, F.; Yang, Q. H.; Cheng, H. M.; Bai, J. B. *Chem. Phys. Lett.* **2003**, *376,* 83.

[10] Ci, L.; Wei, B.; Liang, J.; Xu, C.; Wu, D. *Carbon* **2001**, *39*, 329.

[11] Ago, H.; Ohshima, S.; Tsukuagoshi, K.; Tsuji, M.; Yumura, M. *Curr. Appl. Phys.* **2005**, *5*, 128.

[12] Chen, Y.; Sun, Z.; Li, Y.N.; Tay, B.K.; *Mater. Chem. Phys.,* **2006**, *98*, 256.

[13] Tapasztó, L.; Kertész, K.; Vértesy, Z,; Horváth, Z. E.; Koós, A. A.; Osváth, Z.; Sárközi, Zs.; Darabont, Al.; Biró, L. P. *Carbon* **2005**, *43*, 970.

[14] Zhu, H.; Ci, L.; Xu, C.; Liang, J.; Wu, D. *Diamond and Related Materials* **2002**, *11*, 1349.

[15] Deepak, F. L.; Govindaraj, A.; Rao, C. N. R. *Chem. Phys. Lett.* **2001**, *345*, 5.

[16] (a) Fan, Y.Y.; Cheng, H. M.; Wei, Y.L.; Su, G.; Shen. Z. H. *Carbon* **2000**, *38*, 789. (b) Motojima, S.; Hasegawa, I.; Kagiga, S.; Monijama, M.; Kawaguchi, M.; Iwanaga, H. *Appl. Phys. Lett*. **1993**, *62*, 2322.

[17] Ren, W.C.; Cheng, H. M. *Carbon* **2002**, *41*, 1657.

[18] (a) Zhou, Z.; Ci, L.; Song, L.; Yan, X.; Liu, D.; Yuan, H.; Gao, Y.; Wang, J.; Liu, L.; Zhou, W.; Wang, G.; Xie, X. *Carbon* **2003**, *41*, 2607. (b) Zhou, Z.; Ci, L.; Song, L.; Yan. X.; Liu, D.; Yuan, H.; Gao, Y.; Wang, J.; Liu, L.; Zhou, W.; Wang, G.; Xie, S. *J. Phys.Chem. B* **2004**, *108*, 10751.

[19] Cheng, H. M.; Li, F.; Sun, X.; Brown, S. D. M.; Pimenta, M. A.; Marucci, A.; Dresselhaus, G.; Dresselhaus, M. S. *Chem. Phys. Lett.* **1998**, *289*, 602.

[20] Zhu, H.; Jiang, B.; Xu, C.; Wu D. *Chem. Comm.* **2002**, 1858.

[21] (a) Wei, B.; Vajtai, R.; Choi, Y. Y.; Ajayan, P. M. *Nano Lett*. **2002**, *1***,** 1105. (b) Zhu, H. W.; Xu, C. L.; Wu, D, H.; Wei, B. Q.; Vajtai, R.; Ajayan, P. M. *Science* **2002**, *296***,** 884.

[22] Kim, M. S.; Rodriguez, N. M.; Baker R. T. K. J. *Catalysis* **1993**, *143*, 449. (b) Ci, L.; Zhu, H.; Wei, B.; Liang, J.; Xu, C.; Wu, D. *Carbon* **1999**, *37*, 1652.

[23] (a) Martin-Gullon, I.; Vera, J.; Conesa, J. A.; Gonzalez, J. L.; Merino, C. *Carbon* **2006**, *44,* 1572. (b) Tibbetts, G. G.; Balogh, M. P. *Carbon* **1999**, *37*, 241.

[24] (a) Hutchinson, J. C.; Kiselev, N. A.; Krinichnaya, E. P.; Krestinin, A. V.; Loutfy, R. O.; Morowsky, A. P.; Muradyan, V. E.; Obraztsova, E. D.; Sloan, J.; Terekhov, S. V.; Zakharov, D. N. *Carbon* **2001**, *39,* 761. (b) Oberlin, A. *Carbon* **1984**, *22*, 521.

[25] McCulloch, B.; Ward, D. L.; Woolins, J. D.; Brubaker Jr., CH. *Organometallics* **1985**, *4*, 1425.

[26] Benissad-Aissani, F.; Ait-Amar, H.; Schouler, M. C.; Gadelle, P. *Carbon* **2004**, *42*, 2163.

[27] (a) Liu, X. Y.; Huang, B. C.; Coville, N. J. *Carbon* **2002**, *40*, 2791. (b) Liu, X. Y.; Huang, B. C.; Coville, N. J. *Fullerenes Nanotubes Carbon Nanostruct*. **2002**, *10,* 339. (c) Mohlala, M. S.; Liu, X. Y.; Robinson, J. M.; Coville, N. J. *Organometallics* **2005**; *24*, 972. (d) Mohlala, M. S.; Liu, X. Y.; Coville, N. J. *J. Organomet. Chem.* **2006***, 691,* 4768.

[28] Huh, Y.; Green, M. L. H.; Lee, J. Y.; Lee, C. J. *Diamond and Related Materials*. **2006**, *15*, 100. (b) Harris, J. D.; Raffaelle, R. P.; Gennett, T.; Landi, B. J.; Hepp, A. F. *Mater. Sci. Eng. B* **2005**, *116*, 369.

[29] Cosyns, J.; Verna, F. *Adv. Catal*. **1990**, *37*, 279.

[30] Ago, H.; Ohshima, S.; Uchida, K.; Komatsu, T.; Yumura, M. *Physica B: Condensed Matter.* **2002**, *323*, 306.

[31] Chen, X. H.; Chen, C. S.; Chen, F. Q.; Zhang, G.; Chen, Z. Z. *Mater. Lett.* **2002**, *57*, 734.

4.6 Appendix

Synthesis of 1,1'-bis(methylthio)ferrocene, (FcS_2Me_2) [25]

Ferrocene (3g, 16 mmol) was added to a solution of N,N,N,N-tetramethylethylenediamine (TMEDA) (5.1 ml, 30 mol) and 1.6 M n-butyllithium in hexane (20.67 ml, 33 mol) in dry hexane (100 ml) in a 250 ml three necked flask under nitrogen. The solution was stirred for 3 h, then methyl disulphide (2.96 ml, 33 mmol) was slowly added through a syringe to give a bright orange solution. The solution was left stirring overnight. The resulting brown solution was filtered and the filtrate was evaporated to dryness. The pure compound was achieved by column chromatography, using a hexane: diethylacetate (5:1) solvent mixture. The product was obtained as brown oil. Yield = 0.790, ca. 30%.

^{1}H-NMR: δ = 4.31 (t, 4H, $H_{2,5}$), 4.22 (t, 4H, $H_{3,4}$), 2.30 (s, 6H, CH_3). **^{13}C-NMR**: δ = 85.21 (s, 2C, C_1), 71.72 (d, 4C, $C_{3,4}$), 69.59 (d, 4C, $C_{2,5}$), 19.35 (q, 2C, CH_3).

CHAPTER 5

Synthesis of multi-walled carbon nanotubes catalyzed by alkyl substituted ferrocenes[1]

5.1 Introduction

It has been shown that transition metals such as iron, cobalt and nickel are the most commonly used catalysts for the growth of carbon nanotubes (CNTs) [1]. Typically, there are two methods for using these metals as catalysts. One entails depositing the metals on a support and then passing a carbon source over the catalyst (chemical vapour deposition, CVD method). The other entails using a volatile source of the metal and adding this source of the metal together with a carbon source into a hot zone where CNTs are then synthesized. This method is called the floating catalyst method. Ferrocene, $Fe(C_5H_5)_2$, has been used extensively as a source of Fe catalyst in this method to produce good yields of CNTs since it is volatile and contains both the metal and a carbon source within its structure. In a floating catalyst method, ferrocene is typically dissolved in a hydrocarbon solvent, such as toluene, hexane, xylene, benzene etc. which serves as the carbon feedstock.

There have been numerous reports in the literature in which the floating catalyst procedure has been used with ferrocene as a catalyst and various hydrocarbons as carbon sources. In one of the earliest reports Rao et al. [2] reported on the pyrolysis of hydrocarbons such as benzene in the presence of ferrocene, cobaltocene and nickelocene in a reductive atmosphere to examine in what way the metal particles from metallocenes catalyze the formation of CNTs. Since then many tens of papers have been published using ferrocene as a catalyst [3], and a brief survey of some of this work is given here.

MWCNTs have been synthesized using a CVD method in which the carbon source was either a solid (e.g. camphor) or a liquid (e.g. cyclohexanol), mixed with ferrocene at around 650 °C under a nitrogen atmosphere [4]. SWCNTs have been successfully

[1]Mohlala M. S.; Liu, X. Y.; Coville, N. J. *Journal of Organometallic Chemistry*, **2006**, *691*, 4768.

synthesized from coal gas with ferrocene as a catalyst and coal acting as a carbon source in a two-furnace system at 900 °C [5]. The growth of vertically aligned SWCNTs has been achieved by catalytic pyrolysis of ferrocene and xylene in the 750-900 °C temperature range [3c]. High purity aligned MWCNTs were also synthesized through the catalytic decomposition of a ferrocene-xylene mixture at ~ 675 °C in a two stage tubular reactor in an H_2/Ar mixture atmosphere [1a]. Vertically aligned MWCNTs were synthesized on quartz glass or an Au film by catalytic decomposition of ferrocene and xylene [6]. It was found that CNTs grown on Au are curled and more separated relative to the tubes grown on quartz glass.

Aligned MWCNT bundles have been obtained in copious quantities by the pyrolysis of ferrocene-acetylene mixtures at a temperature of 1370 K in flowing argon [3e]. SWCNTs without amorphous carbon coating were prepared by thermally decomposing acetylene in the temperature range of 750-1200 °C using ferrocene as a catalyst source in an argon atmosphere [7]. Aligned MWCNTs bundles have been produced by pyrolysis of ferrocene with methane, acetylene or butane at 1373 K under an argon atmosphere [3h]. It was observed that a ferrocene-acetylene mixture was the ideal mixture for the growth of aligned nanotubes bundles. SWCNTs have been produced by pyrolyzing ferrocene-ethanol solutions at 800-950 °C under an argon atmosphere [3d]. The diameters of the tubes formed were mainly influenced by increased ferrocene concentration or by increased pyrolysis temperature. It has been demonstrated that MWCNTs can be produced by pyrolysis of ferrocene in a pure H_2 gas stream through a cylindrical furnace at 1000 °C [8].

A vertical flow reactor has been used to synthesize both carbon fibers and CNTs using ferrocene as a catalyst and organic precursors like xylene, benzene and acetylene as carbon sources under argon or an argon/hydrogen atmosphere [9]. It was reported from this study that when the reaction temperature and ferrocene concentration were low, the well aligned MWCNTs were formed, while at high temperatures, large amounts of low quality CNTs were produced. Aligned MWCNTs (30-130 μm long and 10-200 nm outer diameter) have been synthesized in high yield by pyrolysing homogeneously dispersed aerosols which were generated from benzene/ferrocene solutions, at 800 °C or 950 °C using a compressed gas (Ar) driven

atomizer [1e]. Carbon nanostructures including SWCNTs, MWCNTs and CNFs of different diameters were synthesized by a floating catalyst method by controlling the ferrocene and benzene molar ratio [10]. It was found that the diameters of CNFs and CNTs increased with decreased ferrocene/benzene mole ratio. Nebulized spray pyrolysis has also been used to grow MWCNTs in the temperature range 840-960 °C, using ferrocene-toluene solutions under an argon atmosphere [3f]. Aligned MWCNTs with high purity were grown by injecting a solution of ferrocene in toluene into a horizontal furnace using a H_2/Ar mixture as a carrier gas in the temperature range of 590 to 850 °C [1h]. A ferrocene-toluene solution has been shown to yield a mixture of MWCNTs and aligned MWCNTs under an atmosphere of H_2/Ar in the temperature range 800-1000 °C using a floating catalyst method [3a]. The pyrolysis temperature, ferrocene concentration, solution feeding rate and carrier gas flow rate were shown to influence the yield and the thickness of the CNTs.

Alumina (Al_2O_3) - carbon nanotube composite materials were synthesized by spraying slurry of ferrocene and alumina in xylene, at 1000 °C using argon as a carrier gas, without any post deposition processing [11].

Surprisingly, besides the studies on the ferrocene-based reactions listed above, no other studies on the use of substituted ferrocenes as catalysts in the synthesis of tubular carbon materials have been reported. Some early work reported on the use of Cp_2Co as a catalyst but few studies have been reported to follow up on this study [12].

We have commenced a systematic study of the use of organometallic complexes in the synthesis of tubular and other ‘shaped’ carbons by the floating catalyst method [3a, 13]. In this study we report on the use of alkyl substituted ferrocenes or related metallocenes as catalysts to evaluate the role of the ring substituent on filamentous carbon formation.

5.2 Experimental

Ferrocene (Fc) was purchased from Strem Chemicals; acetylferrocene was purchased from Sigma-Aldrich and used as received**.** Dimethylferrocene [14] and diethylferrocene [15] were synthesized as reported in the literature (see appendix at the end of the chapter). Synthesis of CNTs was carried out in the temperature range 800-1000 °C, under 5% H_2 in Argon (v/v) (AFROX) at atmospheric pressure. The flow rate of H_2 in argon was kept constant at 100 ml/min.

Dimethylferrocene and diethylferrocene were dissolved in toluene at weight percentages of 5 wt% and 10 wt%. The catalyst solutions were placed in a 10 ml syringe and injected into the heated quartz tube by means of a SAGE syringe pump (at 0.8 and 0.2 ml/min injection rate). The solutions were injected into the tube reactor via a specially designed quartz tube (2 mm i.d., 200 mm in length), cooled by water. This tube enabled the solution to be injected directly into the high temperature zone of the large quartz tube reactor.

The carbon materials formed were scraped from the inner walls of the quartz tube in both the high temperature region and low temperature region (temperature < 300 °C) in the tube. Carbon products were also collected at the rear end of the quartz tube; these products were carried away from the hot zone of the furnace by the gas stream. The carbon materials were characterized by low magnification transmission electron microscopy (TEM; Jeol JEM 100S), Raman spectroscopy (J-Y T64000) and thermal gravimetric analysis (TGA) measurements were performed on Perkin Elmer TGA 7. The number and size of the carbon materials were obtained from the TEM images by counting procedures and represent average values.

5.3 Results and discussion

A range of ring substituted ferrocenes have been evaluated for making filamentous carbons (CNTs, CFs). In particular ferrocenes, (CpR)(CpR')Fe, with R and R' = H, Me, Et and COMe have been evaluated for MWCNT synthesis in the reaction. The carbon source chosen for the study was toluene, as it has been shown to be a good carbon source in the temperature range 800 to 1000 ^{o}C [13a]. In the reaction, the iron catalyst and toluene (5 and 10 wt% Fe conc.) were injected into the high temperature quartz reactor at two different flow rates (0.8 and 0.2 ml/min).

Ferrocene, which is currently regarded as a standard Fe catalysts source in CNT synthesis, was also tested for CNT synthesis capabilities to provide a standard to compare with the substituted ferrocene complexes.

Table 5.1: Effect of substituted ferrocene on CNTs growth.

Metal Content[a]	Temperature (°C)	Injection rate (ml/min)	Notes[b]	Mean diameter[c] (nm)	Yield (g)
$FcMe_2$, 5.0 wt%	800	0.8	A-C (50%), tubes (50%)	22T	0.087
		0.2	A-C (30%), tubes (60%), fibers (10%)	21T, 100F	0.165
	900	0.8	A-C (80%), tubes (10%), fibers (10%),)	25T,100F	0.197
		0.2	A-C (95%), fibers (5%)	120F	0.256
	1000	0.8	A-C (70%), fibers (30%)	140F	0.848
		0.2	A-C (70%), fibers (30%)	120F	1.302
$FcMe_2$, 10 wt%	800	0.8	A-C (60%), tubes (40%)	17T	0.529
		0.2	A-C (40%), tubes (30%)	22T	0.585
	900	0.8	A-C (95%), tubes (5%)		0.413
		0.2	A-C (40%), tubes (60%)	25T	0.467
	1000	0.8	A-C (70%), tubes (10%), fibers (15%)	50T, 120F	1.150
		0.2	A-C (65%), tubes (5%), fibers (30%)	46T, 120F	1.987
$FcEt_2$, 5 wt%	700 and 800	0.8 and 0.2	No carbon deposit		
	900	0.8	A-C (65%), spheres (25%), fibers (10%)	200S, 150F	0.357
		0.2	A-C (70%), spheres (20%), fibers (10%)	210S, 150F	0.417
	1000	0.8	A-C (80%), spheres (10%), fibers (10%)	200S, 120F	1.432
		0.2	A-C (80%), spheres (15%), fibers (5%)	200S, 140F	1.457
Fc, 5.0 wt%	800	0.8	A-C (10%), tubes (70%), fibers (20%)	45T, 100F	0.008
		0.2	A-C (30%), Tubes (50%), fibers (20%)	43T, 120F	0.012
	900	0.8	A-C (80%), fibers (20%)	120F	0.359
		0.2	A-C (80%), tubes (10%), fibers (10%)	37T, 130F	0.394
	1000	0.8	A-C (80%), fibers (20%)	140F	1.235

Table 5.1 Contd.

		0.2	A-C (60%), tubes (5%), fibers (35%)	60T, 120F	1.152
Fc,10 wt%	800	0.8	A-C (20%), tubes (70%), fibers (10%)	42T,120F	0.504
		0.2	A-C (40%), tubes (60%)	33T	0.572
	900	0.8	A-C (10%), tubes (80%), fibers (10%)	38T, 120F	0.906
		0.2	A-C (40%), tubes (50%), fibers (10%)	33T,140F	0.924
	1000	0.8	A-C (90%), fibers (10%)	120F	1.818
		0.2	A-C (60%), fibers (40%)	140F	0.996
FcAc, 10 wt%	800	0.8	A-C (60%), spheres (40%)	210S	0.081
	900	0.8	A-C (30%), fibers (30%), spheres (40%)	100F, !80S	0.631
	1000	0.8	A-C (20%), fibers (20%), spheres (60%)	120F, 200S	0.861

[a] Fc = ferrocene, $FcMe_2$ = dimethylferrocene, $FcEt_2$ = diethylferrocene, FcAc = acetylferrocene; [b] A-C = amorphous carbon,

[c] F = fibers, T = tubes, S = spheres; H_2 flow rate = 100 ml/min.

The carbonaceous materials produced from all the reactions were weighed (yields given in Table 5.1) and analyzed by SEM and TEM. The compositions of the materials are also given in Table 5.1. In general amorphous carbon, carbon fibers (tubular material which does not show an internal hollow region), MWCNTs and carbon microspheres were produced in different amounts in the reactions. These products are identical to those reported in earlier studies using ferrocene [2, 10]. The average dimensions of the materials produced are also given in Table 5.1.

Ferrocene: Consistent with our earlier study [3a], the reaction produced tubes with micron lengths and diameters of 30-50 nm as well as fibers with larger diameters (100 - 140 nm) (Figures 5.1 and 5.2). No carbon microspheres were noted, even at 1000 ^{o}C. Figures 5.1 and 5.2 show the CNTs formed at 5 wt% and 10 wt% with the injection rate of 0.2 and 0.8 ml/min. It can be observed that the wt% and the injection rate showed no effect in diameters of the tubes and their morphology.

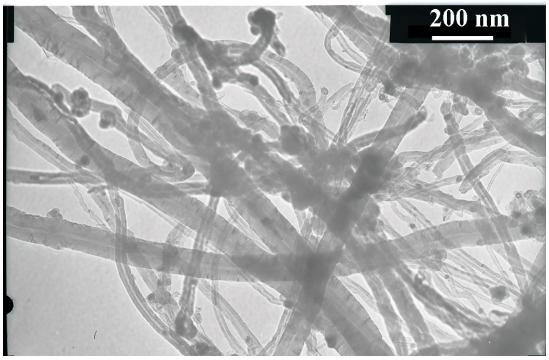

Figure 5.1a: TEM image of CNTs at 800 °C, (ferrocene content: 5 wt.%; 0.2 ml/min injection rate)

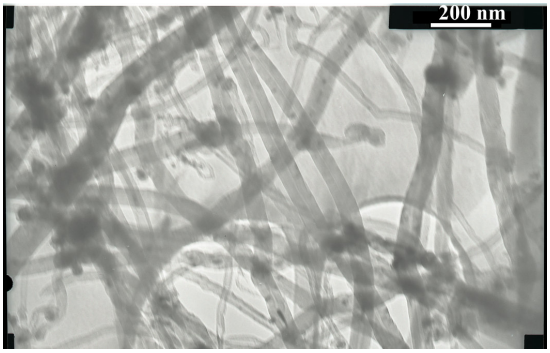

Figure 5.1b: TEM image of CNTs at 800 °C, (ferrocene content: 5 wt.%; 0.8 ml/min injection rate)

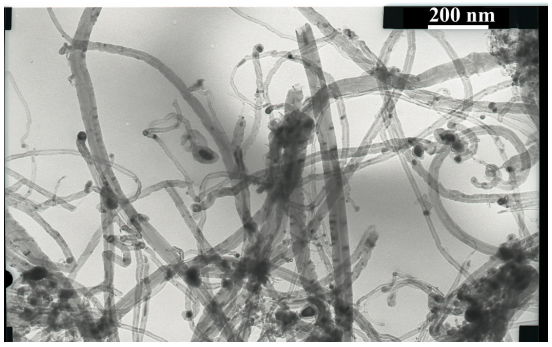

Figure 5.2a: TEM image of CNTs at 800 °C, (ferrocene content: 10 wt.%; 0.2 ml/min injection rate)

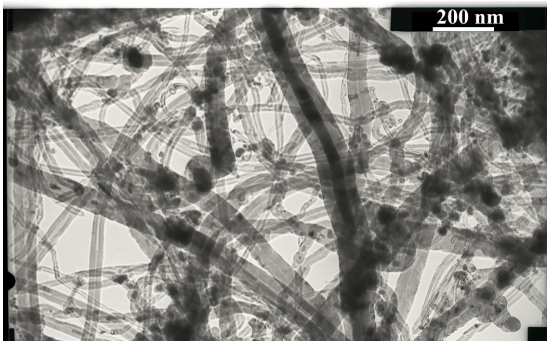

Figure 5.2b: TEM image of CNTs at 800 °C, (ferrocene content: 10 wt.%; 0.8 ml/min injection rate)

Dimethylferrocene. The data reveal that tubes, fibers and amorphous carbon are produced in the reactions (Figures 5.3 and 5.4, Table 5.1). As found for (Figures 5.1 and 5.2) the injection rate and the wt. % Fe had no effect on the diameters of the tubes produced in the reactions.

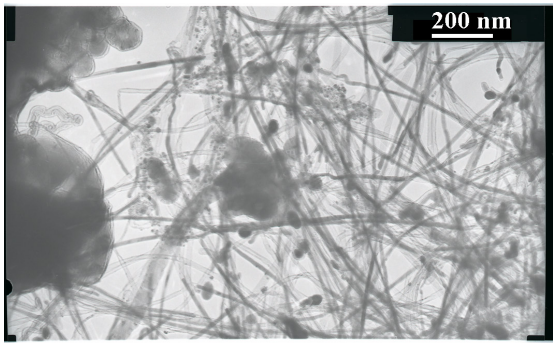

Figure 5.3a: TEM image of CNTs at 800 °C, (dimethylferrocene content: 5 wt.%; 0.2 ml/min injection rate)

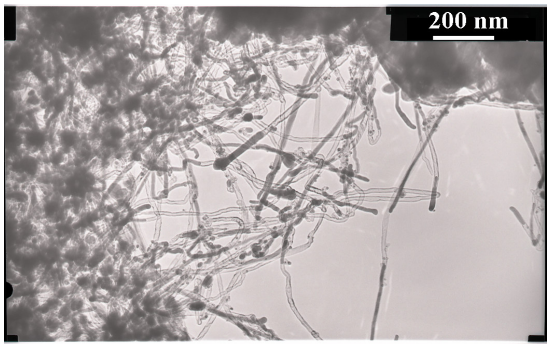

Figure 5.3b: TEM image of CNTs at 800 °C, (dimethylferrocene content: 5 wt.%; 0.8 ml/min injection rate)

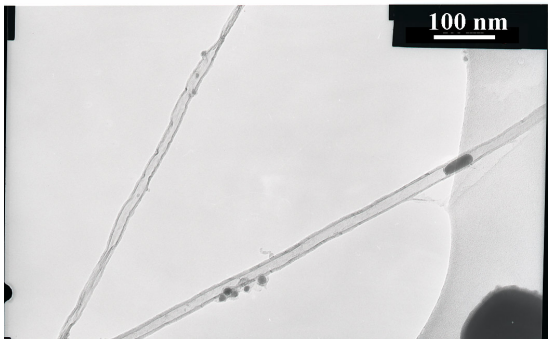

Figure 5.4a: TEM image of CNTs at 800 °C, (dimethylferrocene content: 10.0 wt.%; 0.2 ml/min injection rate)

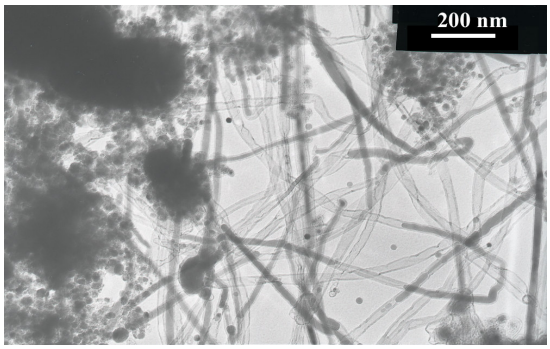

Figure 5.4b: TEM image of CNTs at 800 °C, (dimethylferrocene content: 10.0 wt.%; 0.8 ml/min injection rate)

In summary:

(i) The fibers have the same diameter as those produced from ferrocene (100 - 140 nm). In general the fiber content increased with temperature and with lower Fe content but the flow rate had little effect on the relative fiber yield. The fibers were amorphous rather than graphitic in structure.

(ii) The MWCNTs were, in general, narrower than those produced by ferrocene (typically about 20-25 nm in diameter). The yield decreased with temperature, with lowered Fe content and appeared to be independent of flow rate.

(iii) The overall yields were generally lower than obtained from ferrocene.

Diethylferrocene. A wide range of conditions were studied but no CNTs were formed in this reaction. Carbon microspheres (CSs) and very few carbon fibers were obtained in the temperature range of 900-1000 °C. The diameters of the spheres were about 210 nm and the diameters of the fibers ranged between 100-150 nm (Figure 5.5a)

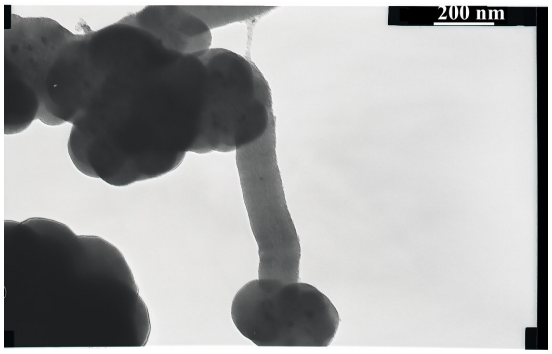

Figure 5.5a: TEM image of CSs at 900 °C, (diethylferrocene content: 5 wt.%; 0.8 ml/min injection rate)

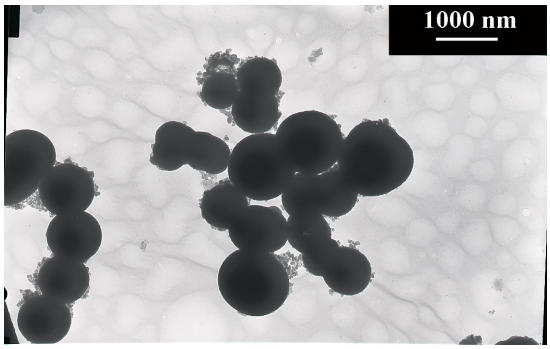

Figure 5.5b: TEM image of CSs at 800 °C, (acetylferrocene content: 5 wt.%; 0.2 ml/min injection rate)

Acetylferrocene. No CNTs were produced in these reactions. The fibers produced had the same dimensions as those described above (100–140 nm). Carbon microspheres were produced at all temperatures (diameter typically about 200 nm, Figure 5.5b), but the yield increased with temperature. This is consistent with other reports on carbon microsphere formation [3a]. The spheres formation does not require an iron catalyst [13a, 16].

Low magnification TEM analysis was performed on samples from all the reactions. Representative TEM pictures are shown in Figures 5.1 to 5.4. After dispersion in a solvent for TEM analysis the products show a mat like appearance, independent of reaction conditions and catalyst used. The lengths of the CNTs could not be easily measured since they were not well aligned. As mentioned above, the CNTs produced from ferrocene have much wider diameters that those produced from dimethylferrocene (see Figures 5.1 to 5.4).

TGA analysis

More quantitative information on the synthesized CNTs was obtained from TGA profiles as shown in Figure 5.6. The thermal decomposition (in air) of CNTs synthesized by dimethylferrocene catalyst showed a major mass loss due to oxidation of CNTs in the interval of 548 to 628 °C. The residual material Fe_2O_3 (4.2 wt.%) was due to oxidation of iron catalyst in air during TGA analysis.

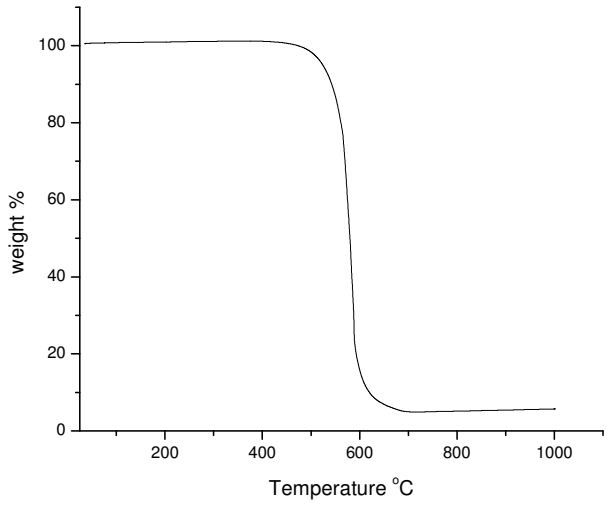

Figure 5.6: TGA profile of CNTs grown using dimethylferrocene (10 wt% , 0.8 ml/min; at 800 °C).

Raman analysis

A Raman spectrum was used to establish the graphitic nature of the CNTs [17]. Thus, a G-peak at about 1590 cm^{-1}, originating mainly from the graphite in plane E_2g vibration mode and a D-peak (at about 1350 cm^{-1}) are attributed to a finite particle size effect and/or structural disorder within the carbon sheet G peak.

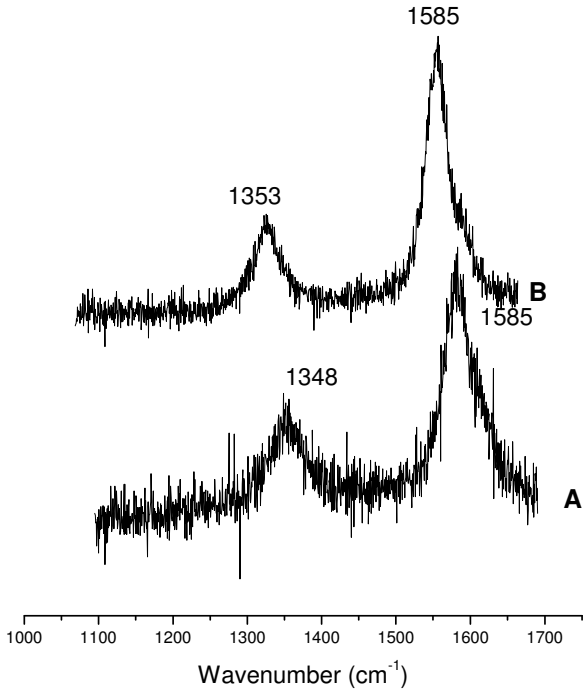

Figure 5.7: Raman spectra of CNTs using (A) dimethylferrocene (10 wt.%), (B) ferrocene (10 wt.%) at 800 °C and 0.8 ml/min injection rate.

The D-peak of the CNTs synthesized from both dimethylferrocene and ferrocene, shown in Figure 5.7, occur at similar positions (about 1350 cm-1). The G-line peak for the CNTs synthesized by both dimethylferrocene and ferrocene appeared at around 1585 cm-1 and the D/G ratio of CNTs synthesized by ferrocene is 0.6 while the D/G ratio of CNTs formed by dimethylferrocene is 0.8. Thus, there is small change in the disorder structure of the two materials, which means CNTs synthesized by dimethylferrocene are more disordered than CNTs formed by ferrocene.

Mechanism of carbon structure formation

The TEM analysis (and other data) also permits for an interpretation of the synthesis data.

(i) Fe particles are found in many of the CNTs. They are generally found at the end of the tube (Figure 5.3) and the type and shape of iron particles are not affected by the ferrocene complexes used. This, as expected, implies that a common mechanism exists for all the catalysts used.

(ii) The iron atoms generated at the high temperatures used, coalesce in the gas phase or on the quartz reactor wall. Once they reach a certain size MWCNTs and fibers commence forming. Control of the metal particle size determines the size of the inner diameter of the tubes and also the number of tubes-within-tubes (MWCNTs) that form. In this case it is apparent that at 800 and 900 ^{o}C, the Fe particles formed from dimethylferrocene are *smaller* than those formed from ferrocene. At the higher temperature (1000 ^{o}C) the particle sizes generated from both catalysts are the same.

(iii) Fiber formation is assumed to be associated with the formation of large iron particles. The data indicate that the synthesis procedure generates particles with a large range of Fe particle sizes. Notwithstanding this, the study still provides *relative* data to assess the effect of ring effects on carbon tubular behaviour.

(iv) The reactions with acetylferrocene lead to the formation of only fibers (no tubes). This implicates the influence of oxygen in the process. The ‘OMe’ group is thus poisoning CNT formation. Reports have, however, shown that CNTs can be grown from alcohols [3d, 18] as carbon source (e.g. ethanol) suggesting that the mere

presence of oxygen atoms in a carbon source is not in itself detrimental to CNT synthesis.

(v) The observation that amorphous carbon and spheres were observed with diethylferrocene as catalyst was unexpected. Indeed, the order for amorphous carbon production follows the sequence: ferrocene < dimethylferrocene < diethylferrocene. This would suggest that ring substituents play a decisive role in tubular carbon formation. However, further studies will be needed to assess whether the observed results are not due to some secondary effect. For example, the volatility of the catalyst sources is quite different - dimethylferrocene has a lower melting point (39-41 °C) than ferrocene (174-176 °C), and therefore it will decompose at lower temperature relative to ferrocene.

(vi) The role of the ring carbon atoms in the CNT synthesis is not known although our data shows that carbon atoms from the Cp ring influence the diameter size of the MWCNTs produced. Isotopic studies have not been performed (by ourselves or others) to evaluate the incorporation of the ring carbon atoms in the tubes using the ferrocene catalysts. However, it is known that the toluene breaks down into smaller carbon fragments/atoms at the high temperatures used. These atoms are proposed to dissolve in the catalyst and precipitate out with formation of the tubular materials [19].

5.4 Conclusions

The effect of ring substitution on the role of ferrocene as catalyst in the formation of tubular carbons has revealed that the substituent can affect the type of carbonaceous material formed. Further, the data show that the ring substituent impacts on the CNT diameter, but does not have an effect on the morphology of the tubes. In all the reactions, injection rate variation did not have any effect on the diameter and morphology of the CNTs formed.

This result suggests that the morphology of CNTs can be influenced by ligands atoms attached to the catalyst. This has implications for the future design of CNT catalysts and the control that may be achieved via this approach to CNT synthesis.

5.5 References

[1] (a) Andrews, R.; Jacques, D.; Rao, A. M.; Derbyshire, F.; Qian, D.; Fan, X.; Dickey, E. C.; Chen, J. *Chem. Phys. Lett*. **1999**, *303*, 467. (b) Kamalakaran, R.; Terrones, M.; Seeger, T.; Kohler-Redlich, Ph.; Rűhle, M. *Appl. Phys. Lett*. **2000**, *77*, 3385. (c) Cao, A.; Ci, L.; Wu, G.; Wei, B.; Xu, C.; Liang, J.; Wu, D. *Carbon* **2001**, *39*, 152. (d) Dickey, E. C.; Grimes, C. A.; Jain, M. K.; Ong, K. G.; Qian, D.; Kichambare, P. D.; Andrews, R.; Jacques, D. *Appl. Phys. Lett*. **2001**, *79*, 4022. (e) Mayne, M.; Grobert, N.; Terrones, M.; Kamalakaran, R.; Rühle, M.; Krato, H. W.; Walton, D. R. M. *Chem. Phys. Lett.* **2001**, *338*, 101. (f) Singh, C.; Shaffer, M.; Kinloch, I.; Windle, A. *Physica B* **2002**, *323*, 339. (g) Wei, B.; Vajtai, R.; Choi, Y. Y.; Ajayan, P. M. Zhu, H.; Xu, C.; Wu, D. *Nano Lett.* **2002**, *2*, 1105. (h) Singh, C.; Shaffer, M. S. P.; Windle, A. H. *Carbon* **2003**, *41*, 359.

[2] Sen, R.; Govindaraj, A.; Rao, C. N. R. *Chem. Phys. Lett.* **1997**, *267*, 276.

[3] (a) Liu, X. Y.; Huang, B. C.; Coville, N. J. *Fullerenes Nanotubes Carbon Nanostruct* **2002**, *10*, 339. (b) Lee, Y. T.; Kim, N. S.; Park, J,; Han, J. B.; Choi, Y. S.; Ryu, H.; Lee, H. J. *Chem. Phys. Lett.* **2003**, *372*, 853. (c) Cao, A.; Zhang, X.; Xu, C.; Liang, J.; Wu, D.; Chen, X.; Wei, B.; Ajayan, P. M. *Appl. Phys. Lett*. **2001**, *79*, 1252. (d) Lupo, F.; Rodriguez-Manzo, J.A.; Zamudio, A.; Elias, A.L.; Kim, Y.A.; Hayashi, T.; Muramatsu, M.; Kamalakaran, R.; Terrones, H.; Endo, M.; Rűhle, M.; Terrones, M.; *Chem. Phys. Lett.,***2005**, *410*, 384. (e) Rao, C. N. R.; Sen, R.; Satishkumar, B. C.; Govindaraj, A. *Chem. Commun*. **1998**, 1525. (f) Vivekchand, S. R. C.; Cele, L.M.; Deepak, F. L.; Raju, A. R.; Govindaraj, A. *Chem. Phys. Lett*. **2004**, *386*, 313. (g) Deepak, F. L.; Govindaraj, A.; Rao, C. N. R. *Chem. Phys. Lett,* **2001**, *345*, 5. (h) Satishkumar, B.C.; Govindaraj, A.; Rao, C.N.R. *Chem. Phys. Lett.* **1999**, *307*, 158. (i) Mondal, K. C.; Coville, N. J. *Submitted for publication*.

[4] Musso, S.; Fanchini, G.; Tagliaferro, A. *Diamond and Related Materials* **2005**, *14*, 784.

[5] Qiu, J.; An, Y.; Zhao, Z.; Li, Y.; Zhou, Y. *Fuel Processing Tech*. **2004**, *85*, 913.

[6] Cao, A.; Ci, L.; Wei, B.; Xu, C.; Liang, J.; Wu, D. *Chem. Phys. Lett*. **2001**, *335*, 150.

[7] Ci, L.; Xie, S.; Tang, D.; Yan, X.; Li, Y.; Liu, Z.; Zou, X.; Zhou, W.; Wang, G. *Chem. Phys. Lett.* **2001**, *349*, 191.

[8] Sano, N.; Akazawa, H.; Kikuchi, T.; Kanki, T. *Carbon* **2003**, *41*, 2159.

[9] Neumayer, H.; Haubner, R. *Diamond and Related Materials* **2004**, *13*, 1191.

[10] Bai, S.; Li, F.; Yang, Q. H.; Cheng, H. M.; Bai, J. B. *Chem. Phys. Lett*. **2003**, *376*, 83.

[11] Kamalakaran, R.; Lupo, F.; Grobert, N.; Lozano-Castello, D.; Jin-Phillipp, N. Y.; Ruhle, M. *Carbon* **2003**, *41*, 2737.

12.(a) Singh, C.; Quested, T.; Boothroyd, C. B.; Thomas, P.; Kinloch, I. A.; Abou-Kandil, A. I.; Windle, A. H. *J. Phys. Chem. B* **2002**, *106*, 10195. (b) Deck, C. P.; Vecchio, K. *Carbon* **2006**, *44*, 267.

[13] (a) Liu, X. Y.; Huang, B. C.; Coville, N. J. *Carbon* **2002**, *40*, 2791. (b) Mohlala, M. S.; Liu, X. Y.; Robinson, J. M.; Coville, N. J. *Organometallics* **2005**, *24*, 972.

[14] McCullosch, B.; Ward, D. L.; Woolins, J. D.; Brubaker, C. H. *Organometallics* **1985**, *4*, 1425.

[15] Bhattacharyya, S. *J. Chem. Soc. Dalton Trans*. **1996**, 4617.

[16] (a) Jin, Y. Z.; Gao, C.; Hsu, W. K.; Zhou, Y.; Huczko, A.; Bystrzewski, M.; Roe, M.; Lee, C. Y.; Acquah, S.; Kroto, H.; Walton, D. R. M. *Carbon* **2005**, *43*, 1944. (b) Qian, H. S.; Han, F. M.; Zhang, B.; Guo, Y. C.; Yue, J.; Peng, B. X. *Carbon* **2004**, *42*, 761.

[17] Belin, T.; Epron, F. *Mater. Sci.Tech.* **2005,** *119*, 105.

[18] (a) Maruyama, S.; Kojima, R.; Miyauchi, Y.; Chiashi, S.; Kohno, M. *Chem. Phys. Lett.* **2002**, *360*, 229. (b) Okazaki, T.; Shinohara, H. *Chem. Phys. Lett.* **2003**, *376*, 606.

[19] (a) Harris, J. D.; Raffaelle, R. P.; Gennett, T.; Landi, B. J.; Hepp, A. F. *Mater. Sci. Eng. B* **2005**, *116*, 369. (b) Wasel, W.; Kuwana, K. Saito, K. *Chem. Phys. Lett*. **2006**, *422*, 470.

5.6 Appendix

Synthesis of 1,1-dimethylferrocene ($FcMe_2$)

To a solution of anhydrous hexane (50 ml) containing ferrocene (2g, 17 mmol) was added n-butyllithium in hexane (20.25 ml, 21 mmol) as well as N,N,N',N'-tetramethylethylenediamine (TMEDA) (3.2 ml, 21 mmol). The reaction was stirred under nitrogen atmosphere for 3 h. MeI (2.9 ml, 20 mmol) was then added to the mixture and the reaction was stirred overnight (14 h). The resulting yellow solution was filtered and the filtrate was evaporated to give the crude product. The crude product was purified by column chromatography using a hexane:diethylacetate (5:1) solvent mixture. Yield = 0.8g, ca. 40%.

^{1}H-NMR: δ = 4.15 (t, 4H, $H_{2,5}$), 3.96 (s, 4H, $H_{3,4}$), 1.96 (s, 6H, CH_3).
^{13}C-NMR: δ = 84.22 (s, 2C, C_1), 69.92 (s, 4C, $C_{3,4}$), 67.54 (s, 4C, $C_{2,5}$), 16.85 (s, 2C, CH_3).

Synthesis of 1,1-diethylferrocene ($FcEt_2$)

Boron trifluoride-diethyl ether (2.84g, 2.5 ml, 20 mmol) was added dropwise to a magnetically stirred solution of the diacetlyferrocene (1.35g, 5 mmol) in anhydrous THF. Sodium cyanotrihydroborate (0.93 g, 1 ml, 10 mmol) was added slowly to the resulting solution over 10 min and the mixture was stirred at r.t for 1 h. The reaction mixture was diluted with dichloromethane (30 ml) and the aqueous ammonia (2 mol/L) was added dropwise until the solution was alkaline (pH = 10) Organic layer was separated and dried over Na_2SO_4. The solvent was removed by vacuum and the crude product was purified by chromatography using a hexane:diethylether (9:1) solvent mixture. Yield = 0.85g, ca. 63%.

^{1}H-NMR: δ = 4.24 (t, 4H, $H_{2,5}$), 4.00 (t, 4H, $H_{3,4}$), 2.36 (q, 4H, CH_2), 1.16 (t, 6H, CH_3).
^{13}C-NMR: δ = 91.35 (s, 2C, C_1), 77.45 (s, 4C, $C_{3,4}$), 77.03 (s, 4C, $C_{2,5}$), 22.53 (s, 2C, CH_2) 15.27 (s, 2C, CH_3).

CHAPTER 6

The use of diisopropylamide and difluoroborate ferrocene substituted compounds as catalysts for the synthesis of doped carbon nanotubes.

6.1 Introduction

Heteroatom doping (e.g., boron, sulfur, phosphorus and nitrogen) of graphitic carbon lattices affects the various physicochemical properties of the sp^2 carbon materials [1]. In particular, doping by nitrogen has received attention because of the significant changes in hardness, electrical conductivity, and chemical reactivity of the CNTs that have been theoretically predicted and experimentally observed [2]. Nitrogen-doped MWCNTs have been synthesized both by chemical vapour deposition (CVD) techniques [3] and aerosol assisted CVD methods [4]. Several authors have demonstrated the possibility of incorporating significant concentrations of nitrogen into MWCNTs (around 20 atom%) by aerosol assisted CVD methods [4].

Boron-containing nanotubes are predicted to behave as semiconductors over a large range of diameters and chiralities and might be a suitable class of materials for nanoelectronics technology. Boron-doped CNTs (B-CNTs) were reported as by-products when BC_2N nanotubes were synthesized by an arc-discharge method [5]. Nanotubes of boron nitride (B-N) were first synthesized by Chopra et al. [6] by a carbon free plasma discharge between a B-N packed tungsten rod and a cooled copper electrode. Most of the recent efforts used to produce boron containing nanotubes employ chemical methods involving suitable catalysts. Boron carbide nitrides (B-C-Ns) have been synthesized by different methods, such as CVD [7], polymer precursor pyrolysis [8] and arc discharge between appropriate electrodes [9]. B-C-Ns are materials in which carbon atoms are partially substituted by boron and nitrogen.

Nitrogen doped CNTs

Ammonia or volatile nitrogen containing organic compounds are generally used as a nitrogen source to produce N-CNTs. Large quantities of CN_x/carbon nanotube intramolecular junctions have been synthesized on a silicon substrate via the CVD method by pyrolysis of ferrocene and melamine [10]. The nanotubes produced have two different sections, one made of carbon with an empty hollow cylinder structure and the other made of carbon nitride with a bamboo-like structure. Films of ordered CN_x nanotubes were vertically grown on different substrates and were obtained by the pyrolysis of nickel phthalocyanine [11]. Vertically aligned nitrogen-doped MWCNTs (N-MWCNTs) were synthesized in an NH_3 environment by thermal decomposition of acetylene using nickel particles as catalyst [12]. N-MWCNTs have also been prepared by the floating catalyst CVD method using ferrocene, xylene, NH_3 and or pyridine [13]. N-MWCNTs were synthesized by pyrolysis of acetonitrile (CH_3CN) over catalytic nanoparticles formed by the thermal decomposition of Co and Ni dimaleates or their solutions [14]. Aligned bamboo-shaped carbon-nitrogen MWCNTs have been produced in large quantities by the pyrolysis of iron pentacarbonyl and acetylene mixtures using ammonia as the source of nitrogen [15]. Synthesis of N-SWCNTs that agglomerate in bundles and form long strands using the thermal decomposition of ferrocene/ethanol/benzylamine solutions in an Ar atmosphere have been reported [16].

Boron doped, Boron Nitride and B-C-N nanotubes

Synthesis of B-CNTs has been achieved by a partial substitution reaction, where some carbon atoms are substituted by boron atoms [17]. Boron oxide vapour reacts with CNTs to form B_xC nanotubes at high temperature under an Ar atmosphere and the B_xC nanotubes have diameters and lengths similar to the starting CNTs.

Synthesis of boron nitride (B-N) nanotubes and nanowires has been reported by Deepak et al. [18]. Their synthesis involved heating boric acid with either activated carbon, MWCNTs and catalytic iron particles or a mixture of activated carbon and iron particles in the presence of NH_3. Activated carbon in the absence of MWCNTs produced boron nitride nanowires, while activated carbon in the presence of MWCNTs formed B-N

MWCNTs. Lourie et al. [19] have synthesized B-N nanotubes by the chemical deposition of borazine over nickel boride catalyst particles at 1100°C. B-N MWCNTs have been synthesized by the reaction of a mixture of B_2O_3 and MWCNTs at 1500°C in a nitrogen atmosphere in the presence of an MoO_3 catalyst [20]. Tang et al. [21] have obtained B-N nanotube and nanobamboo structures by the reaction of boron and iron oxide in a flowing ammonia gas in the 1200-1500°C range.

Pyrolytic methods can be used to generate B-C_x-N nanotubes. Pyrolysis of $CH_3CN.BCl_3$ over cobalt powder at 950-1000°C leads to B-C_2-N nanofibers and nanotubes exhibiting various morphologies [22]. Similarly, B-C-N nanotubes have been prepared by the pyrolysis of $(CH_3)_3N:BH_3$ (1:1) and pyridine over a cobalt powder [23]. It has been shown from the literature that the presence of heteroatom compounds could incorporate into the CNTs and change the morphology and properties of the resulting CNTs.

All the methods described above entailed studies in which the Fe and carbon-boron sources were independently reacted together. In a continuation of our studies in earlier chapters, we have studied the use of substituted ferrocene catalysts containing nitrogen and boron elements to produce B and N containing nanotubes. We have found that nitrogen containing MWCNTs can be produced by use of toluene solutions of 3-ferrocenyl-*N,N*-diisopropyl-3-oxo-propionamide (diisopropylamide) using a single-furnace method under an Ar atmosphere.

6.2 Experimental

The synthesis of 3-ferrocenyl-*N,N*-diisopropyl-3-oxo-propionamide (diisopropylamide complex) and (1Z)-3-(diisopropylamino)-3-oxo-1-ferrocenylprop-1-ene-1-yl diflouroborate (difluoroborate) were performed as described elsewhere [24] (see Appendix at the end of the Chapter for experimental details). Reactions to produce CNTs were carried out in the apparatus shown in Chapter 2 (Figure 2.1). Synthesis of CNTs was carried out in the temperature range 800-1000 °C, under 5% H_2 in argon (v/v) (AFROX) at atmospheric pressure. The flow rate of H_2 in argon was kept constant at 100

ml/min. The diisopropylamide complex was dissolved in toluene (Merck chemicals) to produce different Fe/C ratios. The catalyst solutions were placed in a 10 ml syringe and the syringe was driven by a SAGE pump at various injection rates. The solutions were injected into the quartz tube reactor via a special designed quartz tube (2 mm i.d., 200 mm in length), cooled by water. This specially designed tube enabled the solution to be injected into the high temperature region of the large quartz tube reactor. The carbon deposited materials formed were scraped from the walls of the quartz tube in both the high temperature region and low temperature region (temperature < 300 °C) of the tube (see Chapter 2, Figure 2.1).

The difluoroborate catalyst was insoluble in toluene. Its activity towards CNT growth was hence tested by using a supported CVD method. Carbon nanotubes were synthesized by the catalytic decomposition of acetylene at 700 °C over the iron difluoroborate catalyst supported on $CaCO_3$ as described in the literature [25]. The difluoroborate catalyst (0.4 g; 5% Fe) was dissolved in 30 ml dichloromethane and added dropwise to 0.25 g of $CaCO_3$ support. The resulting precipitate was dried at 120 °C overnight and then calcined at 300 °C in air for 16 hrs. Acetylene was passed through a tubular quartz reactor (51 cm; 1.9 cm i.d.) [26], which was placed horizontally in a single stage furnace. The furnace was electronically controlled and the temperature ramping was readily achieved. The front end of the tube was connected to a glass manifold that allowed gases (nitrogen and acetylene) to be passed through the quartz tube. All reactions were performed at atmospheric pressure in the absence of oxygen. The catalyst (50 mg) was loaded into a quartz boat and placed in the centre of the quartz tube. The tube was flushed with N_2 while the temperature was ramped to the required reaction value for 1 h in situ (700 °C, 300 ml/min). The heating and cooling were automatically controlled and the temperature ramping rate was 10 °C min^{-1}. Acetylene or mixtures of N_2 gas and acetylene were passed through the reactor for 90 min (700 °C, at various flow rates). The reactor was cooled to room temperature under a nitrogen atmosphere (40 ml/min). The boat was removed from the tube reactor and the catalyst support was removed using 30% nitric acid. The carbonaceous materials were weighed to establish the amount of CNT that had been formed.

The carbon materials were characterized by low magnification transmission electron microscopy (TEM) (Jeol JEM 100S) and Raman spectroscopy (J-Y T64000) and thermal gravimetric analysis (TGA) measurements were performed in air on a Perkin Elmer TGA 7. The number and size of the carbon tubes, carbon fibers and spheres were obtained from the TEM images by counting procedures and represent average values.

6.3 Results and discussion

The synthesis of diisopropylamide catalyst is described briefly in the appendix. The reaction scheme to prepare this compound is given below:

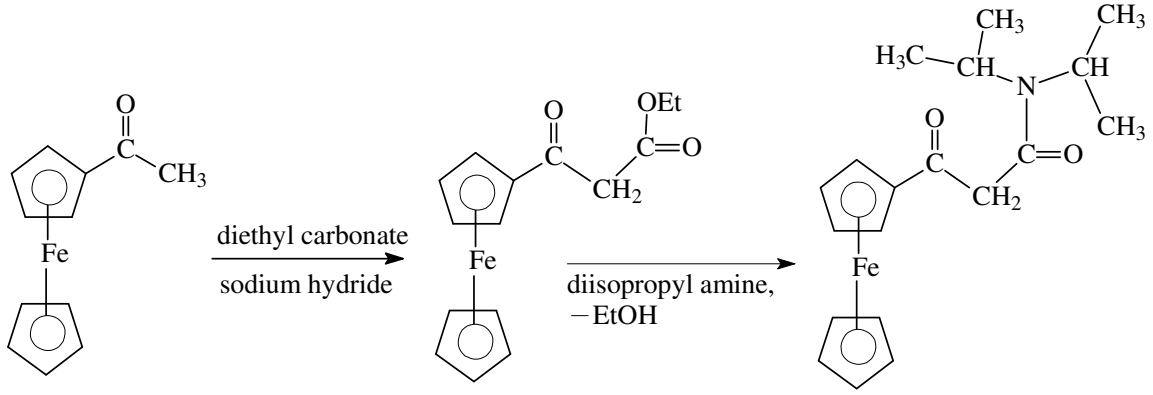

Scheme 1: Preparation of diisopropylamide catalyst [24].

6.3.1 CNTs synthesized by diisopropylamide catalyst.

General results

All reactions were performed at a constant gas flow rate of 100 ml/min and various catalyst concentrations, temperatures and injection rates. TEM was employed to evaluate the morphology and the diameter size distribution of the produced carbonaceous materials. It was observed from the TEM images that CNTs were tangled around each other forming a web-like structure. Analysis of all the samples produced under the different conditions indicates that there were two ranges of outer diameters that were formed. Generally, for nearly all samples, large nanotubes (range: 60-100 nm outer diameter) as well as small nanotubes (range: 20-40 nm outer diameter) were observed as

shown in Figure 6.1-6.7 and Table 6.1. The nanotube diameters for most of the samples were in the small diameter range rather than the large diameter range.

Figure 6.1: TEM image of N-doped MWCNTs formed using diisopropylamide catalyst (800 °C, 0.8 ml/min 2.0 wt%) *(arrow = bamboo structure)*

Effect of temperature

The growth temperature was varied between 800 and 1000 °C. The rate at which carbonaceous material is deposited increases as the pyrolysis temperature increases. CNTs were obtained at 800 °C while few CNTs and largely amorphous carbon were formed at 900 °C. When the growth temperature was 1000 °C only amorphous carbon was formed. The diameters of the grown CNTs were influenced by temperature. Thus, CNTs formed at 900 °C had a wider diameter range while at 800 °C tubes with a small diameter range were formed.

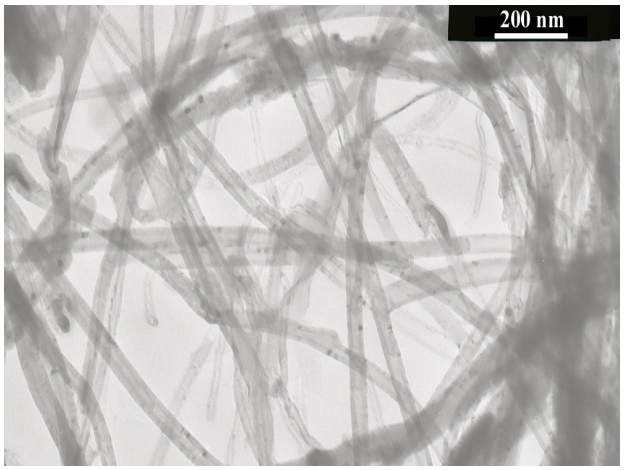

Figure 6.2: TEM image of N-doped MWCNTs formed using diisopropylamide catalyst (800 °C, 0.4 ml/min, 2.0 wt.%)

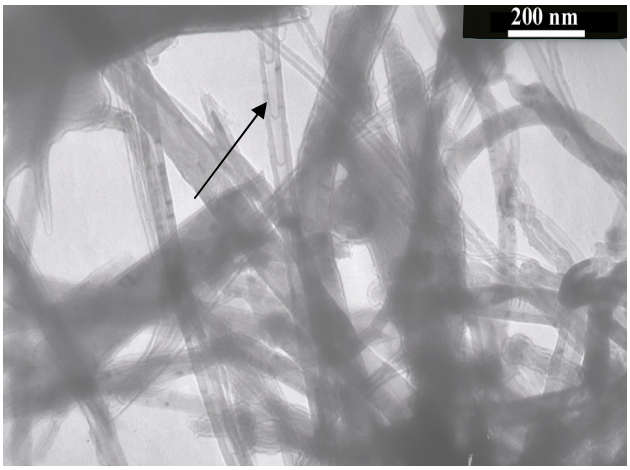

Figure 6.3: TEM image of N-doped MWCNTs formed using diisopropylamide catalyst (800 °C, 0.2 ml/min, 2.0 wt.%) *(arrow = bamboo structure)*

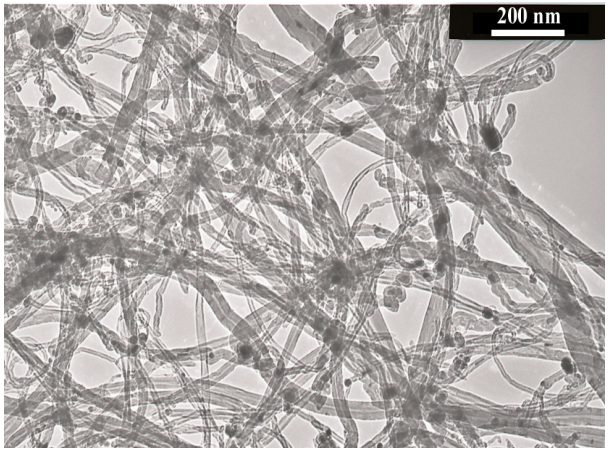

Figure 6.4: TEM image of MWCNT using ferrocene (800 °C, 0.2 ml/min, 2.0 wt.%)

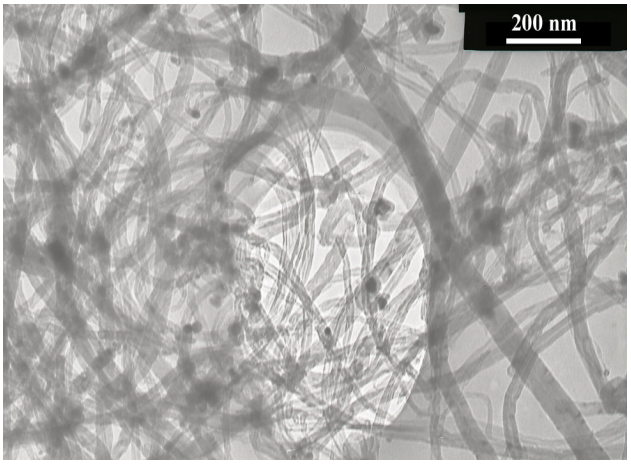

Figure 6.5: TEM image of MWCNT using ferrocene (800 °C, 0.2 ml/min, 1.0 wt.%)

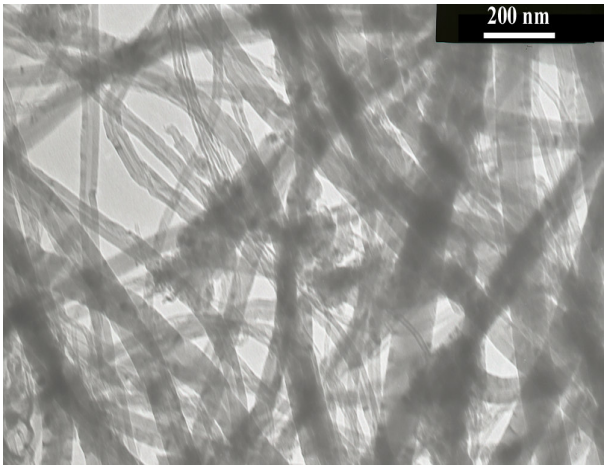

Figure 6.6: TEM image of MWCNT using ferrocene (800 °C, 0.8 ml/min, 2.0 wt.%)

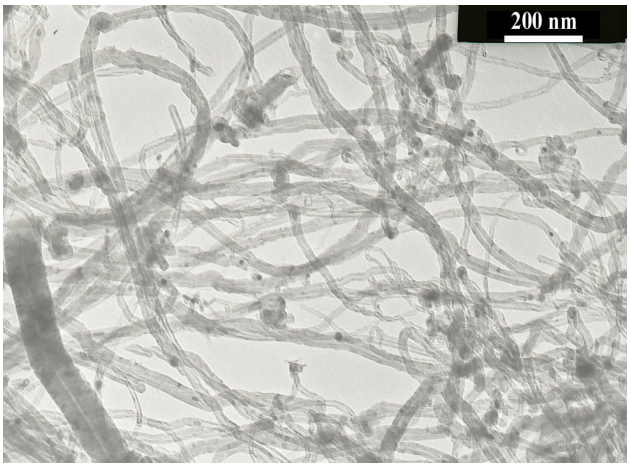

Figure 6.7: TEM image of MWCNT using ferrocene (800 °C, 0.3 ml/min, 2.0 wt.%)

Effect of catalyst and catalyst concentration

When high concentrations of diisopropylamide catalyst were used (5.0 wt.% and 2.5 wt.%) the injection system blocked, therefore lower concentrations were used to catalyze CNT synthesis. Low concentrations of diisopropylamide catalyst (2.0 and 1.0 wt.%) was effective for CNT and fibers synthesis producing MWCNTs with a bimodal diameter distribution (Figures 6.1-6.3) with the lowest concentration of diisopropylamide catalyst (1.0 wt.%) being less effective for CNT synthesis. The lower catalyst concentrations favoured fibers and spheres formation rather than CNTs. The CNTs with diameter range of 24-43 nm were observed to be around 70% yield while the CNTs with diameter range of 43-74 nm were obtained in 30% yield from TEM analysis. More of the grown CNTs were in the small diameter range than in the large diameter range. Ferrocene at lower concentration was also used to prepare CNTs and the results obtained were compared to the results obtained with the diisopropylamide catalyst. The ferrocene reactions also gave CNTs with a bimodal diameter distribution (Figures 6.4-6.7). The morphology of the CNTs formed with diisopropylamide catalyst was different from the tubes grown from ferrocene. Many of the tubes grown from the diisopropylamide catalyst had a bamboo structure (Figures 6.1 and 6.3, arrows) and this bamboo structure is known to be a characteristic of nitrogen-doped MWCNTs. Nitrogen-doped MWCNTs reported in the literature have also exhibited this distinct morphology which is different from undoped MWCNTs [27]. The diameters of the CNTs formed with the diisopropylamide catalyst were comparable to the ones formed using ferrocene as a catalyst, using similar catalyst concentrations (see Table 6.1).

Table 6.1: Effect of diisopropylamide catalyst on CNT synthesis.

Metal content[a]	Temperature (°C)	Injection rate (ml/min)	Notes[b]	Mean diameter (nm)[c]
Amide, 2.5 wt.%	800	3.3	No carbon deposit	–
	900	3.3	A-C	–
	1000	3.3	A-C	–
Amide, 2.5 wt.%	800	1.2	Tubes (20%), a-C (70%), fibers (10%)	28 (12 inn)
	900	1.2	A-C	–
	1000	1.2	A-C	–
Amide, 2.0 wt.%	800	0.8	Tubes (70%), a-C (30%)	28 (15 inn)
	900	0.8	A-C (85%), Fibers (10%), spheres (5%)	120F, 200S
Amide, 2.0 wt.%	800	0.4	Tubes (60%), a-C (40%)	35 (17 inn)
	900	0.4	A-C (75%), fibers(5%), spheres (20%)	150F, 180S
Amide, 2.0 wt.%	800	0.2	Tubes (60%), a-C (20%), fibers (20%)	43T (20 inn), 150F
	900	0.2	A-C (10%), spheres (90%)	240
Amide, 1.0 wt.%	800	0.8	No carbon deposit	–
	900	0.8	Tubes (40%), a-C (50%), spheres (10%)	74 (14 inn)
	1000	0.8	A-C	–
Amide, 1.0 wt.%	800	0.4	Tubes (20%), a-C (80%), fibers (10%)	32 (17 inn)
	900	0.4	A-C	–
	1000	0.4	A-C	–
Amide, 1.0 wt.%	800	0.2	A-C (70%), fibers (30%)	100
	900	0.2	A-C (80%), spheres (20%)	700
	1000	0.2	A-C (80%), spheres (20%)	750
Fc, 2.0 wt.%	800	0.8	Tubes (60%), a-C (40%)	36 (14 inn)
2.0	900	0.8	A-C (80%), fibers (20%)	270
Fc, 2.0 wt.%	800	0.4	Tubes (60%), a-C (40%)	23 (10 inn)

Table 6.1 Contd.

2.0	900	0.4	A-C (90%), fibers (10%)	200
Fc, 2.0 wt.%	800	0.2	Tubes (80%), a-C (20%)	25 (13 inn)
2.0	900	0.2	A-C (90%), fibers (10%)	120
Fc, 1.0	800	0.2	Tubes (60%), a-C (40%)	24 (11 inn)

[a] Amide = diisopropylamide, [b] A-C = amorphous carbon, [c] T = tubes, F = fibers, S = spheres, inn = inner diameter.

Effect of injection rate

Low injection flow rates (0.8, 0.4, and 0.2) and high injection rates (3.3 and 1.2) were used in the CNT synthesis reactions. More CNTs were formed at the lower injection rates while at higher injection rates less CNTs were formed depending on the concentration of the catalyst. Thus more CNTs were formed at an injection rate of 0.8, 0.4 and 0.2 ml/min when using 2 wt.% catalyst. When higher injection rates were used at 2 wt.% of catalyst there was no formation of CNTs (3.3 ml/min) or there was less formation of CNTs (1.2 ml/min). From our earlier studies (Chapter 5), it was also found that low injection rates were more suitable for the production of CNTs rather than fibers and spheres. The diameter and the morphology of the formed CNTs were not influenced by the injection rate as reported in our earlier studies.

Analysis of the synthesized CNTs

CNTs synthesized using diisopropylamide catalysts are less stable and were noted visually to break easily under TEM. TGA measurements of grown MWCNTS (unpurified) were recorded and Figure 6.8 reveal that the sample oxidises at lower temperature than ferrocene grown CNTs. The TGA results for the ferrocene catalyzed CNTs gave the expected properties (Figure 6.8b) in which carbon is lost between 500-600 °C. When the equivalent experiment is performed in the TGA apparatus with the diisopropylamide catalyst a completely different weight loss profile is observed (Figure 6.8a). Indeed the weight loss occurs in three consecutive steps (a) 25-200 °C (b) 200-347 °C and the major weight loss at (c) 347-624 °C. Almost 50% of the mass has been lost

before 500 °C (compared with Figure 6.8 b where weight loss is 25%). It is thus clear that the CNT has been dramatically affected by the catalyst. To date no studies have been performed to identify the gases formed at the different temperatures. These results are however consistent with the literature reports which show that N-doped CNTs are less stable than undoped CNTs [15]. Thus a possible explanation to rationalise the data relates to the inclusion of N into the CNTs. As the TEM data revealed that the tube dimensions have not changed significantly, this would suggest modest N inclusion into the tubular structure. The remaining 17 and 9 % weight loss from both catalysts (Figure 6.8) is due to the iron particles in the sample. The weight loss from 218-344 °C for the MWCNTs synthesized by diisopropyl catalyst could be attributed to the decomposition of amorphous carbon.

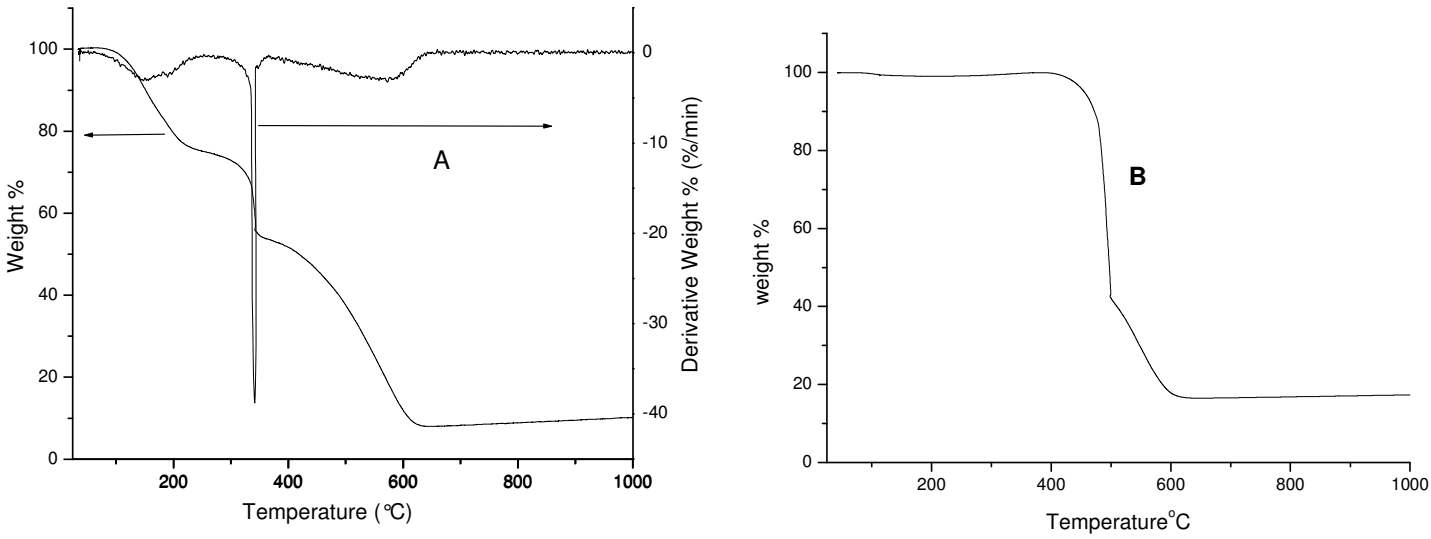

Figure 6.8: TGA of MWCNTs grown from (A) diisopropyl amide complex and (B) ferrocene (800 °C, 0.2 ml/min, 2.0 wt.%)

Figure 6.9 shows Raman spectra of the nanotubes grown at 800 °C using diisopropylamide (Figure 6.9a), and ferrocene (Figure 6.9b) as catalysts. Both spectra show two Raman bands at ~1350 cm^{-1} (D band) and ~1580 cm^{-1} (G band). The D band indicates the defective structure of the graphite sheets [28].

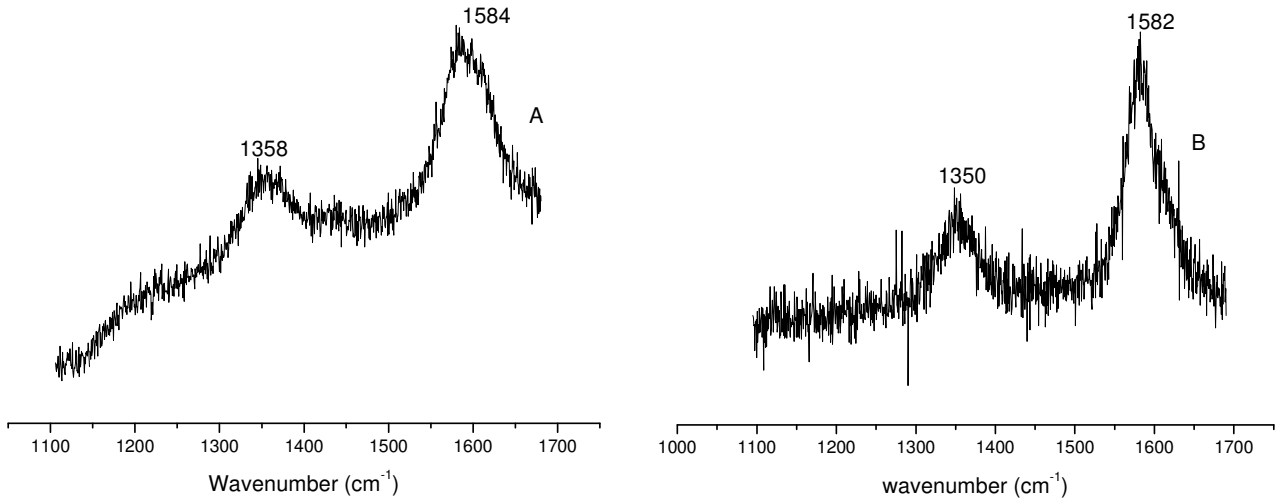

Figure 6.9: Raman spectra of MWCNTs grown using (A) diisopropylamide catalyst and (B) ferrocene (800 °C, 0.2 ml/min, 2.0 wt.%)

The peak intensity ratio of D and G bands of CNTs formed by diisopropylamide catalyst (0.6) is higher than the ratio CNTs formed by ferrocene (0.4). This indicates that the disorder in the nitrogen containing CNTs is higher than that for nanotubes formed by ferrocene.

Proposed mechanism for N-doped MWCNTs

The unusual bamboo structure observed for tubes formed from N containing CNTs cannot be explained by the usual CNT growth models. Thus, an alternative growth mechanism for N-doped MWCNTs was proposed by Terrones et al. [22] which is shown in Figure 6.10. In this growth mechanism cobalt was used as a catalyst instead of iron. It is assumed that reactions that occur over a Fe catalyst will occur in a similar manner.

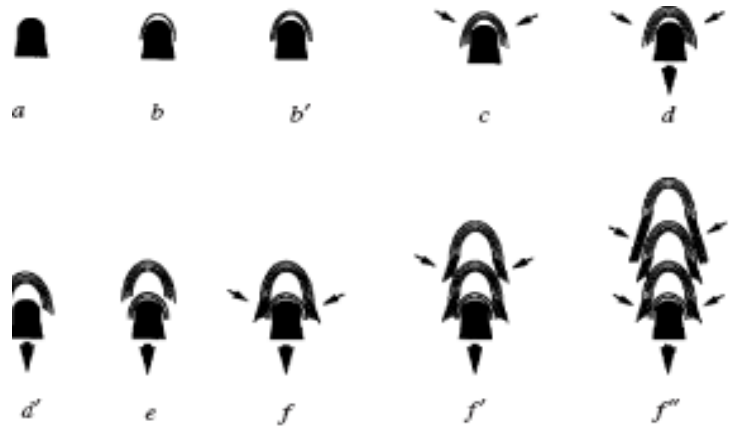

Figure 6.10: Proposed growth mechanism for N-doped MWCNT bamboo or "nanobell" structures.

Figure 6.10 shows the reaction mechanism required to produce the bamboo structure. (a) The catalyst develops a metal carbide interface, (b) before precipitating carbon layers match the particle shape. (b') The addition of new layers (c) increases pressure on the catalyst particle (d) until it is ejected from the inside of the cup (e-f). The strain is relieved and the process can repeat itself. It is worth noting that this growth model differs from that of undoped CNT growth mechanism in that the graphitic layers grow parallel to each other in undoped CNTs, while in doped-CNTs the graphitic layers grow in a shell shaped manner.

6.3.2 CNTs synthesized by difluoroborate-$CaCO_3$ supported catalyst

The synthesis of the difluoroborate catalyst has been carried out as shown in the scheme below:

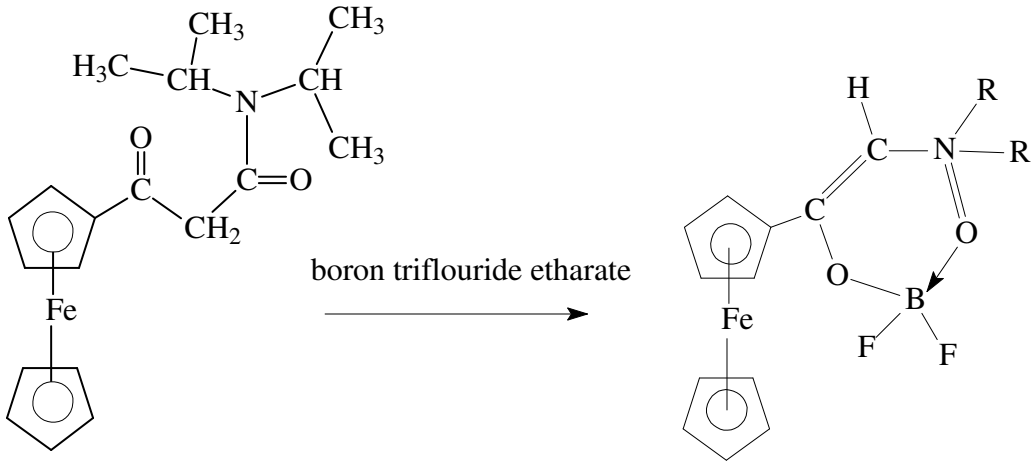

Scheme 2: Preparation of difluoroborate catalyst (R = CH_3) [24]

The difluoroborate catalyst was found to be insoluble in toluene. Its activity could thus only be tested using a CVD method using a support. The support chosen was $CaCO_3$. $CaCO_3$ has been found to be an excellent support for metals since it can support small metal particles. It has a specific surface area of between 10–20 m^2g^{-1}. This means the tubes will not be affected by the acid treatment [29].

Very few reactions were performed with $CaCO_3$ supported catalyst in this study. The reaction conditions used are shown in Table 6.2. The supported catalyst was placed in a boat, which was put in a quartz tube reactor in a hot furnace (700 °C). Acetylene was passed over the supported catalyst as a carbon source and the reactions were performed under nitrogen atmosphere. Hydrogen was not used as a reducing gas in the system, but the catalyst was reduced by the hydrogen atoms which were formed when the carbon source acetylene, C_2H_2, decomposed to form C atoms and H atoms. Nitrogen gas is known to be inactive on its own but, in these reactions it was found that when it is mixed with acetylene it could assist in CNT synthesis. The difluoroborate catalyst was found to be active for MWCNT synthesis (Figure 6.11) when the mixtures of nitrogen and acetylene were used. When pure acetylene was used, spheres were formed with no formation of CNTs. More CNTs were formed when N_2 was used especially at a high nitrogen flow rate. The mean diameter of CNTs formed ranged between 10 to 80 nm with more of the tubes possessing a mean diameter of 20-40 nm. The diameters of CNTs grown using higher nitrogen flow rates were smaller than the diameters of the tubes formed when a higher acetylene flow rate was used (Table 6.2).

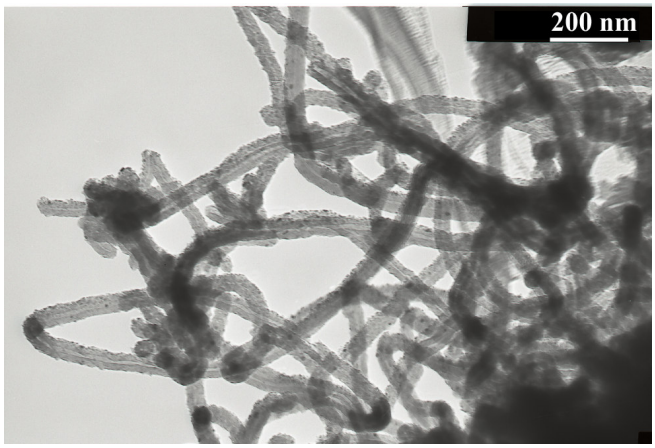

Figure 6.11: TEM image of MWCNTs formed at 700 °C (difluoroborate catalyst, 240 ml/min N_2 flow rate, 90 ml/min C_2H_2 flow rate)

Table 6.2: Effect of difluoroborate on CNTs synthesis.

Acetylene flow rate (ml/min)	Nitrogen flow rate (ml/min)	Total gas flow rate (ml/min)	Notes	Mean diameter (nm)
90	240	330	Tubes (40%) and a-C (60%)	39 (12 inner)
50	280	330	Tubes (60%) and a-C (40%)	24 (10 inner)
165	165	330	Tubes (30%) and a-C (70%)	37 (12 inner)
100	—	100	spheres	500

Reaction temperature: 700 °C, 5 wt.% Fe catalyst.

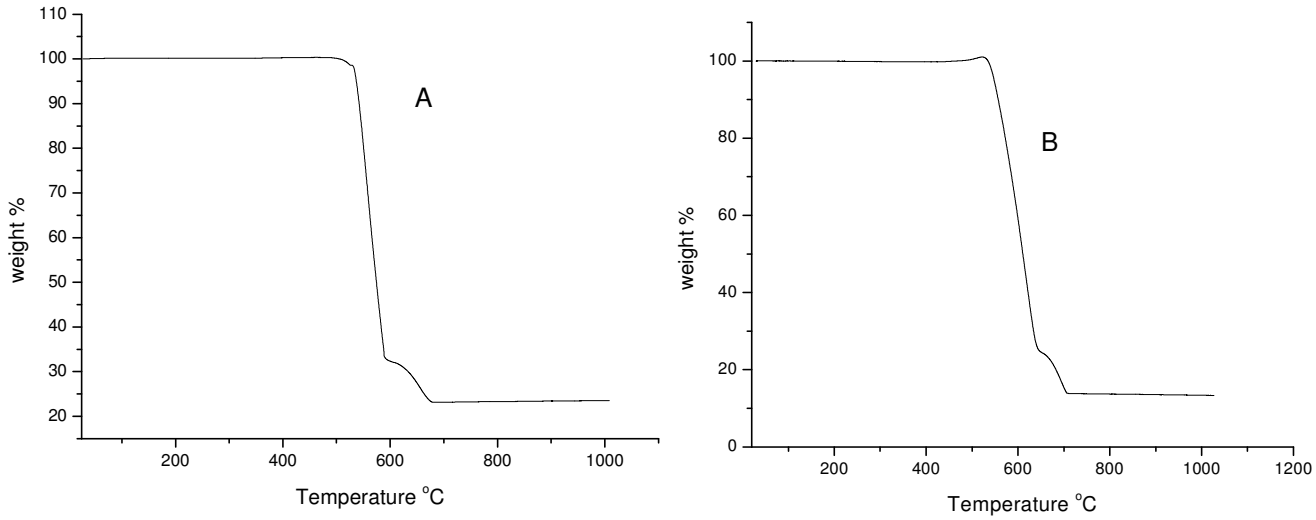

Figure 6.12: TGA of MWCNTs synthesized by (A) difluoroborate catalyst and (B) Fe/$CaCO_3$, without the boron element (700 °C, 240 ml/min N_2 flow rate, 90 ml/min C_2H_2 flow rate)

MWCNTs grown from the difluoroborate catalyst were also characterized by TGA in air (Figure 6.12). The TGA of CNTs synthesized from the difluoroborate catalyst (Figure 6.12a) was found to be similar to the TGA data of CNTs formed by $Fe/CaCO_3$ (Figure 6.12b) without boron. This shows that the boron has no effect on the oxidation properties of the synthesized CNTs. The maximum weight loss occurred at 516 °C with the complete carbon oxidation occurring at 680 °C. The remaining residual mass (23 wt.%) following the complete carbon oxidation is due to the presence of iron particles in the samples.

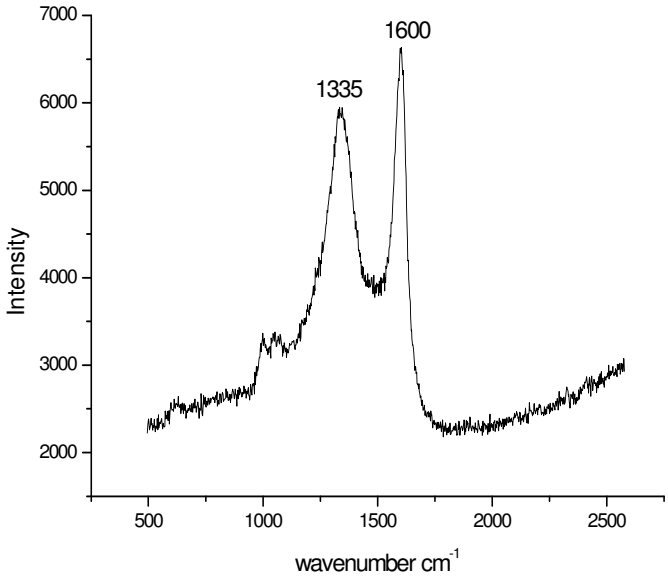

Figure 6.13: Raman spectra of MWCNTs grown using difluoroborate catalyst (700 °C, 240 ml/min N_2 flow rate, 90 ml/min C_2H_2 flow rate)

The Raman spectrum for MWCNTs deposited using difluoroborate reveals strong bands at 1335 cm^{-1} and 1600 cm^{-1} corresponding to the D and G lines respectively (Figure 6.13). The ratio of intensity of the D and G bands (I_D/I_G) is often used as a measure of disorder in CNTs [30]. As evident from Raman spectra there is more disorder (I_D/I_G = 0.73) in the material prepared with the difluoroborate catalyst than other ferrocenyl catalysts described in earlier chapters. Using Raman spectrum, it has been reported in the literature [31] that a the peak at 2700 cm^{-1} is a characteristic of boron-doped CNTs but this peak was not observed in this study suggesting that the CNTs formed were not doped

with boron to any large extent. This could be attributed to the low concentration of boron in the catalyst system (5 wt.%).

6.4 Conclusions

MWCNTs were formed when a diisopropylamide ferrocene was used as a catalyst. More CNTs were grown at low temperature (800 °C) while high temperatures (900-1000 °C) were favourable for amorphous carbon and fiber formation. The injection rate showed no influence on the diameters of grown CNTs. High injection rate reactions produced more amorphous carbon than CNTs. TGA results and Raman results showed that the CNTs synthesized by diisopropylamide catalyst are disordered compared to CNTs synthesized by ferrocene. They also revealed a bamboo structure, controlled with N incorporation into the CNTs.

A difluoroborate-$CaCO_3$ supported catalyst was shown to be active for MWCNT synthesis at 700 °C using mixtures of nitrogen and acetylene. The physical characterization data suggest little if any formation of boron-doped CNTs.

6.5 References

[1] (a) Endo, M.; Hayashi, T.; Hong, S. H.; Enoki, T.; Dresselhaus, M. S. *J. Appl. Phys.* **2001**, *90*, 5670. (b) Glenis, S.; Nelson, A. J.; Labes, M. M. *J. Appl. Phys*. **1999**, *86*, 4464.

[2] (a) Kim, D. P.; Lin, C.L. Mihalisin, T.; Heiney, P. Labes M. M. *Chem. Mater.* **1991**, *3*, 686. (b) Nevidomskyy, A. H.; Csanyi, G.; Payne, M. C. *Phys. Rev. Lett*. **2003**, *91*, 1055021. (c) dos Santos, M. C. Alvares, F. *Phys. Rev. B* **1998**, *58*, 13918.

[3] (a) Yudasaka, M.; Kikuchi, R.; Ohki, Y.; Yoshimura, S. *Carbon* **1997,** *35*, 195. (b) Sung, S. L.; Tsai, S. H.; Tseng, C. H.; Chiang, F. K.; Liu, X. W.; Shih, H. C. *Appl. Phys. Lett.* **1999**, *74*, 197. (c) Ma, X.; Wang, E. G. *Appl. Phys. Lett.* **2001**, *78*, 978.

[4] (a) Glerup, M.; Castignolles, M.; Holzinger, M.; Hug, G.; Loiseau, A.; Bernier, P. *Chem. Commun.* **2003**, *20*, 2542. (b) Tang, C.; Bando, Y.; Golberg, D.; Xu, F.

Carbon **2004**, *42*, 2625. (b) Tang, C.; Bando, Y.; Golberg, D.; Xu, F. *Carbon* **2004**, *42*, 2625.

[5] Redlich, Ph.; Loeffler, J.; Ajayan, P. M.; Aldinger, Ruhle, M. *Chem. Phys. Lett.* **1996**, *260*, 465.

[6] Chopra, N. G.; Luyken, R. J.; Cherry, K.; Crespi, V. H.; Cohen, M. L.; Louie, S. G.; Zettl, A. *Science* **1995**, *269*, 966.

[7] (a) Loeffler, J.; Steinbach, F.; Bill, J.; Mayer, J.; Aldinger, F.; *Z. Metallkd*. **1996**, *87*, 170. (b) Kaner, R. B.; Kouvetakis, J.; Warble, C. E.; Sattler, M. L.; Bartlett, N. *Mater. Res. Bull.* **1987**, *22*, 399.

[8] Bill, J.; Riedel, R.; Passing, G.; *Z. Anorg. Allg. Chem.* **1992**, *610*, 83.

[9] (a) Stephan, O.; Ajayan, P. M.; Colliex, C.; Redlich, P.; Lambert, J. M.; Bernier, P.; Lefin, P. *Science* **1994**, *266*, 1683. (b) Weng-Sieh, Z.; Cherrey, K.; Chopra, N. G.; Blasé, X.; Miyamoto, Y.; Rubio, A.; Cohen, M. L.; Louie, S. G.; Zettl, A.; Gronsky, R. *Phys. Rev. B* **1995**, *51*, 11229.

[10] Chai, Y.; Zhang, Q.F.; Wu, J.L. *Carbon* **2006**, *44*, 687.

[11] Suenaga, K.; Yudasaka, M.; Colliex, C.; Iijima, S. *Chem. Phys. Lett.* **2000**, *316*, 365

[12] Jung, M.; Eun, K. Y.; Lee, J. K.; Baik, Y. J.; Lee, K. R.; Park, J. W. *Diamond and Related Materials* **2001**, *10*, 1235.

[13] Maldonado, S.; Morin, S.; Stevenson, K.J.; *Carbon,* **2006**, *44*, 1429.

[14] Kudashov, A. G.; Okotrub, A.V.; Bulusheva, L. G.; Asanov, I. P.; Shubin, Y. V.; Yudanov, N. F.; Yudanova, L. I.; Danilovich, V. S.; Abrosimov, O. G. *J. Phys. Chem. B* **2004**, *108*, 9048.

[15] Lee, C. J.; Lyu, S. C.; Kim, H. W.; Lee, J. H.; Cho, K. I. *Chem. Phys. Lett*. **2002**, *359*, 115.

[16] Villalpando-Paez, F.; Zamudio, A.; Elias, A. L.; Son, H.; Barros, E. B.; Chou, S. G.; Kim, Y. A.; Muramatsu, H.; Hayashi, T.; Kong, J.; Terrones, H.; Dresselhaus, G.; Endo, M.; Terrones, M.; Dresselhaus, M. S. *Chem. Phys. Lett*. **2006**, *424*, 345.

[17] Han, W.; Bando, Y.; Kurashima, K.; Sato, T. *Chem. Phys. Lett.* **1999**, 299, 368.

[18] Deepak, F. L.; Vinod, C. P.; Mukhopadhyay, K.; Govindaraj, A.; Rao, C. N. R. *Chem. Phys. Lett.* **2002**, *353*, 345.

[19] Lourie, O. R.; Jones, C. R.; Bartlett, B. M.; Gibbons, P. C.; Rouff, R. S.; Buhro, W. E. *Chem. Mater.* **2000,** *12*, 1808.

[20] Goldberg, D.; Bando, Y.; Karashima, K.; Sato, T. *Chem. Phys. Lett.* **2000**, *323*, 185.

[21] Tang, C. C.; de la Chapelle, M. L.; Li, P.; Liu, Y. M.; Dang, H. Y.; Fan, S. S. *Chem. Phys. Lett.* **2001**, *342,* 492.

[22] Terrones, M.; Benito, A. M.; Mantega-Diego, C.; Hsu, W. K.; Osman, O. I.; Hare, J. P.; Reid, D. G.; Terrones, H.; Cheetham, A. K.; Prassides, K.; Kroto, H. W.; Walton, D. R. M. *Chem Phys. Lett.* **1996**, *257*, 576.

[23] Sen, R.; Satishkumar, B. C.; Govindaraj, A.; Harikumar, K. R.; Raina, G.; Zhang, J. P.; Cheethan, A. K.; Rao, C. N. R. *Chem. Phys. Lett*. **1998**, *287*, 671.

[24] Coville, N. J.; Ramsden, J. A.; Staskun, B. *S. Afr. Tydskr. Chem.* **1980**, *33*, 71.

[25] Bahome, M. C.; Jewell, L. L.; Hildebrandt, D.; Glasser, D.; Coville, N. J. *Appl. Catal. A* **2005**, *287*, 60.

[26] Mabudafhasi, M. L.; Bodkin, R.; Nicolaides, C. P.; Liu, X. Y., Witcomb, M. J.; Coville, N. J. *Carbon* **2002**, *40*, 2737.

[27] Ewels, C. P.; Glerup, C. P. *J. Nanoscience and Nanotechnology* **2005**, *5*, 1345.

[28] Tuinstra, F.; Koenig, J. L. *J. Chem. Phys.* **1970**, *53*, 1126.

[29] Couteau, E.; Hernadi, K.; Seo, J. W.; Thiên-Nga, L.; Mikó, Cs.; Gaál, R.; Forró, L. *Chem. Phys. Lett.* **2003**, *378*, 9.

[30] (a) Singh, C.; Shaffer, M. S. P.; Windle, A. H. *Carbon* **2003**, *41*, 359. (b) Endo, M.; Kim, Y. A.; Fukai, Y.; Hayashi, T.; Terrones, M.; Terrones, H.; Dresselhaus, M. S. *Appl. Phys. Lett.* **2001**, *79*, 1531.

[31] Mennela, V.; Monaco, G.; Golangeli, L.; Bussoleti, E. *Carbon* **1995**, *33*, 115.

6.6 Appendix

Synthesis of diisopropylamide catalyst [24]

Ethyl ferrocenoylacetate (3g, 9,9 mmol), which was obtained from the reaction of acetylferrocene and diethyl carbonate [R], was added to diisopropylamine (0.84 g, 1.16 ml, 8.3 mmol) in a 50 ml round bottom flask purged with nitrogen. The mixture was stirred and heated at ca. 140 C under nitrogen for 5 h. The reaction mixture was cooled, and then toluene (10 ml) and 'kieselgel 60' (3 g) were added to the mixture. The solvent was removed in vacuum and the residual mass was adsorbed on silica gel. The product was purified by column chromatography with ethyl acetate:hexane (1:5) solvent mixture to give a brown oil in 40% yield.

^{1}H-NMR ($CDCl_3$) δ: 1,32 (d, 6H, CH(**CH_3**)$_2$), 1.43 (d, 6H, CH(**CH_3**)$_2$), 3.44 (m, 1H, **CH**$(CH_3)_2$), 3.83 (s, 2H, CH_2), 4.06 (m, 1H, **CH**$(CH_3)_2$), 4.26 (s, 5H, C_5H_5), 4.55 (t, 2H, C_5H_4), 4,87 (t, 2H, C_5H_4). **IR** (CH_2Cl_2) ν = 1633 cm^{-1} (amide CO).

Synthesis of difluoroborate catalyst [24]

Boron trifluoride-etherate (0.156 g, 1.1 mmol) was added dropwise to a stirring solution of diisopropylamide ferrocene (0.299 g, 1 mmol) in anhydrous toluene (10 ml) at room temperature. An immediate reaction occurred with formation of a purple precipitate. Addition of wet toluene gave an orange solution. The solvent was removed in vacuum and the crude product was purified by chromatography, eluting with ethyl acetate:hexane (1:7) mixture to give the difluoroborate ferrocene complex as an orange-red solid. The desired product was isolated in 60% yield.

^{1}H-NMR ($CDCl_3$) δ: 1,34 (d, 6H, CH(**CH_3**)$_2$), 1.37 (d, 6H, CH(**CH_3**)$_2$), 2.57 (m, 1H, F_2B**CH**=C) 4.46 (s, 5H, C_5H_5), 4.24 (t, 2H, C5H4), 4.78 (t, 2H, C5H4), 5.49 (s, 1H, C-**CH**=C).

CHAPTER 7

Carbon nanotubes obtained by injection CVD method using cyclopentadienyldicarbonylmethyl(iodo)iron[4]

7.1 Introduction

Carbon nanotubes (CNTs) have been synthesized in the presence of a metal using different techniques. A facile method for producing CNTs is through the floating catalyst method in which the catalyst is introduced into a hot reaction zone by (i) a syringe process using the catalyst dissolved in a carbon source [1] (ii) by sublimation of the catalyst at elevated temperatures (solid to gas phase) [2] or (iii) using a gaseous catalyst source e.g., $Fe(CO)_5$) [3]. These methods do not require a support for the catalyst and the catalyst and the carbon source are directly reacted in the gas phase. The carbon source decomposes to form carbon nanostructures. The catalysts that are commonly used are organometallic compounds such as metallocenes typically $Fe(C_5H_5)_2$ [2] and [$Fe(CO)_5$] [4].

In previous chapters, studies were focused on ferrocene derivatives as catalysts. In this chapter we report on the use of iron carbonyl containing complexes as catalysts for CNT synthesis. One of the earliest reports on the use of $Fe(CO)_5$ as a catalyst for CNT synthesis in the gas phase was reported by Nikolaev et al. [3]. They reported the catalytic production of SWCNTs in a continuous-flow gas phase reactor using CO as a carbon feedstock and $Fe(CO)_5$ as the iron containing catalyst precursor. Vertically aligned and non-aligned MWCNT films have also been synthesized by decomposition of acetylene and methane using $Fe(CO)_5$ as a catalyst, CO/Ar as carrier gases and hydrogen as a reducing agent [5]. Using a similar method, SWCNTs have also been synthesized by the thermal decomposition of $Fe(CO)_5$ in the presence of CO but this required use of an ambient pressure laminar flow reactor [6]. Liu et al. have synthesized aligned and non-

[4]Mohlala M. S.; Coville, N. J. *Journal of Organometallic Chemistry,* **In Press**.

aligned MWCNTs by pyrolysis of $Fe(CO)_5$/pentane using the floating CVD method under a nitrogen atmosphere [7]. Solutions of $Fe(CO)_5$ and $Fe_3(CO)_{12}$ were atomized by electrohydrodynamic means and the resultant aerosols were reacted with ethyne in the gas phase to form CNTs [8]. The aerosol of $Fe(CO)_5$ resulted in the formation of MWCNTs with a narrow diameter range (≤ 10 nm), whereas the $Fe_3(CO)_{12}$ aerosol gave MWCNTs with a wider diameter range (≥19 nm). Synthesis of large arrays of aligned MWCNTs from the thermal decomposition of $Fe(CO)_5$ using acetylene as a carbon feedstock have been reported by Rohmund et al. [9]. Pyrolysis of $Fe(CO)_5$ in the presence of thiophene under an argon atmosphere has been shown to favour the production of Y-junction MWCNTs [10].

MWCNTs have also been prepared by an injection CVD method using a cyclopentadienyl dicarbonyl iron dimer; ($[CpFe(CO)_2]_2$) or a cyclooctatetraene iron tricarbonyl complex, ($C_8H_8Fe(CO)_3$) as the iron catalyst source, toluene as carbon source and H_2 in a Ar/N_2 mixture as carrier gases [1a].

In our work we have investigated the effect of organometallic catalyst precursors in an effort to generate an efficient catalyst system for CNT synthesis. Here, we present our study on the synthesis of MWCNT growth using cyclopentadienyldicarbonylmethyliron ($CpFe(CO)_2Me$) and cyclopentadienyldicarbonyliodoiron ($CpFe(CO)_2I$) complexes as iron catalysts.

7.2 Experimental

The complexes, $CpFe(CO)_2I$ [11] and $CpFe(CO)_2Me$ [12] were synthesized as described elsewhere (see Appendix at the end of the Chapter). Reactions were performed in the apparatus shown in Chapter 2 (Figure 2.1). Synthesis of CNTs was carried out in the temperature range 800-1000 °C, under 5% H_2 in argon (v/v) (AFROX) at atmospheric pressure. The flow rate of H_2 in argon was kept constant at 100 ml/min. $CpFe(CO)_2Me$ and $CpFe(CO)_2I$ with different weight ratios were dissolved in toluene (Merck chemicals). The catalyst solutions were placed in a 10 ml syringe driven by a SAGE

syringe pump at rates of ~0.8 and ~0.2 ml/min. The solutions were injected into the quartz tube reactor via the specially designed quartz tube (2 mm i.d., 200 mm in length), described previously and cooled by water [1b]. The carbon deposited materials formed were scraped from the walls of the quartz tube in both the high temperature region and low temperature region (temperature < 300 °C) of the tube (see Chapter 2, Figure 2.1). The carbon materials were characterized by low magnification transmission electron microscopy (TEM) (Jeol JEM 100S) and Raman spectroscopy (J-Y T64000). Thermal gravimetric analysis (TGA) measurements were performed in air on a Perkin Elmer TGA 7 to determine the characteristics of the nanotubes and the iron residue content. The number and size of the carbon tubes and spheres formed were obtained from the TEM images by counting procedures and represent average values.

7.3 Results and discussion

General Results

Synthesis of various carbon nanostructures were carried out using toluene solutions of $CpFe(CO)_2Me$ and $CpFe(CO)_2I$ complexes as catalysts. Using the preparation conditions described in Table 7.1, carbon products such as carbon fibers (CFs), carbon spheres (CSs) and carbon nanotubes (CNTs) were obtained. (Figures 7.1-7.6).

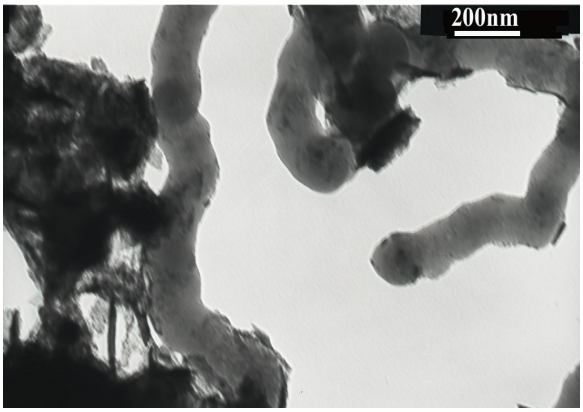

Figure 7.1: TEM image of CFs formed at 800 °C, ($CpFe(CO)_2I$: 5 wt.%; 0.8 ml/min injection rate)

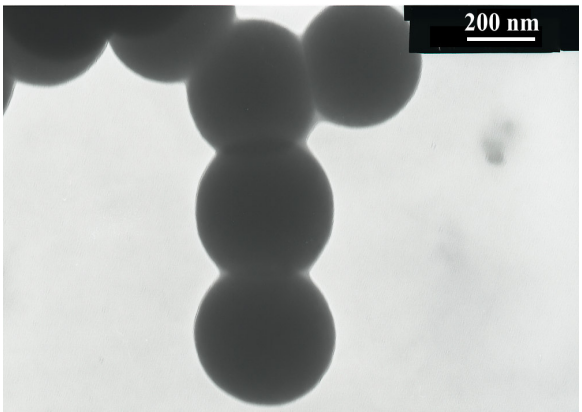

Figure 7.2: TEM image of CSs formed at 800 °C, ($CpFe(CO)_2I$: 10 wt.%; 0.8 ml/min injection rate)

Table 7.1: Effect of $CpFe(CO)_2Me$ and $CpFe(CO)_2I$ on CNTs growth.

Metal content[a]	Temperature (°C)	Injection rate (ml/min)	Yield (g)	Notes[b]	Mean diameter[c] (nm)
$CpFe(CO)_2I$ 5.0 wt.%	800	0.8	0.002	A-C (90%), fibers (10%)	144 F
$CpFe(CO)_2I$ 5.0 wt.%	900	0.8	0.012	A-C (20%), spheres (80%)	439 S
$CpFe(CO)_2I$ 5.0 wt.%	1000	0.8	0.829	A-C (5%), spheres (95%)	276 S
$CpFe(CO)_2I$ 10.0 wt.%	800	0.8	0.009	A-C (95%), fibers (5%)	150 F
$CpFe(CO)_2I$ 10.0 wt.%	900	0.8	0.011	A-C (10%), spheres (90%)	631 S
$CpFe(CO)_2I$ 10.0 wt.%	1000	0.8	0.905	A-C (5%), spheres (95%)	223 S
$CpFe(CO)_2Me$ 5.0 wt.%	800	0.8	0.124	Tubes (70%), fibers (10%), a-C (20%)	25T (10 inn), 120F
$CpFe(CO)_2Me$ 5.0 wt.%	900	0.8	0.198	Tubes (10%), fibers (20%), a-C (70%)	25T (10 inn), 100F
$CpFe(CO)_2Me$ 5.0 wt.%	1000	0.8	0.295	Tubes (5%), fibers (30%), a-C (60%), spheres (5%)	30T(14 inn), 115F
$CpFe(CO)_2Me$ 5.0 wt.%	800	0.2	0.109	Tubes (70%), fibers (20%), a-C (10%)	27T (15 inn); 200F
$CpFe(CO)_2Me$ 5.0 wt.%	900	0.2	0.228	Tubes (10%), fibers (60%), a-C (30%)	32T (14 inn), 150F
$CpFe(CO)_2Me$ 5.0 wt.%	1000	0.2	0.345	Tubes (10%), fibers (70%), a-C (20%)	33T (12 inn), 140F
$CpFe(CO)_2Me$ 10.0 wt.%	800	0.8	0.157	Tubes (30%), a-C (70%)	19T (15 inn)

Table 7.1 Contd.

$CpFe(CO)_2Me$ 10.0 wt.%	900	0.8	0.250	Tubes (5%), fibers (25%), a-C (70%)	37T (11 inn), 70F
$CpFe(CO)_2Me$ 10.0 wt.%	1000	0.8	1.395	Tubes (10%), fibers (10%), a-C (80%)	30T (13 inn), 100F
$CpFe(CO)_2Me$ 10.0 wt.%	800	0.2	0.198	Tubes (40%), a-C (60%)	20T (12 inn)
$CpFe(CO)_2Me$ 10.0 wt.%	900	0.2	0.394	Tubes (5%), fibers (10%), a-C (85%)	41T (11 inn), 80F
$CpFe(CO)_2Me$ 10.0 wt.%	1000	0.2	1.536	Tubes (10%), fibers (20%), a-C (70%)	35T (14 inn), 120F
$[CpFe(CO)_2]_2$ 10.0 wt.%	800	0.8	0.023	Tubes (70%), a-C (30%)	37 (12 inn)
Fc:I (50:1) 5.0 wt.%	800	0.8	0.280	Tubes (80%), a-C (20%)	36 (12 inn)
Fc:I (50:1) 5.0 wt.%	900	0.8	0.314	Tubes (60%), fibers (20%), a-C (20%)	34T (11 inn), 120F
Fc:I (1:1) 5.0 wt.%	800	0.8	0.003	Tubes (20%), a-C (80%)	33 (15 inn)
$[CpFe(CO)_2]_2$:I (10:1) 5.0 wt.%	800	0.8	0.006	Tubes (40%), a-C (60%)	34 (19 inn)
$[CpFe(CO)_2]_2$:I (1:1) 5.0 wt.%	800	0.8	0.005	Tubes (15%), a-C (75%)	33 (17 inn)

[a]$CpFe(CO)_2Me$ = cyclopentadienyl dicarbonyl methyl iron, $CpFe(CO)_2I$ = cyclopentadienyl dicarbonyl iodine iron, Fc = ferrocene, $[CpFe(CO)_2]_2$ = cyclopentadienyliron dicarbonyl dimer; [b]A-C = amorphous carbon; [c]F = fibers, T = tubes, S = spheres, inn = inner diameter.

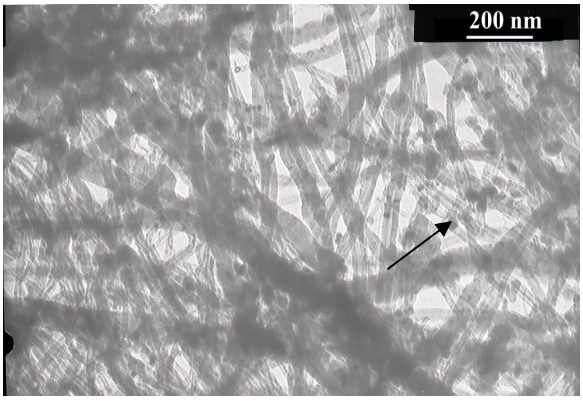

Figure 7.3: TEM image of CNTs formed at 800 °C, ($CpFe(CO)_2Me$: 5 wt.%; 0.8 ml/min injection rate) *(arrow = metal particle)*

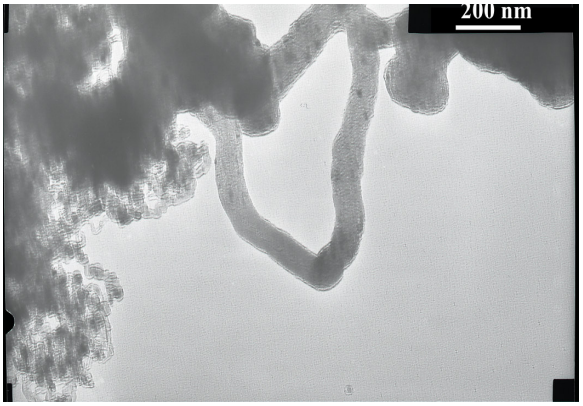

Figure 7.4: TEM image of CFs formed at 900 °C, ($CpFe(CO)_2Me$: 5 wt.%; 0.8 ml/min injection rate)

Figures 7.1, 7.2 and 7.4 show low magnification TEM images of CFs and CSs. The average diameter of the fibers ranged from 70-200 nm while the mean diameter of spheres ranged between 223 and 439 nm. Figures 7.3, 7.5 and 7.6 show TEM images of as-synthesized CNTs. The outer diameter of the nanotubes ranged from 19 to 41 nm with the inner diameter ranging from 11 to 15 nm. Metal particles were observed inside the tubes by TEM (shown by the arrow in Figure 7.3). The presence of an iron particle inside the tube shows that iron acts as a catalyst for CNT formation. Indeed it has been shown in the literature that no CNTs prepared by the CVD method form in the absence of a catalyst [1b].

The injection rate was observed to have no effect on the morphology and size of the CNTs formed, as reported by others [1a,b, 13], but did affect the amount of carbonaceous material formed. At the lower injection (0.2 ml/min) rate more carbonaceous materials were formed.

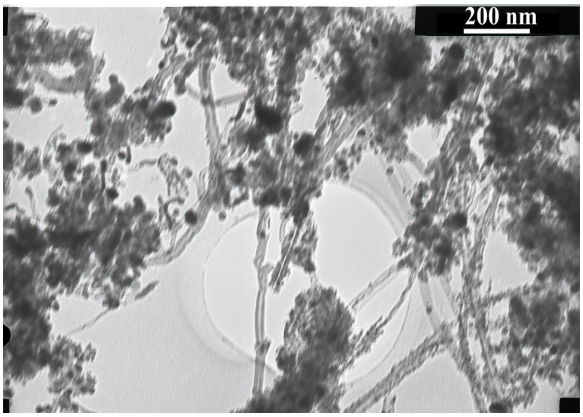

Figure 7.5: TEM image of CNTs formed at 800 °C, ($CpFe(CO)_2Me$: 10 wt.%; 0.8 ml/min injection rate)

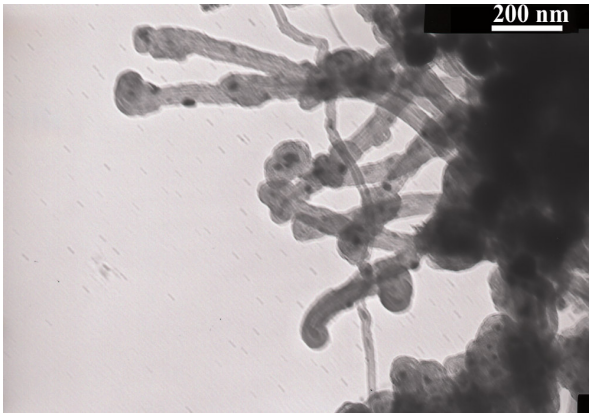

Figure 7.6: TEM image of CNTs formed at 900 °C, ($CpFe(CO)_2Me$: 10 wt.%; 0.8 ml/min injection rate)

Effect of catalyst and catalyst concentration

Pyrolysis of $CpFe(CO)_2I$-toluene solution produced CFs and CSs with no formation of CNTs (Figure 7.1 and 7.2). Reaction conditions were varied but no CNTs were ever formed. This could be attributed to the high concentration of iodide (radicals or ions) which are formed by decomposition of the Fe-I bond at high temperature. This was confirmed by performing a reaction of Fe with varying amounts of I_2. For example, when I_2 was added to a solution of ferrocene (Fc) in toluene (Fc:I = 50:1 molar ratio) MWCNTs were obtained (Figure 7.7). The outer diameter of these CNTs were found to be similar to the diameter of the tubes grown from ferrocene (5 wt.%, 800 °C) reported in Chapter 5. However, when a high ratio of iodine Fc:I (1:1) was used, more amorphous carbon (80%) was formed with poor formation of CNTs (20%) (see Table 7.1).

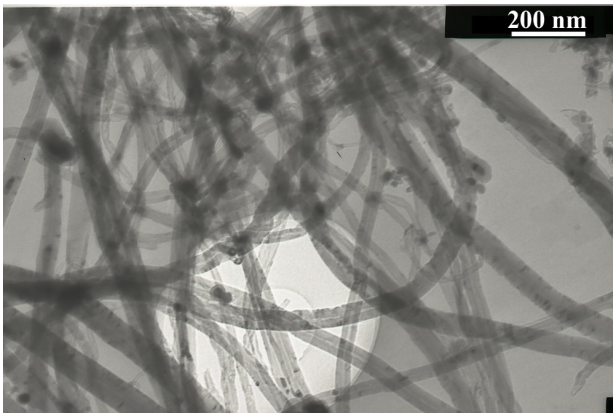

Figure 7.7: TEM image of CNTs formed at 800 °C, (Fc:I = 50:1 (5 wt.%); 0.8 ml/min injection rate)

When $CpFe(CO)_2Me$ was used as a catalyst, high yields of MWCNTs were obtained using various reaction conditions (Figures 7.3, 7.5 and 7.6). A low catalyst concentration (5 wt.%) yielded more CNT films relative to a high catalyst concentration (10 wt%) (Table 7.1). These results are consistent with what others have obtained when catalyst concentrations are too high for optimal deposition of CNTs [1a,b].

Harris et al. have shown that MWCNTs could be grown by pyrolysis of toluene solutions of cyclopentadienyliron dicarbonyl dimer using a two-stage furnace [1a]. It was reported from this study that low concentrations of the dimer were effective for formation of aligned MWCNTs. MWCNTs were also produced in our study from a toluene solution of cyclopentadienyliron dicarbonyl dimer using a single-stage furnace at 800 °C (Figure 7.8). The outer diameters (ranging from 20 to 80 nm) of the grown CNTs were comparable to the diameters of CNTs synthesized by Harris et al (15-200 nm*).* Small amounts of iodine were also added to $[CpFe(CO)_2]_2$ at a ratio of 10:1 (10 wt.%, $[CpFe(CO)_2]_2$:I) to look at the effect of iodine on CNT synthesis. The results showed the formation of more amorphous carbon (90%) than CNTs (10%) than when $[CpFe(CO)_2]_2$ was used without the addition of iodine. This latter reaction resulted in the formation of more CNTs (70%) than amorphous carbon (30%).

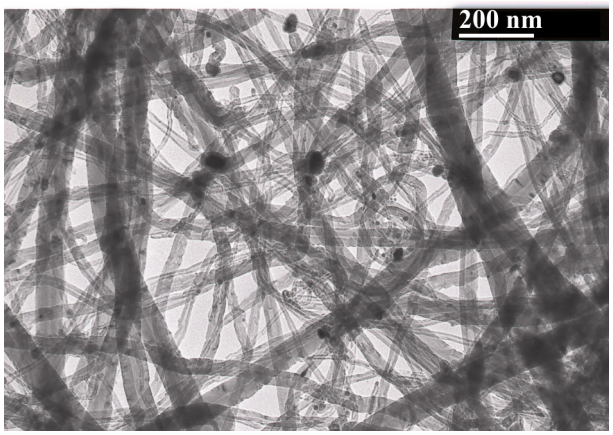

Figure 7.8: TEM image of MWCNTs formed at 800 °C (cyclopentadienyliron dicarbonyl dimer: 5 wt.%; 0.8 ml/min injection rate)

Effect of growth temperature

Products at various reaction temperatures had different morphologies as identified by TEM images. Table 7.1 shows the effect of temperature on the synthesized products. For $CpFe(CO)_2I$ catalyzed reactions amorphous carbon, fibers and spheres were produced. $CpFe(CO)_2Me$ catalyzed reactions were studied at 800 to 1000 °C. When a lower temperature (800 °C) was used the $CpFe(CO)_2Me$ catalyst formed more CNTs than amorphous carbon and carbon fibers. At higher temperatures (1000 °C), more fibers and amorphous carbon were produced. The outer diameter of the nanotubes generally increased with the reaction temperature. For example, the diameters of the tubes formed at 800 °C are smaller than the diameter of the tubes formed at 1000 °C (Table 7.1). Thus the reaction temperature has an obvious influence on the morphology of the deposited carbonaceous materials and their sizes. The yield of carbon deposit increased with temperature, but more CNTs were formed at the lower temperature. When $[CpFe(CO)_2]_2$ was used as a catalyst similar results were obtained with more CNTs formed at 800 °C than at higher temperatures.

Analysis of CNTs

Synthesized MWCNTs were further characterized by TGA in air as shown in Figure 7.9 The weight loss is due to the combustion of carbon with oxygen and therefore, corresponds to the carbon content in the sample. There is one major mass loss observed (67%) in the temperature range of 420-584 °C. This weight loss is a result of oxidation of carbon nanotubes which is consistent with other studies as reported in the literature [14].

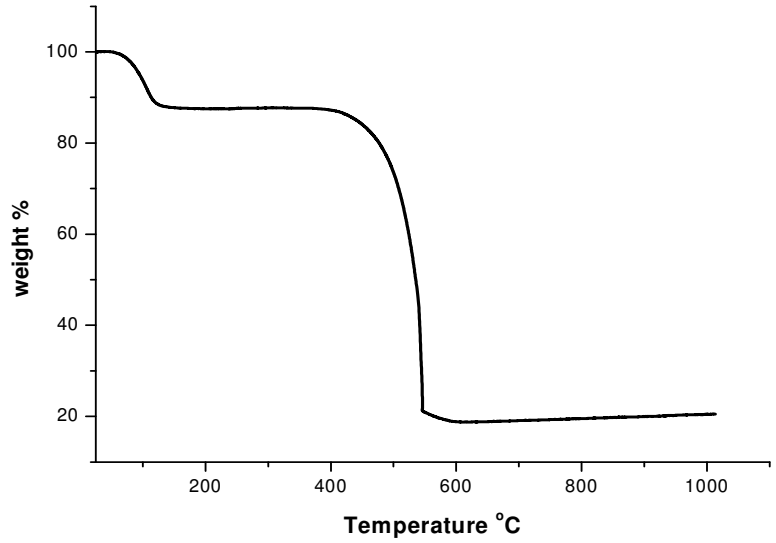

Figure 7.9: TGA of CNTs grown using $CpFe(CO)_2Me$ (5 wt.%, at 800 °C, 0.8 ml/min injection rate) (Weight loss between 24-135 °C is due to moisture).

The residue after complete carbon oxidation was 18.8 wt.% of the original mass which is the iron content in the untreated sample. Similar results were obtained by Harris et al. where they observed 17.6 wt.% for the iron content after complete oxidation when low concentrations of catalyst were applied [1a].

Figure 7.10 shows the first order Raman spectra of CNTs obtained using $CpFe(CO)_2Me$ and ferrocene as catalysts. In Figure 7.10a broad peaks at 1358 cm^{-1} and 1583 cm^{-1} correspond to D and G-bands respectively as reported in the literature [15]. These Raman lines shift slightly to a higher wavenumber (1355 and 1581 cm^{-1}) in samples prepared by ferrocene (Figure 7.10b) but are still within the range of what others have measured [16]. CNTs synthesized by ferrocene showed to have the weak D' band at 1615 cm^{-1} which is normally positioned next to the G-band, while CNTs formed by $CpFe(CO)_2Me$ have a less pronounce D' band. This D' band is due to the presence of defects of the D band. The ratio of the intensity of the D and the G peaks (I_D/I_G) is used to measure the disorder in the CNTs [17]. The I_D/I_G ratio of CNTs formed using $CpFe(CO)_2Me$ was found to be 0.4 while the I_D/I_G ratio of tubes formed by ferrocene was 0.5. This indicates that CNTs formed from ferrocene are more disordered when compared to the tubes formed using $CpFe(CO)_2Me$.

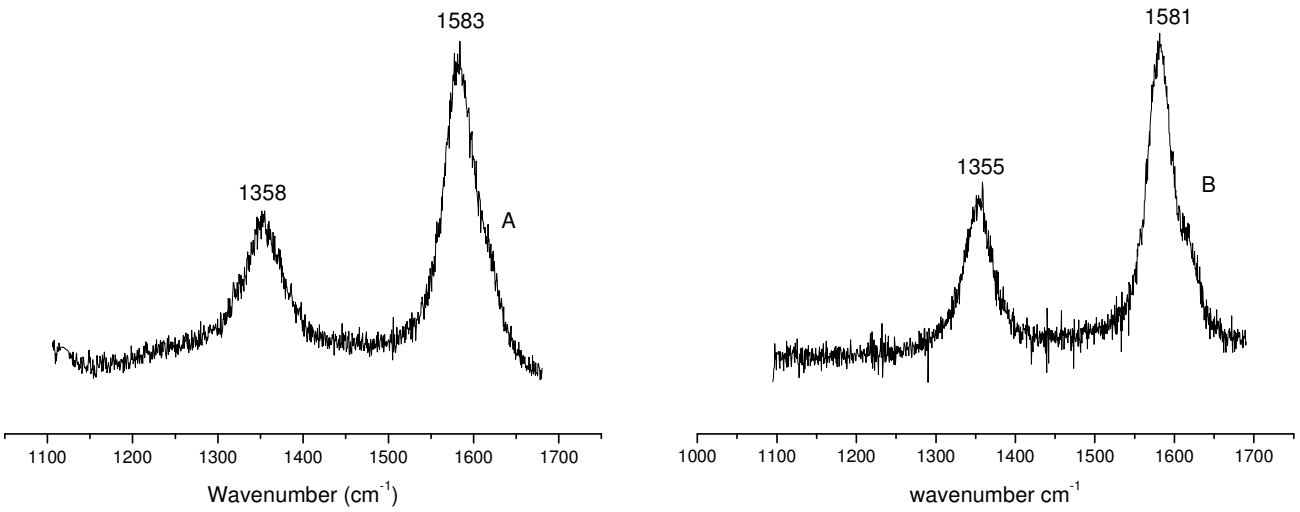

Figure 7.10: Raman spectra of MWCNTs grown from (A) $CpFe(CO)_2Me$ (5 wt.%, at 800 °C, 0.8 ml/min injection rate) and (B) ferrocene (5 wt.%, at 800°C, 0.8 ml/min injection rate).

7.4 Conclusions

MWCNTs with outer diameters in the range of 19-41 nm have been synthesized by an injection CVD method using solutions of $CpFe(CO)_2Me$ dissolved in toluene in a single-furnace. $CpFe(CO)_2I$-toluene solutions were shown to be inactive for CNT growth. The best yield of CNTs were formed at low temperature (800 °C) for $CpFe(CO)_2Me$. The yield of carbonaceous materials increased with temperature. Low injection rates produced high yields of carbonaceous materials. Injection rates were observed to have little effect on the morphology or size distribution of the CNTs. Addition of a large amount of iodine to ferrocene or $[CpFe(CO)_2]_2$ gave low yields of CNTs indicating the negative effect of iodine on CNT growth.

7.5 References

[1] (a) Harris, J. D.; Raffaelle, R. P.; Gennett, T.; Landi, B. J.; Hepp, A. F. *Mater. Sci. Eng. B* **2005**, *116*, 369. (b) Liu, X. Y.; Huang, B. C.; Coville, N.J. *Fullerenes Nanotubes Carbon Nanostruct* **2002**, *10*, 339. (c) Mohlala, M. S.; Liu, X. Y.; Robinson, J. M.; Coville, N. J. *Organometallics* **2005**, *24*, 972.

[2] Satishkumar, B.C.; Govindaraj, A.; Rao, C.N.R. *Chem. Phys. Lett.* **1999**, *307*, 158.

[3] (a) Nikolaev, P.; Bronikowski, J.; Bradley, R. K.; Rohmund, F.; Colbert, D. T.; Smith, K. A.; Smalley, R. E. *Chem. Phys. Lett.* **1999**, *313*, 91. (b) Nerushev, O. A.; Sveningsson, M.; Falk, L. K. L.; Rohmund, F. *J. Mater. Chem*. **2001**, *11*, 1122.

[4] Lee, C. J.; Lyu, S. C.; Kim, H. W.; Park, C. Y.; Yang, C. W. *Chem Phys. Lett*. **2002**, *359*, 109.

[5] Nerushev, O. A.; Sveningsson, M.; Falk, L. K. L.; Rohmund, F. *J. Mater. Chem*. **2001**, *11*, 1122

[6] Moisala, A.; Nasibulin, A. G.; Brown, D. P.; Jiang, H.; Khriachtchev, L.; Kauppinen, E. I. *Chem. Eng. Sci*. **2006**, *61*, 4393.

[7] Liu, X. Y.; Huang, B. C.; Coville, N. J. *Carbon* **2002**, *40*, 2799.

[8] Edgar, K.; Spencer, J. L. *Curr. Appl. Phys.* **2004**, *4*, 121.

[9] Rohmund, F.; Falk, L.K.L.; Campbell, E.E.B; *Chem. Phys. Lett.,* **2000**, *328*, 369.

[10] Deepak, F. L.; Govindaraj, A.; Rao, C. N. R. *Chem. Phys. Lett,* **2001**, *345*, 5.

[11] Piper, T. S.; Wilkinson, G. *J. Inorg. Nucl. Chem.* **1956,** *3*, 104.

[12] King, R. B. "Organometallic Synthesis", Academic Press: New York, 1965; vol I, p114.

[13] Andrews, R.; Jacques, D.; Rao, A. M.; Derbyshire, F.; Qian, D.; Fan, X.; Dickey, E. C.; Chen, J. *Chem. Phys. Lett*. **1999**, *303*, 467.

[14] Das, N.; Dalai, A.; Mohammadzadeh, J. S. S.; Adjaye, J. *Carbon* **2006**, *44*, 2236.

[15] Belin, T.; Epron, F. *Mater. Sci. Eng.B* **2005,** *119*, 105.

[16] Chen, Y.; Sun, Z.; Li, Y. N.; Tay, B. K. *Mater. Chem. Phys.* **2006**, *98*, 256.

[17] (a) Singh, C.; Shaffer, M. S. P.; Windle, A. H. *Carbon* **2003**, *41*, 359. (b) Endo, M.; Kim, Y. A.; Fukai, Y.; Hayashi, T.; Terrones, M.; Terrones, H.; Dresselhaus, M. S. *Appl. Phys. Lett.* **2001**, *79*, 1531.

7.6 Appendix

*Synthesis of $CpFe(CO)_2I$ **[1]*** [11]

The iodine complex, **[1]** was prepared from the reaction of $[CpFe(CO)_2]_2$ (2 g, 5.6 mmol) and iodine (1.43 g, 5 mmol) in dichloromethane (30 ml) at room temperature. The reaction was stirred for 4 hours and the solvent was evaporated. The crude material was dissolved in dichloromethane. Sodium thiosulphate (2g) was dissolved in distilled water and mixed with the dichloromethane solution of the crude product to remove excess iodine. The organic layer was extracted and evaporated to give complex [1]. Yield = 1.8 g, ca. 90%.

^{1}H-NMR ($CDCl_3$)**:** δ = 5.04 (s, 5H, (C_5H_5-Fe); **IR** (CH_2Cl_2)**:**ν = 2041, 1996 cm^{-1} (CO); **m.p** = 117 °C.

*Synthesis of $CpFe(CO)_2Me$ **[2]*** **[**12]

The methyl complex, [**2]** was prepared according to the procedure of Piper and Wilkinson. The preparation of a Na amalgam was done by cutting fresh (shiny) small portions of Na metal (1.0 g, 43 mmol) under paraffin and adding them slowly to vigorously stirring mercury (10 ml). The dimer $(CpFe(CO)_2)_2$ (2,5 g, 7 mmol) was dissolved in dry THF (50 ml) and then added slowly to the sodium amalgam. The mixture was stirred vigorously for 3 hours. MeI (2 ml, 32 mmol) was added and the mixture was stirred for another 6 hours. The mercury was separated from the solvent layer and the solvent was removed under vacuum. The dry mixture was placed in a cooling flask and the pure compound was achieved by sublimation at 60 °C under vacuum yielding a fatty yellow crystalline compound [**2**] with a camphor smell.

The product is air sensitive and changes from yellow to brown with time. Yield = 1.0 g, *ca.* 45%.

^{1}H-NMR ($CDCl_3$)**:** δ = 4.65 (s, 5H, (C_5H_5-Fe), 0.12 (s, 3H, Fe-Me); **IR** (CH_2Cl_2): ν= 2006, 1948 cm-1 (CO); **m.p**. = 59-67 °C.

CHAPTER 8

Conclusions

Numerous methods have been used to synthesize CNTs. These methods include: arc discharge, laser ablation and CVD methods, with the latter method been the most widely used because large amounts of CNTs can be achieved from this method. The CVD methods (gas phase, floating or injection) have been used to synthesize different types of CNTs (aligned, coiled, N/B doped) using various transition metals as catalysts in the presence of hydrocarbon sources. The catalysts which have been used to produce high yields and reasonable quality CNTs were mainly comprise of iron and cobalt metals. These issues were described in chapter 1.

Chapter 2 described the use of the injection CVD method to synthesize MWCNTs in the presence of a reducing gas (5% H_2 in Ar) and a hydrocarbon solvent. MWCNTs synthesized in this study were mainly characterized by Raman spectroscopy, TGA analysis, SEM and TEM analysis. The methods are classical methods and have now been well established in the research literature and a brief outline of the issues relating to the use of these techniques was described in chapter 2.

The results presented in this research project show that the use of organometallic iron catalysts, carbon containing gases and hydrocarbon liquids which can be easily handled are sufficient to efficiently synthesize MWCNTs in a single-furnace experimental method via an injection CVD route. A range of conditions used in this work, showed that variables must be selected carefully to produce the CNTs. The variables included: temperature, injection rate, catalyst concentrations and gas flow rates.

Many studies have been reported in the CNT synthesis literature using Fe/Mo supported catalysts but to date there are no reports in which CNT synthesis was effected using Fe/Mo gas phase catalysts. Therefore, it was of interest to study the use of Fe/Mo catalysts for CNT synthesis using the *injection* CVD method. It was shown in Chapter 3

that mixtures of transition metals of Fe and Mo, could efficiently produce CNTs at various metal concentrations. A series of experiments were performed in which mixtures of ferrocene (Fc) and $M(CO)_5{}^tBuNC$ (M = Mo, W) were decomposed in the presence of toluene at high temperature (700–900 ^oC). The low solubility of $Mo(CO)_6$ prevented formation of any carbonaceous materials from this metal source in the temperature range 700-900 °C. Carbon spheres were formed from toluene in the absence of the metal and when a single metal source, $M(CO)_5{}^tBuNC$ or Fc/W bimetallic catalyst were used. In fact the synthesis of CSs does not require a catalyst and the results suggest that the metal systems were inactive in the reaction. CNTs were mainly synthesized by Fc or Fc/Mo bimetallic mixtures. HMTEM results revealed that metal particles, comprising of Fe or Fe-Mo alloys were present in the MWCNTs produced. It was observed from this study that the formation of MWCNTs produced by Fe-Mo catalysts exhibited broad outer diameters (200-467 nm). The large size of the metal particles produced in this study is believed to be responsible for the limited formation of CNTs produced in the reaction.

Addition of element sulphur to the metal catalysts has shown by many researchers to influence the diameters of the synthesized CNTs. Amongst all these studies reported to date there has not been any mention of the use of sulphur containing compound in which the sulphur is directly attached to the catalyst. In Chapter 4, it was shown that mixtures of ferrocene and sulphur containing compound can form CNTs. The sulphur containing compound that was used in this study was 1,1'-bis(methylthio)ferrocene (ferrocenyl sulphide). The presence of sulphur as expected did modify both the tube diameter and the product yield of the CNTs. In our studies, the presence of sulphur gave MWCNTs instead of DWCNTs or SWCNTs as reported by others on related but different systems. MWCNTs and fibers synthesized from the ferrocenyl sulphide were shown to have wider diameters relative to the tubes and fibers synthesized from ferrocene. More importantly it was observed that *less* sulphur was required to induce the changes when compared to using sulphur added from an external source (S_8, thiophene). More CNTs were grown at high temperature (1000 °C), while amorphous carbon, spheres and fibers were mostly formed at lower temperatures (800-900 °C).

From the literature, CNTs have been synthesized mainly from ferrocene and other iron containing compounds using both supported and unsupported CVD methods. But there have not been any studies on the synthesis of CNTs using substituted ferrocenes as catalysts. In Chapter 5, the use of alkyl ferrocenes (1,1-dimethylferrocene and 1,1-diethylferrocene) as catalyst for MWCNTs was discussed. Dimethylferrocene was shown to be active for the growth of CNTs while diethylferrocene was found to be inactive for CNT formation. The effect of ring substitution on the role of ferrocene as catalyst in the formation of tubular carbons has revealed that the substituent can affect the type of carbonaceous material formed. Furthermore, the results showed that the ring substituent impacts on the CNT diameter, but does not have an effect on the morphology of the tubes. MWCNTs grown from 1,1-dimethylferrocene were observed to have narrow outer diameters relative to tubes formed from ferrocene. A relatively low temperature (800 °C) was found to be appropriate for formation of CNTs. The injection rate variation did not have any effect on the diameter and morphology of the CNTs formed. These results suggest that the morphology of CNTs can be influenced by ligands atoms attached to the catalyst. This has implications for the future design of CNT catalysts and the control that may be achieved via this approach to CNT synthesis.

Nitrogen doped and boron doped CNTs have been widely synthesized using various catalysts. Nitrogen doped nanotubes have previously been prepared under N_2 and NH_3 atmospheres while the boron doped CNTs have been prepared by a range of boron containing compounds. Up to date there has not been any study on N-doped CNTs synthesis using ferrocenyl compounds containing nitrogen. In Chapter 6, ferrocenyl compounds containing nitrogen and boron elements, 3-ferrocenyl-*N,N*-diisopropyl-3-oxo-propionamide (diisopropylamide complex) and (1Z)-3-(diisopropylamino)-3-oxo-1-ferrocenylprop-1-ene-1-yl difluoroborate (difluoroborate) were used as catalyst for CNT synthesis. It was shown that by using the nitrogen containing ferrocene compounds, MWCNTs with different morphology and properties could be synthesized. MWCNTs containing nitrogen were formed when diisopropylamide ferrocene was used as a catalysts at low concentrations (2.0 and 1.0 wt.%). More CNTs were grown at low temperature (800 °C) while high temperatures (900-1000 °C) were favourable for the

formation of amorphous carbon and fibers. A difluoroborate ferrocene-$CaCO_3$ supported catalyst was shown to be active for MWCNTs synthesis at 700 °C using mixtures of nitrogen and acetylene.

Organometallic compounds containing carbonyl groups such as $Fe(CO)_5$, $(CpFe(CO)_2)_2$ and $(C_8H_8Fe(CO)_3)$ have been used to synthesize CNTs using gas phase and injection CVD methods. In this chapter we have sought to expand on this approach by using other organometallic compounds containing carbonyl groups. In Chapter 7 the effect of $CpFe(CO)_2Me$ and $CpFe(CO)_2I$ catalysts for MWCNT production was described. MWCNTs with outer diameters in the range of 19-41 nm were synthesized by toluene solutions of $CpFe(CO)_2Me$. Toluene solutions of $CpFe(CO)_2I$ were shown to be inactive for CNT growth. More CNTs were formed at lower temperatures (800 °C). The yield of carbonaceous materials increased with temperature. Low injection rates produced high yields of carbonaceous materials. Injection rates were shown to have no effect on the morphology or size distribution of the CNTs produced. Addition of iodine to ferrocene and $(CpFe(CO)_2)_2$ gave low yields of CNTs indicating the negative effect of iodine on CNT growth.

In general, CNTs synthesized in this study was influenced by various parameters. Thus, temperature, catalyst concentration and injection flow rates were shown to impact on CNT synthesis across a range of different iron organometallic complexes. It was found that various temperatures can be suitable for CNT synthesis only when certain catalysts were used at certain injection rate.

These results from this study open the door for formation of CNTs using different organometallic complexes. Further work will focus on the use of different substituents on ferrocene and organometallic iron complexes as catalysts for CNT synthesis. These substituents include: the hydroxyl group and aromatic groups attached to the ferrocene ring. The effect of a solid hydrocarbon source using ferrocenyl compounds as catalysts could also be studied by synthesizing CNTs using pyrolysis methods instead of injection CVD methods.